Perineuronal Nets & Parvalbumin Interneurons in the PolyI:C Model of Schizophrenia

by

John Wesley Paylor

A thesis submitted in partial fulfillment of the requirements for the degree of

Master of Science

Centre for Neuroscience
University of Alberta

Abstract

Schizophrenia (SCZ) is a psychiatric disorder that, despite a high prevalence (1% population worldwide) and burden of disease (1% global burden of disease), has a poorly understood etiology. While symptoms of SCZ typically manifest during adolescence and early adulthood, there is a substantial body of research linking prenatal events (e.g. early infection) to one's risk for developing SCZ. Human post-mortem analyses have suggested perineuronal nets (PNNs) as a potential biomarker for SCZ, as PNNs are deficient in a number of disease-specific regions of SCZ patients. PNNs, which surround parvalbumin positive (PV) inhibitory interneurons, typically mature during late adolescence and early adulthood when SCZ symptoms often first present. As such, I sought to examine whether a developmental PNN deficit is present in a maternal immune activation model of SCZ in rats.

Long-Evans rat dams were treated at gestational day 15 with polyriboinosinic-polyribocytidilic acid (PolyI:C) to induce a strong maternal immune response. The litters were carried to birth and offspring allowed to develop to postnatal days 7 (PND7), 21, 35, and 90. I used histochemistry to assess PNNs, staining with the lectin *Wisteria Floribunda Agglutinin,* and examined their integrity using epifluorescent and confocal microscopy across a number of brain regions: frontal association cortex, prelimbic cortex, reticular thalamic nucleus, primary auditory cortex, amygdala, and the dorsal and ventral hippocampus. Additionally, I stained for microglia (anti-IBA1) and astrocytes (GFAP) as well as PV interneurons (anti-PV) to assess immune activation and PV neuronal integrity respectively.

Consistent with previous research, I find that PNNs increase throughout postnatal development in all regions examined. During adolescence a deficit emerged in the number of PNNs in both the frontal association cortex and medial prelimbic cortex of PolyI:C treated animals. I did not

however replicate previous human studies showing PNN associated dysfunction in the primary auditory cortex or amygdala. My examination of PV+ interneurons also showed developmental effects of reduced PV+ interneurons within the basolateral amygdala and a trend towards a reduction in the frontal association cortex. I found that there were no differences in microglial cell density and only minor changes to GFAP immunoreactivity, neither of which were associated with the PNN deficits in the prefrontal cortex.

Remarkably, this study shows that a prenatal immune challenge event can result in deficits in PNNs that are not apparent until much later in development during adulthood. Furthermore, my results add to the list of shared pathological features between the PolyI:C model and SCZ itself, as PNNs are disturbed in the prefrontal cortex in both. PNNs along with PV+ interneurons are important regulators of critical windows of heightened plasticity during development. A deficit in PNNs could lead to a permanent pathological upregulation of structural plasticity into adulthood, as well as PV interneuron and cortical inhibitory network dysfunction. These deficits may contribute to a number of behavioural symptoms that appear within the same developmental periods, many of which are associated with the prefrontal cortex.

Preface

This research was conducted in collaboration with Dr. Ian Winship at the University of Alberta and Dr. John Howland at the University of Saskatchewan. Dr. Howland's lab raised the animals used in the study and induced the model. After the animals were euthanized and tissue extracted, all samples were sent to Dr. Winship's lab at the University of Alberta where I conducted my work. This included processing the tissue, sectioning the brains, all immunohistochemistry and subsequent analysis of the data. Writing and preparation of the thesis was entirely conducted by my own accord, with edits suggested by the examining committee. The project was conducted under ethical approval of the University of Saskatchewan Animal Research Ethics Board.

Acknowledgements

First and foremost, I would like to thank my supervisor Dr. Ian Winship for his wisdom and guidance in the course of this project and my education as a whole. Thank you for taking a chance on me as your student and providing an environment within which I can thrive. Thank you also to my colleagues Mischa, Sam, Anna, Junqiang, Nick, Reiner, and Eszter for their assistance and friendship throughout the course of this work. Thank you to our laboratory technician Jocelyn for going above and beyond in every way to facilitate my own work and everyone else's in the lab.

Additionally, I would like to thank Dr. Bradley Kerr and Dr. Karim Fouad of my supervisory committee for making their immense backgrounds of knowledge available to myself and my work. Thank you to Dr. John Howland and his entire team at the University of Saskatchewan for their role in my thesis project and the years they spent developing this model in their laboratory. Thank you to Dr. Kathryn Todd for making her lab equipment and her student's minds available to me for the benefit of my work.

Thank you to my parents, Debbi and Jay as well as my step dad Allen for providing me with every opportunity possible to pursue a career and a life that I love. Thank you to my brothers Benjamin and Jeremy for their everlasting support and encouragement to achieve my dreams and making sure that I want for nothing along the way. Thank you to Ian for being the friend that you are to me. In everything I have done you and your family have been there for me, and each of my accomplishments is a reflection of the care and love that you've shown me. Lastly, thank you Chantalle for being a perfect example and the only inspiration necessary to want to achieve something greater than oneself.

Table of Contents

List of Tables

List of Figures

Glossary of Terms & Abbreviations

Schizophrenia: SCZ

Parvalbumin: PV+

Perineuronal Nets: PNNs

Polyriboinosinic-polyribocytodilic acid: PolyI:C

Chondroitin Sulfate Proteoglycans: CSGPs

Chondroitinase ABC: ChABC

Matrix Metalloproteinases: MMPs

A disintegrin and metallopeptidase with thrombospondin motifs: ADAMTSs

Prefrontal Cortex: PFC

Reticular Thalamic Nucleus: RTN

Basolateral Amygdala: BLA

1. Introduction

1.1 Introduction to Schizophrenia

Schizophrenia (SCZ) is a devastating neuropsychiatric disorder characterized primarily by profound mental disturbances in the form of hallucinations and delusions. Twenty-six million suffer from the disorder worldwide and 60% will suffer life-long disability (Hor & Taylor, 2010; World Health Organization, 2014). Among individuals with SCZ, the average life expectancy is 10-15 years shorter than the general population and 10% of those individuals will commit suicide (Miles, 1977; Caldwell & Gottesman, 1990; Laursen et al., 2012; Crump et al., 2013). In addition to the persistent burden this chronic disorder places on patients individually, it also accounts for about 1% of the global burden of disease which is considered a moderate to high factor in the worldwide burden (World Health Organization, 2014).

While the presentation of SCZ is heterogeneous within patients, the incidence is largely consistent across cultural and ethnic groups (Ayuso-Mateos, 2002). Patients' symptoms generally fall into one of three clusters: the positive symptoms (e.g. hallucinations and delusions), negative symptoms (e.g. social isolation, avolition, anhedonia), and cognitive symptoms (e.g. impairments in working memory, sensory processing, and higher order cognition). Symptoms most typically begin to manifest during the late teens and early adulthood with a decline in incidence in the late twenties (Sham et al., 1994; Murray & Van Os, 1998). However, in recent years it has become widely accepted that certain subtle cognitive disturbances are present well before the first presentation of psychotic symptoms (Malla et al., 1994; Jones, 1997; Klosterkötter et al., 2001; Liebermen et al., 2001; Perkins, 2004).

1.2 Schizophrenia Pathology

Unfortunately, little is currently known about the underlying pathology that gives rise to SCZ. Much of our understanding stems from the observation that therapeutic drugs with known mechanisms alleviate symptom clusters of SCZ and inferences on pathophysiology are made based on those mechanisms. By this method one of the leading hypotheses of SCZ pathophysiology, the dopamine hypothesis, was suggested based upon the observed therapeutic efficacy of antipsychotic agents that act by blocking dopamine receptors in the brain (Van Rossum, 1967). However, the dopamine hypothesis and traditional antipsychotic medications cannot account for all the symptoms of schizophrenia. Several other hypotheses have been proposed, including the glutamate hypothesis, serotonin hypothesis, and GABA hypothesis (Wooley & Shaw, 1954; Gaddum & Hameed, 1954; Kim et al., 1980; Benes et al., 1996; Javitt et al., 2012). Each, like the dopamine hypothesis, is not a comprehensive explanation of the disease process. More recently it has been suggested that SCZ could arise from a disruption during development, giving rise to the neurodevelopmental hypothesis (Murray & Lewis, 1987; Weinberger, 1987). This idea has gained significant interest as a disturbance during these critical early stages could feasibly disrupt the developmental trajectories of multiple neurotransmitter systems and thus provide some coherence between other hypotheses (Butler et al., 1994). In support of this suggestion, several of the risk factors for developing SCZ that have been identified stem from early developmental time points such as maternal exposure to infection or stress, malnutrition before birth, and obstetrics complications (Xu et al., 2009; Brown & Derkits, 2010; Lumey et al., 2011; Margari et al., 2011; Brown, 2012; Suvisaari et al., 2013).

Despite our limited mechanistic understanding of SCZ, a number of pathophysiological features have been identified. Both imaging and post-mortem studies have identified that SCZ patients have impaired synaptic connectivity, delayed or dysfunctional maturation of cortical

inhibitory networks, and deficits in perineuronal nets (PNNs) in disease specific regions (McGlashan and Hoffman, 2000; Volk and Lewis 2002; Lewis et al., 2005; Stephan et al., 2009; Gonzalez-Burgos et al., 2010; Pantazopoulos et al., 2010; Mauney et al., 2013; Pantazopoulos et al., 2013; Seshadri et al., 2013; Volk and Lewis 2013; Pietersen et al., 2014). While other types of dysfunction have been identified (e.g. dopamine hyperactivity), these pathological features of the disease highlight the role of the inhibitory system and its importance in SCZ (for review see Lewis et al., 2011; Volk & Lewis, 2014). At the centre of this focus are parvalbumin positive (PV+) inhibitory interneurons, a particular subtype of interneuron defined by their expression of the calcium binding protein parvalbumin (Celio, 1990). PV+ interneurons have been shown in several studies to be lost or down-regulated at both the protein and mRNA level in SCZ brains post-mortem (Hashimoto et al., 2003; Mellios et al., 2009; Fung et al., 2010; Curley & Lewis, 2012; Volk et al., 2012; Glausier et al., 2014). In SCZ, about 50% of PV+ interneurons entirely fail to express the synthesizing enzyme from the primary inhibitory neurotransmitter, GABA, called GAD67 (Hashimoto et al., 2003). Functionally, PV+ interneuron activity varies with network activity and during oscillatory activity can fire at rates up to ~120 Hz (Hu et al., 2014). This high frequency firing rate has been shown to be both necessary and sufficient for the generation of gamma oscillations (30-80 Hz) of cortical pyramidal neurons (Cardin et al., 2009; Sohal et al., 2009) Fittingly, gamma oscillations have been repeatedly shown to be perturbed in electrophysiological recordings from SCZ patients (Cho et al., 2006; Basar-Eroglu et al., 2007; Spencer et al., 2008; Farzan et al., 2010; Uhlhaas & Singer et al., 2010; Woo et al., 2010; Sun et al., 2011; Kirihara et al., 2012; Grutzner et al., 2013). PV+ interneurons also play crucial roles in the opening of critical windows such as is seen in the visual cortex, within which the cortical tissue undergoes dramatic structural and functional reorganization in response to activity

(Hensch, 2005; Takensian & Hensch, 2013). PV+ expression is highly upregulated prior to the opening of a critical window, and any disturbance of this maturation can delay or disrupt this trajectory (Del Rio et al., 1994; Maffei et al., 2010; Takesian et al., 2013). PV+ interneurons are also involved in the closure of critical windows and in this case it is the upregulation of perineuronal nets (PNNs) surrounding PV+ interneurons that signals stabilization (Pizzorusso et al., 2002; Gogolla et al., 2009; Takesian & Hensch, 2013).

1.3 Perineuronal Nets

PNNs are highly organized components of the extracellular matrix that surround the cell body, initial axon segment, and proximal dendrites of PV+ inhibitory interneurons (Brückner et al., 1993, 1996; Koppe et al., 1997; Kwok et al., 2010). The percentage of PV+ interneurons that have PNNs can vary greatly depending on region, but in some areas up to 90% of PV+ interneurons are surrounded by PNNs (Yamada et al., 2015). They have also been reported in smaller proportions surrounding other inhibitory interneuron subtypes (e.g. calrentin, calbindin) as well as sparsely on cortical pyramidal cells (Alpár et al., 2006; Morishita et al., 2015). These structures have been shown to play a variety of roles including surrounding and stabilizing synaptic structures, restricting plasticity, and in the maintenance of ion homeostasis of highly active PV+ interneurons (Hockfield et al., 1990; Brückner et al., 1993; Brückner et al., 1996; Hartig et al., 2001; Fox & Caterson, 2002; Pizzorusso et al., 2002; Berardi et al., 2003; Rhodes & Fawcett, 2004). Structurally, PNNs are composed of multiple ECM proteins including hyaluronic acid, chondroitin sulphate proteoglycans (CSPGs), tenascins, and link proteins (Celio & Blumcke, 1994; Carulli et al., 2007; Morawski et al., 2009; Kwok et al., 2010). In addition to these, PNNs can sequester a number of growth-promoting and -inhibitory factors within their

interlaced network (Celio & Blumcke, 1994; Pesold et al., 1999; Galtrey & Fawcett, 2007; Fawcett, 2009; Beurdeley et al., 2012; Vo et al. 2013).

PNNs have been perhaps best studied in regards to their role in the stabilization of critical periods as their maturation coincides with the cessation of these heightened periods of plasticity. This has been well described in the visual system, where PNN expression increases throughout postnatal developmental and plateaus with the closure of ocular dominance plasticity within the primary visual cortex (Sur et al., 1988; Pizzorusso et al., 2002). PNN maturation has also been examined in several other modalities and been shown to protect and ensure permanence of learned behaviours, suggestive of their stabilization of critical period remodeling. For example, in the high vocal centre nucleus of the zebra finch song bird, the percentage of PV+ cells ensheathed in PNNs increases dramatically during the course of song learning and plateaus with song maturity (Balmer et al., 2009). In the amygdala, PNNs see their greatest upregulation during the same developmental period in which a dramatic shift in fear extinction phenotype occurs. Prior to PNN formation, learned fear memories can be entirely extinguished by retraining, but when learned as adults in the presence of PNNs these memories are robust to extinction (Gogolla et al., 2009). The formation of PNNs is also disturbed by manipulations that delay the closure of critical periods. Visual deprivation, whisker-trimming, and acoustic isolation, which starve critical windows of neural activity, have all been shown to disrupt the appropriate expression of PNNs (Sur et al., 1988; McRae et al., 2007; Balmer et al., 2009; Ye & Maio, 2013). Lastly, consistent with their role in heightened periods of plasticity, genetic knockouts of PNN components such as tenascin-R, cartilage-link protein 1 (ctrl1) or link protein can result in failure of PNNs to form and plasticity to be permanently upregulated into adulthood (Bruckner et al., 2000; Carulli et al., 2010; Romberg et al., 2013).

While the process by which PNN formation occurs is not entirely understood, many studies have begun to elucidate the complex signalling cascades of the critical period. The opening of the critical period is closely associated with the upregulation of factors like brain-derived neurotrophic factor and orthodentricle homeobox 2 (Otx2) protein. Otx2 in particular is thought to be an essential regulator of the onset of the critical period, as it is captured and internalized just prior to the opening of the window (Sugiyama et al., 2008; Beurdeley et al., 2012). With internalization, Otx2 enhances the expression of markers of PV+ cell maturation, including further PNN development. BDNF has also been shown to be an important regulator of the critical period. Genetic enhancement of BDNF triggers the critical period early in the primary visual cortex and direct BDNF infusion into the primary auditory cortex amplifies tonotopic map plasticity in response to pure tone exposures (Hanover et al., 1999; Huang et al., 1999; Anomal et al., 2013). Conversely to this, blocking BDNF prevents critical period plasticity in both the visual and auditory modalities (Cabelli et al., 1997; Anomal et al., 2013). Stimulants of the inhibitory system like benzodiazepines, which act on $GABA_A$ receptors, can also trigger the critical period early (Hensch et al., 1998; Fagiolini & Hensch, 2000; Iwai et al., 2003; Fagiolini et al., 2004).

Once matured PNNs stabilize and prevent further structural reorganization of the cortex. For example, monocular deprivation during the critical period of visual plasticity can cause loss of visual acuity in the deprived eye, called amblyopia, which persists throughout adulthood (Sur et al., 1988; Ye & Maio, 2013). However, the same manipulation has no effect when introduced after the critical period in the presence of mature PNNs and visual acuity remains intact (McRae et al., 2007; Sur et al., 1988). These stabilizing effects can be reversed by degradation of PNNs using targeted enzymes like chondroitinase ABC (ChABC), which cleaves constituent CSPG

chains of PNNs. Treatment with ChABC renders the mature visual cortex sensitive again to monocular deprivation, or in the case of previous deprivation the cortex can be reorganized with appropriate stimulation and visual acuity restored (Pizzorusso et al., 2002; 2006). Similarly, in the amygdala where fear extinction phenotypes are encoded, adult rats who are otherwise resistant to retraining of their fear memories can have them entirely extinguished by combined treatment with ChABC and retraining (Gogolla et al., 2009).

1.4 Perineuronal Net Deficits in Schizophrenia

Interest into the structural and functional role of PNNs has increased with the observation that PNNs are disturbed in SCZ. Studies in recent years have shown deficits in PNNs in the dorsolateral prefrontal cortex, olfactory epithelium, entorhinal cortex, and amygdala of SCZ patients brains post-mortem (Pantazopoulos et al., 2010; Mauney et al., 2013; Pantazopoulos et al., 2013; Pantazopoulos et al., 2015). These observations are of particular interest due to the coincidental developmental timeline of SCZ and PNNs. SCZ generally begins to manifest during the late adolescent and early adult periods of development, between the ages of 15-25. A study of healthy human post-mortem tissue has shown that this is also the age range within which the greatest increase in PNNs occurs, at least in the prefrontal cortex (Mauney et al., 2013). Animal studies from a variety of species and contexts also corroborate this timeline, showing that the largest upregulation of PNNs in multiple brain regions occurs during species-equivalent periods of late adolescence and early adulthood (Pizzorusso et al., 2002; Gogolla et al., 2009). In the seminal work that described PNN development in the human prefrontal cortex, it was also shown that adult SCZ patient's brains post-mortem had a deficit in PNNs compared to matched controls (Mauney et al., 2013). This suggests that the overt manifestation of schizophrenia may be linked, at least temporally, to the maturation of PNNs and stabilization of the networks within which

they reside. It is of note that the prefrontal cortex where the deficit was observed is thought to be involved in a variety functions within the cognitive symptom cluster of SCZ, including executive functions, working memory, and planning (Roberts et al., 1998). Similar deficits in other brain regions of interest to SCZ including the olfactory epithelium, entorhinal cortex, and amygdala have been reported. Within the amygdala, several subnuclei were individually examined and it was found that the deficits were specific to certain subnuclei whereas others maintained control levels of PNNs (Pantazopoulos et al., 2010; 2015). Furthermore, the number of PV+ interneurons were unchanged in the amygdala and entorhinal cortex despite a diminished number of PNNs. Taken together, these suggest that the loss of PNNs observed in SCZ is not a global deficit, nor is it simply a loss of host PV+ interneurons (Mauney et al., 2010; Pantazopoulos et al., 2010; 2015).

The observation that PNNs are deficient above and beyond that of their close association with PV+ interneurons could provide some mechanistic understanding into several pathological features of SCZ. Firstly, PNNs have well defined roles in the healthy progression of critical periods, within which synaptic growth and later pruning occurs. Malformation of PNNs in SCZ could disturb this trajectory and contribute to the aberrant synaptic connectivity that is also observed in SCZ patient's brains post-mortem (Do et al., 2015). During the critical period, as PV+ interneurons mature they respond rapidly to discordant sensory input and later induce a sequence of synaptic pruning in pyramidal cells (Bavelier et al., 2010; Takesian & Hensch, 2013). This heightened period of pruning ends with the closure of the critical period coincidentally with PNN maturation. In SCZ it has been observed that dendritic spine number and density are reduced in a number of regions of interest, including the prefrontal cortex, superior temporal cortex and several subcortical structures (Garey et al., 1998; Roberts et al.,

2005a,b; Kolomeets et al., 2005; Sweet et al., 2009; Moyer et al., 2012; Konopaske et al., 2014). Fittingly, spine deficits in a variety of animal models have been shown to have an impact on a number of SCZ-related symptoms such as impairments in working memory, attention, sensorimotor processing, and sociability (Liston et al., 2006; Cahill et al., 2009; Hains et al., 2009; Brennaman et al., 2011). Disruption or malformation of PNNs could result in a prolonging of this otherwise healthy period of synaptic pruning and a destabilization of functional synaptic contacts. Not only do PNNs form physical barriers to the degradation of these synapses, but also have a variety of complex interactions with receptors (e.g. Nogo receptor) that can limit critical period plasticity (Dickendesher et al., 2012; Bochner et al., 2014).

A wealth of research suggests a variety of forms of GABAergic and inhibitory dysfunction in SCZ patients, especially in the prefrontal cortex. Preventing the upregulation of PNNs during the critical period using ChABC has been shown to cause GABAergic inhibitory post-synaptic currents to stagnate in their immature form (Liu et al., 2013). This suggests that GABAergic receptor maturation is either dependant on or coincidental to the consolidation of PNNs and the disruption of the process can result in a persistently immature inhibitory system. Consistent with this, enzymatic degradation of PNNs with ChABC results in increased excitability of interneurons and can affect gamma oscillatory activity generated by PV+ interneurons, which is consistently reported to be dysfunctional in SCZ (Carter et al., 1998; Cho et al., 2006; Basar-Eroglu et al., 2007; Dityatev et al., 2007; Lewis & Gonzalez-Burgos, 2008; Spencer et al., 2008; Farzan et al., 2010; Uhlhaas & Singer, 2010; Woo et al., 2010; Sun et al., 2011; Kirihara et al., 2012; Grutzner et al., 2013). Furthermore, direct ChABC infusion into the ventral hippocampus to remove PNNs has been to shown enhance hippocampal activity, increase dopamine system function, and augment locomotor responses to amphetamines, a phenomenon

also observed in SCZ patients (Shah & Lodge, 2013). Disruption of PNNs by other means can also disturb inhibitory function. Chronic treatment with the SSRI fluoxetine has been shown to downregulate PNNs, decrease perisomatic inhibitory puncta on pyramidal neurons in the medial prefrontal cortex and concurrently increase critical period plasticity markers (Giurado et al., 2014). Chronic fluoxetine has been shown to enable fear erasure in adult mice in combination with extinction training similar to what has been reported after treatment with ChABC (Gogolla et al., 2009; Karpova et al., 2011).

In a recent study it was shown that PV+ protein and mRNA expression decreased in areas where PNNs were degraded using ChABC (Yamada et al., 2015). This suggests that the loss of PNNs surrounding a host PV+ interneuron can result in decreased PV expression on that neuron. With regards to SCZ, while studies have consistently shown that while PV protein and mRNA levels are decreased few have found direct histological evidence of decreased cell numbers (Hashimoto et al., 2003; Mellios et al., 2009; Fung et al., 2010; Curley & Lewis, 2012; Lewis et al., 2012; Glausier et al., 2014). If a loss of PNNs is indeed an integral feature of SCZ, the hallmark loss of PV+ protein and mRNA expression without a decrease in actual cell number could be explained a deficit in PNNs.

While the developmental trajectory as well as functional and structural role of PNNs point to them having some part to play in SCZ pathogenesis, there have also been significant limitations to furthering our understanding. One major obstacle to date is that human post-mortem studies have only ever been able to examine individual end stage time points as tissue cannot be obtained earlier in development prior to a SCZ diagnosis. Considering the suspected developmental nature of SCZ, in particular PNN development, these studies can only provide a limited end-stage view point. Additionally, studies to date have only ever been able to examine a

limited number of brain structures. It is not yet known the full extent of the deficit in PNNs in the brain of SCZ patients and what other brain structures are affected beyond those already studied. Traditionally, the solution to these issues would be to turn to animal models of the disease to garner further understanding into potential human pathological processes. However, that is also problematic in that until recently it has proven difficult to create an effective model of schizophrenia due to the diversity of known risk factors, the breadth of symptoms, and unknown underlying pathology.

1.5 PolyI:C Model of Schizophrenia

In recent years one animal model that has had a significant impact in the field is the PolyI:C model of SCZ. PolyI:C is a maternal immune activation model whereby pregnant animals are treated with a synthetic double-stranded RNA analog called polyinosinic-polyribocytodilic acid (PolyI:C; for review see Meyer & Feldon, 2012; Meyer, 2014). This treatment, in the form of a single injection, causes a profound immune response in the mother that is short-lasting with well characterized effects (Alexopoulo et al., 2001; Takeuchi & Akira, 2007). This method of induction replicates epidemiological data suggesting that maternal infections during pregnancy can increase one's offspring's risk for developing SCZ (Brown, 2012; Brown & Derkits, 2010). Treatment with PolyI:C during specific gestational periods has been shown in a both rodents and non-human primates to induce behavioural and cognitive deficits in the offspring, many of which are consistent with a SCZ phenotype (Meyer et al., 2009; Brown & Derkits, 2010; Brown & Patterson, 2011; Howland et al., 2012; Zhang et al., 2012; Sangha et al., 2014; Meyer et al., 2014; Meyer et al., 2012; Machado et al., 2015). This includes impairments in working memory, latent inhibition, behavioural flexibility, fear processing and object recognition. Additionally, PolyI:C treated offspring display enhanced social withdrawal

and isolation as well as augmented responses to amphetamines, similar to that of SCZ patients. Notably, the majority of these symptoms are not present during rearing or childhood but manifest in late adolescence and early adulthood similar to the onset of SCZ.

In addition to their behavioural dysfunction, PolyI:C offspring also display a number of other shared pathophysiological features to that of SCZ patients. PolyI:C treated offspring have been shown to have more dopamine producing neurons in the ventral tegmental area, increased basal levels of dopamine and dopamine turnover (Ozawa et al., 2006; Winter et al., 2009; Li et al., 2014). Studies *in vitro* similarly show dopamine hyperactivity in PolyI:C as it has been reported that striatal slices from juvenile affected offspring have heightened dopaminergic release (Zuckerman et al., 2003). There is also evidence of shared immune system dysfunction between SCZ patients and PolyI:C treated offspring. PolyI:C is recognized via Toll-like receptor 3 (TLR3) and is a potent activator of many inflammatory markers, including IL-1, IL-6, TNF-a, and interferons (Fortier et al., 2004b, Traynor et al., 2004; Gilmore et al., 2005). However, it has been shown that among these only maternal IL-6 is necessary and sufficient for the behavioural deficits observed in PolyI:C offspring (Smith et al., 2007). In SCZ, multiple studies have identified elevated levels of IL-6 (Ganguli et al., 1994; Maes et al., 1995; Lin et al., 1998). Heightened IL-6 levels have also been related to the duration of the disorder and treatment resistance, identifying IL-6 as a marker for poor long term outcomes (Ganguli et al., 1994; Lin et al., 1998). Interestingly, IL-6 has been shown both in vitro and in vivo to enhance dopaminergic signalling in the rodent brain (Hama et al., 1991; Zalcman et al., 1994).

Another aspect of the PolyI:C that lends support to its validity as a model is the sensitivity of PolyI:C affected offspring to antipsychotic agents. Several studies have reported that treatment with the antipsychotic agents clozapine, risperidone, or haloperidol during the

adolescence of PolyI:C treated animals prevents the manifestation of behavioural deficits in adulthood (Meyer et al., 2010; Piontkewitz et al., 2012). The beneficial effects of antipsychotics also extend to the structural abnormalities of PolyI:C treated offspring, where both clozapine and risperidone can prevent the enlargement of the lateral ventricles and reduction in hippocampal volumes (Piontkewitz et al., 2012). These beneficial effects may be in part related to inflammatory cytokines like IL-6, as antipsychotic treatment has also been shown to reduce IL-6 and soluble IL-6 receptors in human SCZ patients (Maes et al., 1995; Muller et al., 1997)

One feature of this model that has yet to be explored is whether it also shares the PNN deficit that has been shown in SCZ patient's brains post-mortem. If a PNN deficit is indeed an integral feature to SCZ dysfunction, models that share this pathology would provide an intriguing platform from which to examine PNNs exact role and how they contribute to the disorder. Only one previous study has examined PNN expression in an SCZ model in mice, the neonatal ventral hippocampal lesion model. These animals had reduced numbers of PNNs in the anterior cingulate cortex and displayed disturbed prepulse inhibition as well as potentiated prefrontal cortex responses to ventral tegmental area stimulation (Cabungcal et al., 2014). Interestingly these animals also had increased markers of oxidative stress and adolescent antioxidant treatment reversed both the PNN and behavioural deficits (for review of PNNs, oxidative stress & SCZ, see Do et al., 2015). While few studies have examined PNNs in SCZ models or PolyI:C specifically, several have observed PV+ interneuron disturbances in PolyI:C treated offspring. PolyI:C treatment alone does not appear to have an effect on PV+ development, but when treatment is administered to mutant Disrupted-in-Schizophrenia 1 (DISC1) mice or co-administered along with peripubertal stress PV+ expression is dramatically reduced (Ibi et al., 2010; Giovanoli et al., 2014). Again, while treatment with PolyI:C doesn't

decrease PV+ expression, it has been shown to decrease GAD67 expression on PV+ interneurons, similar to as has been shown in SCZ patients (Dickerson et al., 2014).

1.6 Present Study: Perineuronal Nets in the PolyI:C Model of Schizophrenia

The present study sought to determine whether the PolyI:C model has a deficiency in PNN formation, to identify when this disturbance may occur during development, and to evaluate the integrity of closely-associated PV+ interneurons. Utilizing an animal model of SCZ allowed us to ask several important questions not readily performed in human clinical studies. Firstly, I investigated the temporal profile of PNN and PV+ cell expression to determine if and when PNN and PV+ interneuron deficits emerge during development. To do this, I examined PolyI:C offspring and control treated animals at several developmental time points, including early infancy, adolescence, early adulthood, and as mature adults. These observations are crucial in understanding when anatomical disturbances in PNNs and PV+ interneurons emerge in relation to the manifestation of SCZ-like symptoms in these animals. Secondly, I examined a wide breadth of brain regions relevant to SCZ dysfunction (see Table 1), including the frontal association cortex, prelimbic cortex, reticular thalamic nucleus (RTN), primary auditory cortex, the basolateral amygdala (BLA), as well as both the dorsal and ventral hippocampus. The frontal association cortex is a region of the rodent brain involved in the integration of emotional and contextual information as well as a number of executive functions (Hebb et al., 1945; Nakayama et al., 2015). It is analogous to the human dorsal prefrontal cortex, which has been shown in SCZ to have deficient PNN formation, reduced GAD67 mRNA and protein expression as well as decreased cortical gray matter and dendritic spine density (Rajkowska et al., 1998; Glantz et al., 2000; Guidotti et al., 2000; Gonzalez-Burgos et al., 2010; Curley et al., 2011; Mauney et al., 2013). The medial prelimbic cortex is analogous to the medial prefrontal cortex in the human

brain. In rodents, it is associated with working memory, executive functions, and attentional control (Zahrt et al., 1997; Miner et al., 1997; Passetti et al., 2000). In SCZ patient's brain post-mortem, the medial prefrontal cortex has been shown to have reduced volume but increased cell density and elevated dopamine synthesis (Selemon et al., 1995; Lindström et al., 1999; Pomarol-Clotet et al., 2010). The reticular thalamic nucleus is one of several thalamic nuclei that does not itself send direct projections to the cortex, but rather functions to organize and modulate the activity of other thalamic nuclei (Guillery & Harting, 2003; Ferrarelli & Tononi, 2011). Within the brain, it is entirely composed of GABAergic neurons and has one of the highest PV+ interneuron densities of all brain regions (Cowan et al., 1990; FitzGibbon et al., 2000). In rats, it has been shown that the nucleus is critical to sensorimotor gating and highly sensitive to pharmacological manipulations (Cochran et al., 2003; Krause et al., 2003; Troyano-Rodriguez et al., 2014). While the activity of the reticular thalamic nucleus is difficult to measure in humans, EEG recordings suggest it generates dysfunctional oscillatory activity in SCZ patients (Krause et al., 2003; Ferrarelli et al., 2010). The amygdala is a structure shared between both rodents and humans, and in both is involved in emotional processing, fear, and anxiety (Davis, 1992; Davidson, 2002; Gogolla et al., 2009). In human SCZ patients, there has been reported widespread dysfunction within certain sub-nuclei including total volume reduction, dopamine hyperactivity, and deficits in perineuronal nets (Reynolds, 1983; Lawrie & Abukmeil, 1998; Wright et al., 2000; Pantazopoulos et al., 2010; 2015). The primary auditory cortex is a region of interest to schizophrenia in that the hallucinations SCZ patients experience are primarily auditory in nature (Thomas et al., 2007). While PNNs have not been directly examined in this region, it has been shown that multiple genes encoding for components of PNNs, including CSPGs, are downregulated in SCZ patients (Pietersen et al., 2014). Additionally, genes encoding for

enzymes like ADAMTS-1 and -6 (a disintegrin and mettalopeptidase with thrombrospondin motifs) and MMPs (matrix matelloproteinases) which degrade PNNs and the ECM were heightened within the superior temporal cortex. Other studies of this region have also identified reduced dendritic spine density and reduced pyramidal cell soma size (Sweet et al., 2004; 2009). Lastly, I examined the hippocampus, a structure best known for its role in memory formation and retrieval (Cohen & Eichenbaum, 1993; McClelland et al., 1995; Norman & O'Reilly, 2003). SCZ patients show generalized dysfunction in multiple aspects of memory, including verbal declarative memory, working memory, and processing speed (Saykin et al., 1991; 1994; Heinrichs & Zakzanis, 1998; Dickinson et al., 2004; Neuchterlein et al., 2004). Among these, one of the most consistently impaired functions in SCZ is declarative memory and alterations in declarative memory performance are associated with reductions in hippocampal volume and activity (Saykin et al., 1991; McCarley et al., 1993; Keefe et al., 1997; Stone et al., 1998; Neuchterlein et al., 2004; Weiss et al., 2004; Ranganath et al., 2008;). SCZ patients show both reduced hippocampal volume and activity in conjunction with their declarative memory deficits (Suddath et al., 1989; Bogerts et al., 1990; McCarley et al., 1993; Bilder et al., 1995; Becker et al., 1996; Heckers et al., 1998; Cirillo & Seidman, 2003; Jessen et al., 2003; Weiss et al., 2003; Weiss et al., 2004; Achim et al., 2007). The hippocampus is also a region identified in SCZ patients as having reduced PV+ and GAD67 mRNA expression which may contribute to gamma oscillatory asynchrony observed in electrophysiological recordings from SCZ patients (Gonzalez-Burgos et al., 2010; Heckers & Konradi, 2014)

Table 1. Regions of interest for the present study and their relevance to SCZ.

Brain Region Examined	Associated Functions in Rodents	Human Anatomical Correlate	Known Disturbances in SCZ
Frontal Association Cortex	Executive functions Integration of emotional and contextual information	Dorsal Prefrontal Cortex	**Perineuronal net deficits** Reduced GAD67 protein and mRNA Decreased cortical gray matter volumes Reduced dendritic spine density
Prelimbic Cortex	Working memory Executive functions Attention	Medial Prefrontal Cortex	Volume reduction and dysfunction Increased cell density Elevated dopamine synthesis
Reticular Thalamic Nucleus	Sensorimotor gating	Reticular Thalamic Nucleus	Dysfunctional EEG oscillations
Amygdala	Fear processing Emotional processing	Amygdala	**Perineuronal net deficits** Volume reduction Dopamine hyperactivity
Primary Auditory Cortex	Auditory processing	Superior Temporal Cortex	**PNN related gene dysfunction** Reduced dendritic spine density Reduced pyramidal cell soma size
Dorsal Hippocampus	Memory formation Memory retrieval	Dorsal Hippocampus	**Reduced PV+ and GAD67 mRNA** Reduced volume Decreased neuronal size Disturbed GABA distribution Gamma oscillatory asynchrony
Ventral Hippocampus		Ventral Hippocampus	

Lastly, as PolyI:C treatment induces a maternal inflammatory response I also conducted a preliminary examination of the glial cells of central nervous system throughout the same developmental windows. Both microglia (the immune cells of the brain) and astrocytes have important roles in the formation and maintenance of the extracellular matrix and have been shown to be disturbed in SCZ (Gottschall & Deb, 1996; Maeda & Sobel, 1996; Bayer et al., 1999; Webster et al., 2001; Matute et al., 2005; Faissner et al., 2010; Klausmeyer et al., 2011; Wiese et al., 2012). As such, any disturbances in these systems developmental trajectories might identify a potential target for the mechanism by which PNN malformation occurs (Berretta et al., 2015; Pantazopoulos et al., 2015).

My results suggest that PolyI:C treated offspring have pronounced PNN deficits in the prefrontal cortex that emerge between adolescence and adulthood, during the same window within which behavioural dysfunction has been previously reported. However, several brains regions important to SCZ-related behaviours like the primary auditory cortex did not have deficits. I also find that the basolateral amygdala has reduced PV+ cell density throughout development. A similar trend was observed in the frontal association cortex. Furthermore, PolyI:C treated animals had profound deficits in PV+ cell density in the reticular thalamic nucleus during infancy. A preliminary evaluation of microglia and astrocytes revealed no signs of ongoing inflammatory processes in PolyI:C treated offspring.

2. Methods

2.1 Project Outline. This project was conducted as a collaborative engagement between Dr. Ian Winship at the University of Alberta and Dr. John Howland at the University of Saskatchewan. The outline for this work is described in the following paragraph. Dr. John Howland and his lab carried out methods sections *2.1 – 2.4*, which included housing and rearing of the animals,

induction of PolyI:C treatment, and tissue extraction at appropriate time points. Once extracted, the tissue was shipped to Dr. Winship's lab at the University of Alberta. I was responsible for methods sections *2.4 – 2.10*, which included processing of the tissue, freezing and cryosectioning, all histochemistry and immunohistochemistry, imaging and subsequent analyses of the data. All writing for the final thesis as well as figure preparation was conducted by myself.

2.2 Subjects and Housing. Timed-pregnant Long-Evans rats (n=17) from Charles River Laboratory, Quebec, Canada arrived at the animal holding facility on GD7. Rats were single housed in clear, ventilated plastic cages in a temperature-controlled vivarium. Lighting was controlled automatically on a 12:12 hour cycle with lights on at 7:00 am. All handling and experimentation occurred within the light phase. Food (Purina Rat Chow) and water were available *ad libitum*. All experiments were performed in accordance with the standards of the Canadian Council on Animal Care and were approved by the University of Saskatchewan Animal Research Ethics Board.

2.3 Treatment Procedure. Upon delivery to the animal holding facility, rats were left undisturbed until gestational day 15 (GD 15). Baseline body weight and rectal temperature were recorded (Homeothermic Blanket System, Harvard Instruments, MA, USA). Dams were anesthetised for approximately 6 minutes using isoflurane (5% induction, 3% maintenance) and administered a single tail vein injection of either saline or PolyI:C (4 mg/kg, high molecular weight; InVivoGen, San Diego, CA, USA).

2.4 Follow-up Care of Dams and Pups. Dam body weight and rectal temperature measurements were taken at 8, 24, and 48 hrs post treatment and then left undisturbed to give birth naturally. On postnatal day (PND) 1, pups were weighed, sexed, and culled to a maximum of 10 per litter. Cage changes were scheduled twice per week and were otherwise left undisturbed. Weaning

occurred at PND 21 when pups were placed in same-sex sibling groups of 2 or 3 and received standard care provided by vivarium staff.

2.5 Tissue Collection Procedure. On PND 7, 21, 35, or 90, pups (n= 8-16 per time point) were deeply anesthetised with isoflurane and perfused intracardially with saline followed by 4% paraformaldehyde using infusion pumps. Flow rate and volume of perfusate were adjusted based on pup size. Following perfusion, the brains were carefully extracted and stored in a solution of 4% paraformaldehyde at 4 degrees Celsius. After overnight incubation the brains were transferred to a 30% sucrose solution for several days and then flash frozen in isopentane. Frozen brains were then mounted and sectioned on a cryostat at 25um thickness.

2.6 Immunohistochemistry. Slides were let thaw to room temperature for 20 mins and then given three washes in 1X PBS for 10 mins each. They were then incubated for 1 hour with 10% Protein Block, Serum-Free (Dako, Mississauga, ON) in 1X PBS. After this, slides were incubated overnight at room temperature with a primary antibody in an antibody solution of 1% Protein Block, 1% Bovine Serum Albumin and 98% 1X PBS with 0.1% Triton X-100. The following primary antibodies were used: Wisteria Floribunda Agglutinin (WFA; 1:1000; Vector Labs, Philadelphia, PA), mouse anti-Parvalbumin (1:2000; Swant, Switzerland), rabbit anti-IBA1 (1:200; Dako, Mississauga, ON); and mouse anti-GFAP (1:200; Sigma-Aldrich, Oakville, ON). Slides were washed again three times, twice in 1X PBS with 1% tween-20 and then once in 1X PBS. Sections were then incubated for 1 hour at room temperature with secondary antibodies in antibody solution. Secondary antibodies were as follows: Streptavidin 647 (1:200; Invitrogen, Burlington, ON), donkey anti-mouse Alexa Fluor® 488 (1:200; Molecular Probes, Eugene, OR) and donkey anti-rabbit Alexa Fluor® 647 (1:200; Molecular Probes, Eugene, OR). Slides were

again washed three times, twice in PBS with 1% tween-20 and once in 1X PBS. Slides were mounted with DAPI (4′, 6-diamidino-2-phenylindole in vectashield mounting medium).

2.7 Imaging. Images were captured on a Leica DMI6000B Microscope and processed with LAS AF computer software. All images were captured at 5X magnification over target regions, with a total of 4-6 images taken bilaterally in adjacent sections. Within each region and each cohort a constant gain, exposure, and light intensity were used for all images. Images for insets were captured using a Leica DMI4000 confocal microscope. All confocal images were captured with a 40X objective lens and within each region constant imaging parameters were used for all images.

2.8 Identification of Brain Regions. All brain structures were identified using The Rat Brain in Stereotaxic Coordinates (Paxinos & Watson, 1986) and selected based on their DAPI nuclear staining pattern. The frontal association cortex (region FrA) was identified between Bregma +4.70 mm to +5.20 mm with the imaging area adjusted to the dorsal edge of the slice extending through cortical layers 1-6. The prelimbic cortex (region PrL) was identified between Bregma +3.20 mm to +3.70 mm where the imaging area was centered over the anterior longitudinal sulcus capturing the all layers of the prelimbic cortex bilaterally in a single image. The reticular thalamic nucleus (region Rt) was identified between Bremga -1.88 mm to -2.80 mm beginning just ventral to the fimbria of the hippocampus extending down the entire length of the nucleus. The basolateral nucleus of the amygdala (region BLA) was identified between Bregma -2.12 mm and -2.80 mm based on its teardrop nuclear staining pattern which is also readily identifiable by its parvalbumin staining distribution. The primary auditory cortex (region Au1) was identified between Bregma -4.16 mm and -5.20 mm and selected from the most lateral point of the cortical surface extending upwards. The dorsal hippocampus (regions CA1, CA2, CA3) was identified between Bregma -2.80 mm and -3.30mm and the imaging region beginning at the most lateral

edge of the hippocampus and ending medially towards the dorsal third ventricle. The ventral hippocampus (regions CA1, CA3) was identified between Bregma -4.80 mm and -5.80 mm.

2.9 Quantification. All quantification was completed on unmodified images by an observer blind to the specific experimental conditions of tissue analyzed. Cell counts for DAPI+, IBA+, and PV+ cells were all counted using the Image-based Tool for Counting Nuclei (Centre for Bio-image Informatics, UC Santa Barbara, CA, USA) plugin for NIH ImageJ software. Within a target region, a standard total area was measured over the region of interest within which cells were identified and cell counting parameters kept constant. PNNs were counted manually using the ImageJ Cell Counter function within a standard total area over the target region. For each stain and each region, measurements of mean brightness within the area were also taken. All measurements and counts are the average of 2 images bilaterally from 2 sections (4 total images per animal).

2.10 Statistical Analyses. Statistical analyses were carried out in PRISM Software (Prism Software, Irvine, CA, USA) using two-way ANOVAs with Bonferroni post hoc tests. Significance was set at $p < 0.05$.

3. Results

We examined six different brain regions: the frontal association cortex, the prelimbic cortex, the reticular thalamic nucleus, the amygdala, the dorsal hippocampus (CA1, CA2, & CA3), the ventral hippocampus (CA1 & CA3) and the primary auditory cortex. For each, I measured either total PNN count or WFA staining intensity (where no PNNs were present), PV+ cell density, DAPI+ nuclei density, IBA1+ cell density, and overall GFAP staining intensity.

3.1 Frontal Association Cortex. I examined the frontal association cortex as it is the most anterior cortical structure in the rodent brain and is analogous to the dorsal prefrontal cortex in the human brain. The dorsolateral prefrontal cortex in particular has been shown to be disturbed in SCZ (Rajkowska et al., 1998; Glantz & Lewis, 2000, Guillozet-Bongaarts et al., 2014; Radhu et al., 2015). In both humans and rodents, these regions are thought to be involved in higher order cognitive functions like working memory, attention, and associative learning (Hebb et al., 1945; Nakayama et al., 2015).

Perineuronal Nets. I examined the number of PNNs present within the frontal association cortex throughout all developmental cohorts (Fig. 1). Consistent with previous research in human post mortem tissue, PNNs increased throughout postnatal development. A two-way ANOVA revealed a significant overall effect of age, $F(3,48) = 313.40$, $p < 0.0001$. There was no significant overall effect of treatment condition, $F(1,48) = 2.356$, ns. There was a trend towards a significant interaction between treatment and age, $F(3,48) = 2.470$, $p = 0.073$. Post hoc comparisons indicated that there was a significant difference between PolyI:C treated offspring and controls at PND90, SAL (M=139.85 ± 3.19) vs. POL (M=120.39 ± 6.20), $t = 3.098$, $p < 0.05$. There were no significant differences between other cohorts.

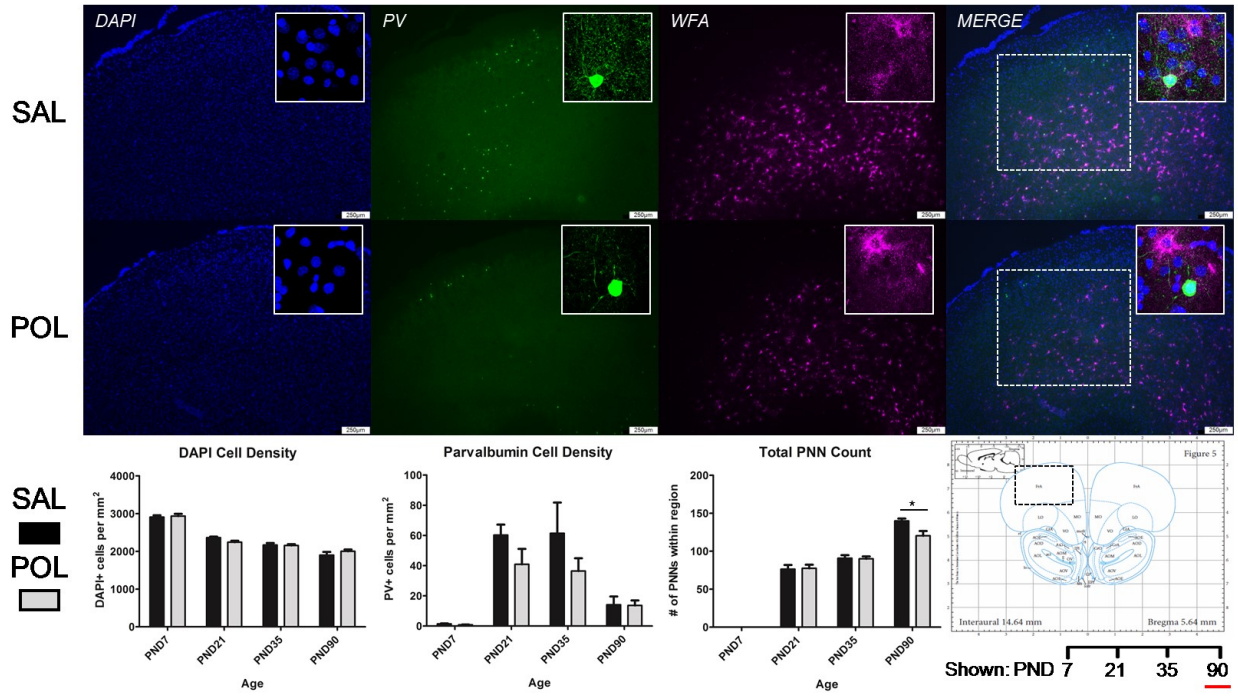

Figure 1. Perineuronal nets stained with WFA and parvalbumin interneurons in the frontal association cortex (postnatal day 90 shown). Across both conditions the total number of DAPI labelled nuclei decreased throughout postnatal development (main effect of Age, $p < 0.0001$). PV+ interneurons increased from PND7 to PND21 before declining at PND90 (main effect of Age, $p < 0.0001$). There was a trend towards a significant overall effect of treatment on PV+ cell density (main effect of Treatment, $p = 0.0596$). The number of perineuronal nets increased throughout postnatal development in the frontal association cortex (main effect of Age, $p < 0.0001$). A significant deficit in the total number of perineuronal nets emerged in PolyI:C treated offspring as compared to saline in the PND90 cohort ($p < 0.05$). The frontal association cortex was identified using The Rat Brain in Stereotaxic Coordinates (Paxinos & Watson, 1986) as region FrA, between Bregma +4.70 mm to +5.20 mm. Black bars represent Saline treated offspring, light grey bars PolyI:C treated offspring. Insets are representative images from each condition. Scale bar represents 250 μm. *p<0.05, 2X2 ANOVA followed by *post hoc* Bonferroni t-tests. Data is mean ± SEM.

Parvalbumin Interneurons. Next I evaluated the number of PV+ interneurons within the same region across all cohorts. The density of PV+ interneurons increased from infancy into childhood, surprisingly however PV+ interneuron density decreased into adulthood. A two-way ANOVA revealed a significant effect of age $F(3,48) = 18.15$, $p < 0.0001$. There was a trend towards a main effect of treatment, $F(1,48) = 3.72$, $p = 0.0596$. There was no significant interaction between treatment and age, $F(3,48) = 1.17$, ns. There were no significant differences between treatment groups at any of the developmental ages.

DAPI Nuclear Stain. Counts of the total number of DAPI+ positive cells were assessed using an automated counter. A two-way ANOVA revealed a significant effect of age, $F(3,47) = 134.90$, $p < 0.0001$. There was no significant effect of treatment, $F(1,47) = 0.001$, ns. There was no interaction between treatment and age, $F(3,47) = 1.66$, ns. There were no significant differences between treatment groups at any of the developmental ages.

Microglia. Counts of the total number of microglia were assessed using an automated counter of IBA1+ cells (Fig. 2). A two-way ANOVA revealed a significant effect of age, $F(3,48) = 53.13$, $p < 0.0001$. Microglial density peaked during childhood before decreasing and plateauing into maturity. There was no significant effect of treatment, $F(1,48) = 0.70$, ns. There was no interaction between treatment and age, $F(3,48) = 1.47$, ns.

Astrocytes. To assess the degree of astrocytic activity throughout development, I examined the optical density of GFAP staining within regions of measure. A two-way ANOVA revealed a significant effect of age, $F(3,48) = 31.39$, $p < 0.0001$. There was no significant effect of treatment, $F(1,48) = 2.11$, ns. There was no interaction between treatment and age, $F(3,48) = 0.16$, ns.. GFAP immunoreactivity was sparsely present in infancy and childhood, but increased during adolescence.

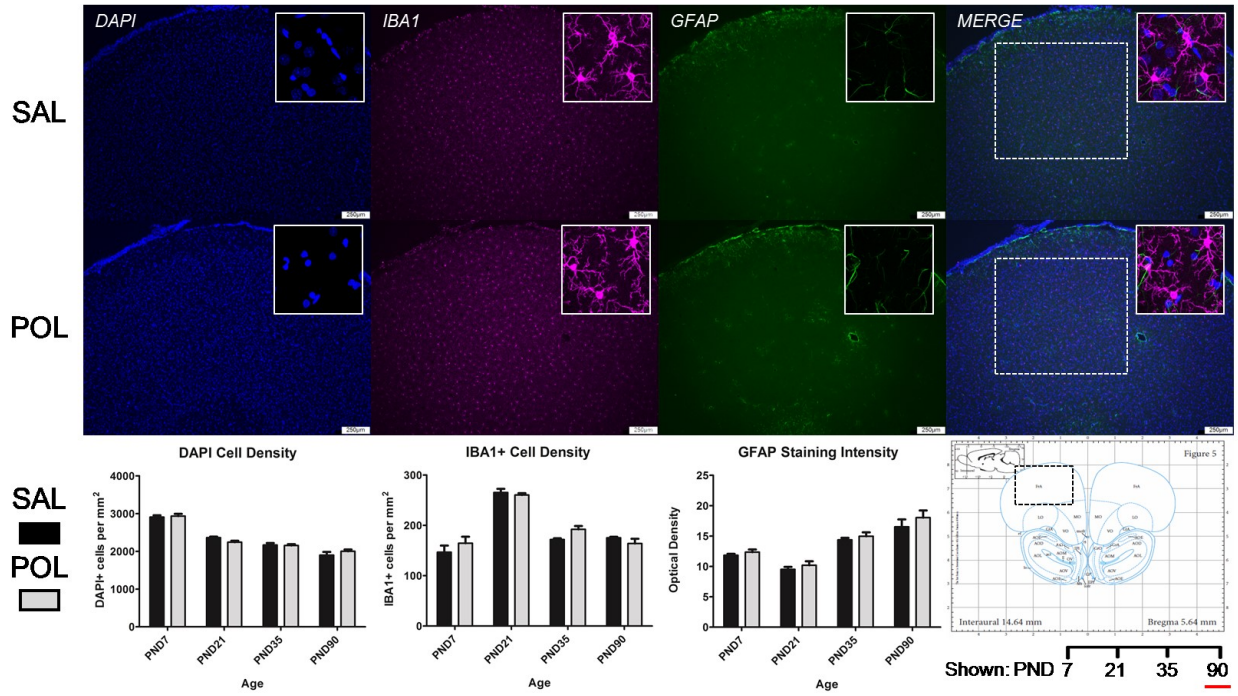

Figure 2. Microglia stained with IBA1 and astrocytes with GFAP in the frontal association cortex (postnatal day 90 shown). Across both conditions the total number of DAPI labelled nuclei decreased throughout postnatal development (main effect of Age, $p < 0.0001$). Microglial density was relatively stable throughout development aside from a dramatic increase in the PND21 cohort (main effect of Age, $p < 0.0001$). GFAP staining was sparsely present within the cortical parenchyma, instead clustering around the cortical surface and blood vessels throughout the tissue. Overall, GFAP staining intensity increased throughout postnatal development (main effect of Age, $p < 0.0001$). Neither PolyI:C treated animals or controls showed significant differences between either of these immune markers. The frontal association cortex was identified using The Rat Brain in Stereotaxic Coordinates (Paxinos & Watson, 1986) as region FrA, between Bregma +4.70 mm to +5.20 mm. Black bars represent Saline treated offspring, light grey bars PolyI:C treated offspring. Insets are representative images from each condition. Scale bar represents 250 μm. *p<0.05, 2X2 ANOVA followed by *post hoc* Bonferroni t-tests. Data is mean ± SEM.

3.2 Prelimbic Cortex. I targeted the prelimbic cortex as it is analogous to the medial prefrontal cortex in humans and these structures have functional similarities relevant to schizophrenia, including fear responses, information processing and sensorimotor gating (Zahrt et al., 1997; Miner et al., 1997; Passetti et al., 2000; Burrell & Brown, 2000). It is also an area that has shown to be anatomically disturbed in SCZ and contains high concentrations of dopamine receptors involved in SCZ (Selemon et al., 1995; Lindström et al., 1999; Pomarol-Clotet et al., 2010).

Perineuronal Nets. I examined the number of PNNs present within the frontal association cortex throughout all developmental cohorts (Fig. 3). The number of PNNs increased during the transition from infancy to childhood and from early adolescence into adulthood. There was a significant effect of age, $F(3,48) = 539.40$, $p < 0.0001$. There was a trend towards a significant effect of treatment, $F(1,48) = 3.34$, $p = 0.074$. There was a significant interaction between treatment and age, $F(3,48) = 12.91$, $p < 0.0001$. Post hoc comparisons indicated that there was a significant difference between PolyI:C treated offspring and controls at PND90, SAL (M=68.20 ± 2.41) vs. POL (M=55.00 ± 1.11), $t = 5.986$, $p < 0.0001$. There were no significant differences between treatment groups at any other ages.

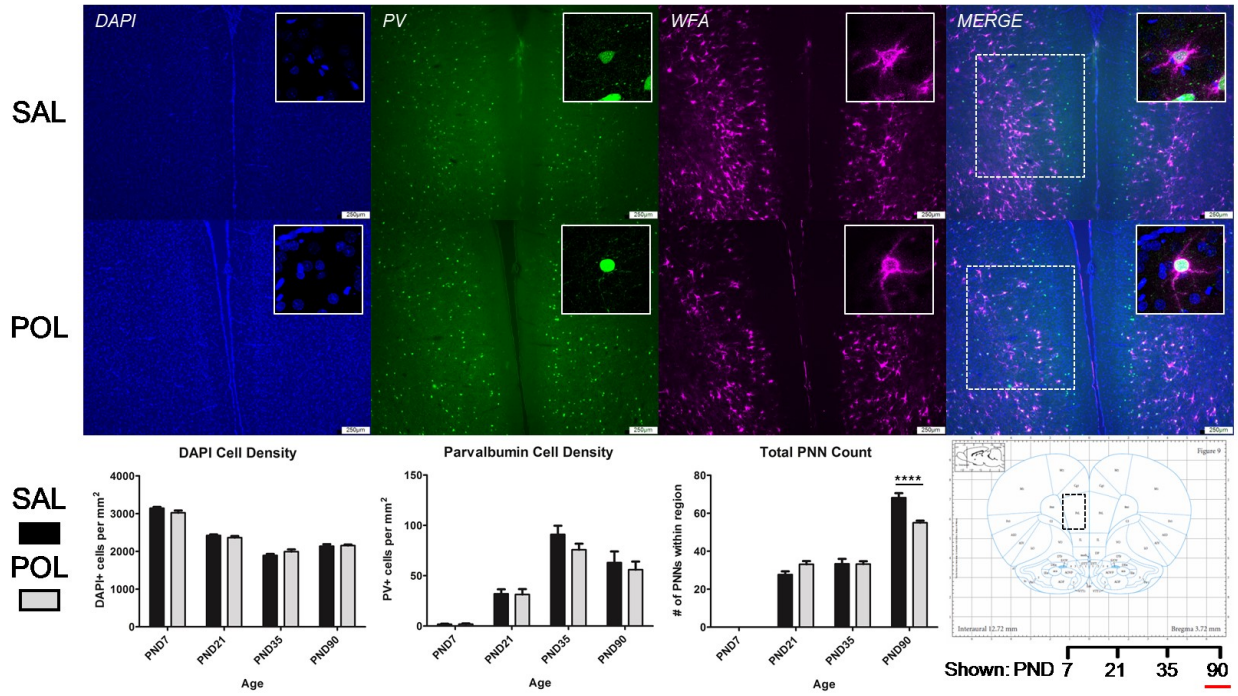

Figure 3. Perineuronal nets stained with WFA and parvalbumin interneurons in the prelimbic cortex (postnatal day 90 shown). Across both conditions the total number of DAPI labelled nuclei decreased throughout postnatal development before plateauing in the PND35 and 90 cohorts (main effect of Age, $p < 0.0001$). PV+ interneurons increased from PND7 to PND35 before declining at PND90 (main effect of Age, $p < 0.0001$). The number of perineuronal nets increased throughout postnatal development with the greatest increases occurring from PND7 to 21, and PND35 to 90 (main effect of Age, $p < 0.0001$; Age x Treatment, $p < 0.0001$; Treatment, $p = 0.074$). In the PND90 cohort, a significant deficit emerged in PolyI:C treated animals as compared to saline treated in total number of PNNs ($p < 0.0001$). The prelimbic cortex was identified using The Rat Brain in Stereotaxic Coordinates (Paxinos & Watson, 1986) as region PrL, between Bregma +3.20 mm to +3.70 mm. Black bars represent Saline treated offspring, light grey bars PolyI:C treated offspring. Insets are representative images from each condition. Scale bar represents 250 µm. ****p<0.0001, 2X2 ANOVA followed by *post hoc* Bonferroni t-tests. Data is mean ± SEM.

Parvalbumin Interneurons. Next I evaluated the density of PV+ interneurons within the same region across all cohorts. A two-way ANOVA revealed a significant effect of age, $F(3,46) = 55.67$, $p < 0.0001$. PV+ counts increased during childhood and adolescence before decreasing in adulthood. There was no significant effect of treatment condition, $F(1,46) = 1.44$, ns. There was no significant interaction between treatment and age, $F(3,46) = 0.572$, ns.

DAPI Nuclear Stain. The density of DAPI+ positive cells were assessed using an automated counter. A two-way ANOVA revealed a significant effect of age, $F(1,47) = 200.80$, ns. DAPI+ cells decreased from infancy into early adolescence before plateauing into adulthood. There was no significant effect of treatment, $F(1,47) = 0.19$, ns. There was no interaction between treatment and age, $F(3,47) = 1.80$, ns.

Microglia. Cellular density of microglia were assessed using an automated counter of IBA1+ cells (Fig. 4). A two-way ANOVA revealed a significant effect of age, $F(3,49) = 70.55$, $p < 0.0001$. Microglia density increased during childhood before it plateaued into maturity. There was no significant effect of treatment, $F(1,49) = 1.51$, ns. There was an interaction between treatment and age, $F(3,49) = 3.33$, $p < 0.05$. There were no significant differences between treatment groups at any developmental age.

Astrocytes. To assess the degree of astrocytic activity throughout development, I examined the optical density of GFAP staining within regions of measure. A two-way ANOVA revealed a significant effect of age, $F(3,49) = 31.07$, $p < 0.0001$. GFAP immunoreactivity was sparsely present in infancy and childhood, but increased during adolescence. There was no significant effect of treatment, $F(1,49) = 0.06$, ns. There was no interaction between treatment and age, $F(3,49) = 0.71$, ns.

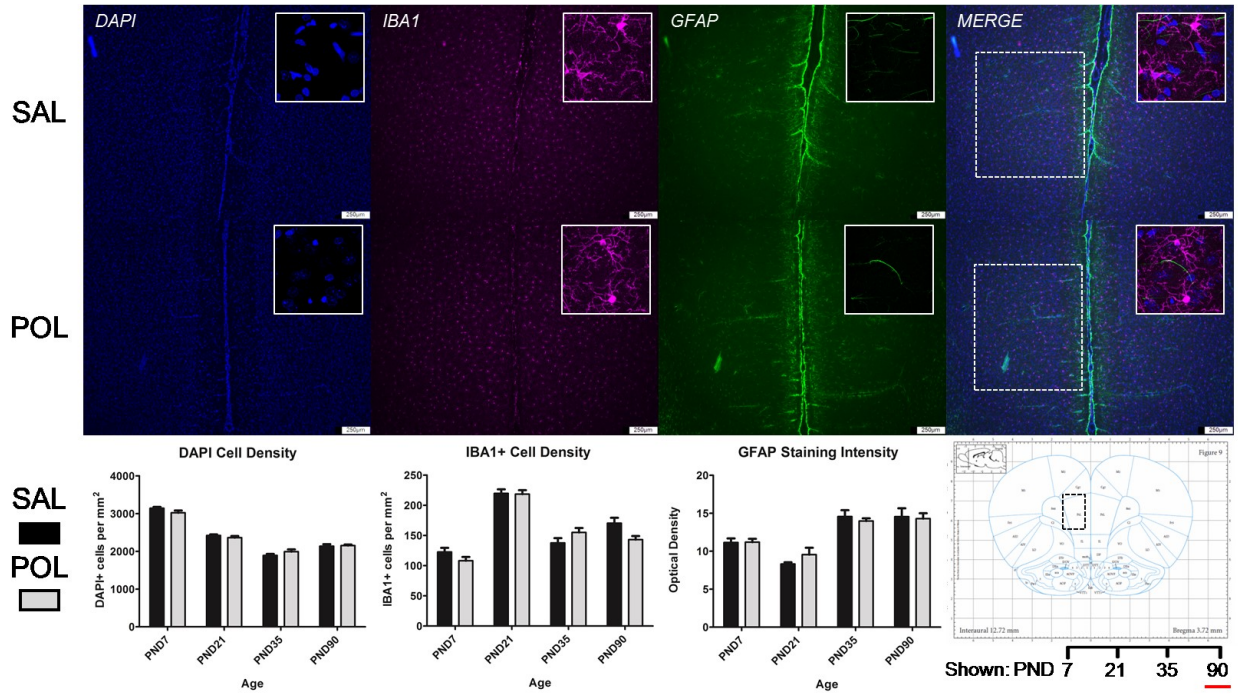

Figure 4. Microglia stained with IBA1 and astrocytes with GFAP in the prelimbic cortex (postnatal day 90 shown). Across both conditions the total number of DAPI labelled nuclei decreased throughout postnatal development (main effect of Age, $p < 0.0001$). Microglial density was increased slightly throughout postnatal development aside from a dramatic spike in density in the PND21 cohort (main effect of Age, $p < 0.001$; Age x Treatment, $p < 0.05$). GFAP staining was sparsely present within the cortical parenchyma, instead clustering around the cortical surface and blood vessels throughout the tissue. GFAP staining intensity increased from PND21 to PND35 where it leveled off into maturity (main effect of Age, $p < 0.0001$). Neither PolyI:C treated animals or controls showed significant differences between either of these immune markers. The prelimbic cortex was identified using The Rat Brain in Stereotaxic Coordinates (Paxinos & Watson, 1986) as region PrL, between Bregma +3.20 mm to +3.70 mm. Black bars represent Saline treated offspring, light grey bars PolyI:C treated offspring. Insets are representative images from each condition. Scale bar represents 250 µm. *p<0.05, 2X2 ANOVA followed by *post hoc* Bonferroni t-tests. Data is mean ± SEM.

3.3 Reticular Thalamic Nucleus. The thalamus is a critical sensory integration centre that is shared between rodents and humans. This reticular thalamic nucleus in particular is of interest to schizophrenia as serves to modulate the function of all other thalamic nuclei and has a topographical sensory distribution (Ferrarrelli & Tononi, 2010; Pratt & Morris, 2015). This area has both an extremely high density of PV+ interneurons which are disturbed in SCZ and highly expresses the DISC1 gene throughout development.

Perineuronal Nets. Within the reticular thalamic nucleus no distinguishable PNNs were identifiable, but rather a diffuse or reticular WFA staining pattern (Fig. 5). As such I measured the optical density within the region rather than PNN counts. A two-way ANOVA of WFA optical density revealed a significant effect of age, $F(3,46) = 80.01$, $p < 0.0001$. WFA staining intensity increased throughout postnatal development. There was no effect of treatment condition, $F(1,46) = 0.14$, ns. There was no interaction between treatment and age, $F(3,46) = 1.10$, ns.

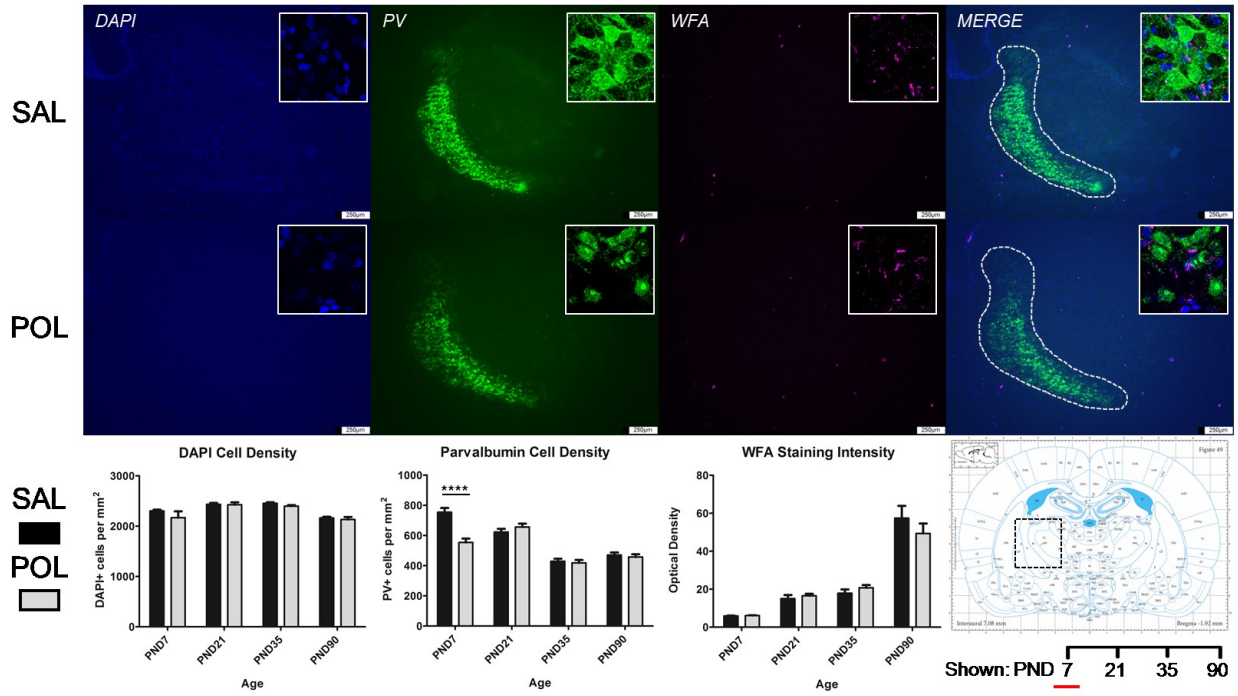

Figure 5. Parvalbumin interneurons and WFA immunoreactivity in the reticular thalamic nucleus (postnatal day 7 shown). In contrast to many other regions, DAPI cell density in the RTN was relatively stable but density was highest during PND21 and PND35 before decreasing at PND90 (main effect of Age, $p < 0.0001$). Across all brain regions, only the RTN had PV+ cells as early as PND7. I observed a significant reduction in PV+ cell density in the PND7 cohort of PolyI:C treated offspring as compared to controls ($p < 0.0001$). Overall, PV+ cell density decreased throughout postnatal development (main effect of Age, $p < 0.0001$; Treatment, $p < 0.01$; Age x Treatment, $p < 0.0001$). While no distinguishable PNNs were present within the RTN, there was an intense WFA staining pattern that emerged at PND21 and saw a dramatic increase at PND90 (main effect of Age, $p < 0.0001$). As such, rather than count PNNs I measured overall WFA staining intensity of the RTN but there were no differences between PolyI:C and saline treated offspring. The reticular thalamic nucleus was identified using The Rat Brain in Stereotaxic Coordinates (Paxinos & Watson, 1986) as region Rt, between Bregma -1.88 mm to -2.80 mm. Black bars represent Saline treated offspring, light grey bars PolyI:C treated offspring. Insets are representative images from each condition. Scale bar represents 250 μm. ****$p<0.0001$, 2X2 ANOVA followed by *post hoc* Bonferroni t-tests. Data is mean ± SEM.

Parvalbumin Interneurons. Next I evaluated the density of PV+ interneurons within the same region across all cohorts. A two-way ANOVA revealed an overall significant effect of age, $F(3,46) = 51.22$, $p < 0.0001$. PV+ density in the reticular thalamic nucleus decreased throughout postnatal development. There was a significant effect of treatment, $F(1,46) = 8.42$, $p < 0.01$. There was also a significant interaction between treatment and age, $F(3,46) = 10.63$, $p < 0.0001$. Post hoc comparisons showed that there was a significant difference between PolyI:C treated animals and saline animals in the PND7 cohort, SAL (M= 754.29 ± 27.79) vs. POL (M= 553.81 ± 23.38), $t = 6.36$, $p <$ 0.0001. There were no significant differences between treatment groups at any of the developmental ages.

DAPI Nuclear Stain. Cellular density of DAPI+ positive cells were assessed using an automated counter. A two-way ANOVA revealed a significant effect of age, $F(3,45) = 10.92$, $p < 0.0001$. There was no significant effect of treatment, $F(1,46) = 1.74$, ns. There was no interaction between treatment and age, $F(3,46) = 0.44$, ns.

Microglia. Microglial cell density was assessed using an automated counter of IBA1+ cells (Fig. 6). A two-way ANOVA revealed a significant effect of treatment, $F(3,48) = 52.64$, $p < 0.0001$. Microglial density peaked during childhood before decreasing into maturity. There was no significant effect of treatment, $F(3,48) = 2.00$, ns. There was no interaction between treatment and age, $F(3,46) = 0.52$, ns.

Astrocytes. To assess the degree of astrocytic activity throughout development, I examined the optical density of GFAP staining. A two-way ANOVA revealed a significant overall effect of age, $F(3,48) = 35.32$, $p < 0.0001$. GFAP immunoreactivity increased throughout postnatal development. There was no significant effect of treatment, $F(1,48) = 0.83$, ns. There was no interaction between treatment and age, $F(3,48) = 0.99$, ns.

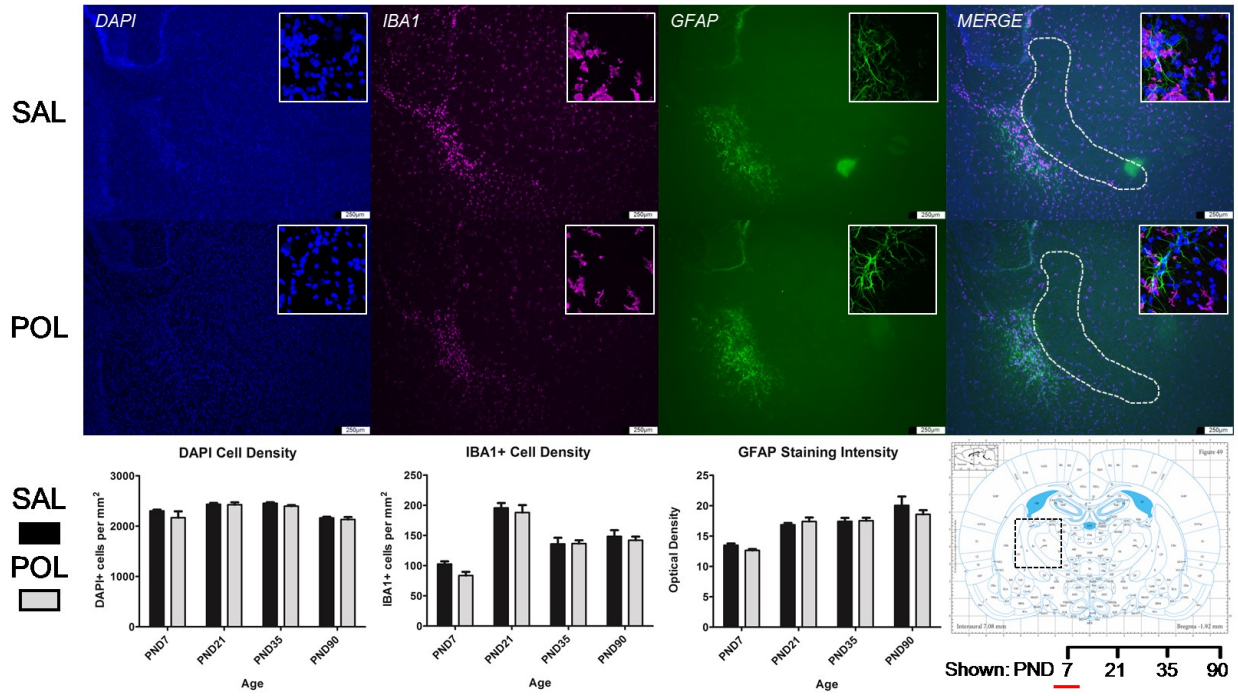

Figure 6. Microglia stained with IBA1 and astrocytes with GFAP in the reticular thalamic nucleus (postnatal day 7 shown). In contrast to many other regions, DAPI cell density in the RTN was relatively stable but density was highest during PND21 and PND35 before decreasing at PND90 (main effect of Age, $p < 0.0001$). Overall, microglial density increased throughout postnatal development with a massive spike in the PND21 cohort (main effect of Age, $p < 0.0001$). GFAP staining was sparsely present at PND7 but increased steadily throughout postnatal development (main effect of Age, $p < 0.0001$). Neither PolyI:C treated animals or controls showed significant differences between either of these immune markers. The reticular thalamic nucleus was identified using The Rat Brain in Stereotaxic Coordinates (Paxinos & Watson, 1986) as region Rt, between Bregma -1.88 mm to -2.80 mm. Black bars represent Saline treated offspring, light grey bars PolyI:C treated offspring. Insets are representative images from each condition. Scale bar represents 250 μm. *p<0.05, 2X2 ANOVA followed by *post hoc* Bonferroni t-tests. Data is mean ± SEM.

3.4 Basolateral Amygdala. This nucleus of the amygdala is shared anatomically between both rodents and humans. It has been associated with fear processing and learning, as well as emotionality (Davis, 1992; Davidson, 2002; Gogolla et al., 2009). Importantly, the basolateral amygdala has been shown to have projections to the frontal association cortex in rodents which contribute to associative learning in fear-associated tasks (Nakayama et al., 2015). The basolateral amygdala has also been shown to have deficits in PNNs in SCZ patient's brains post-mortem (Pantazopoulos et al., 2010; 2015).

Perineuronal Nets. I examined the total number of PNNs present within the basolateral amygdala (Fig. 7). A two-way ANOVA revealed a significant effect of age of the number of PNNs, $F(3,43) = 74.47$, $p < 0.0001$. The number of PNNs in the basolateral amygdala increased from infancy to childhood where it plateaued into maturity. There was no significant effect of treatment, $F(1,43) = 1.27$, ns. There was no interaction between treatment and age, $F(3,43) = 1.15$, ns.

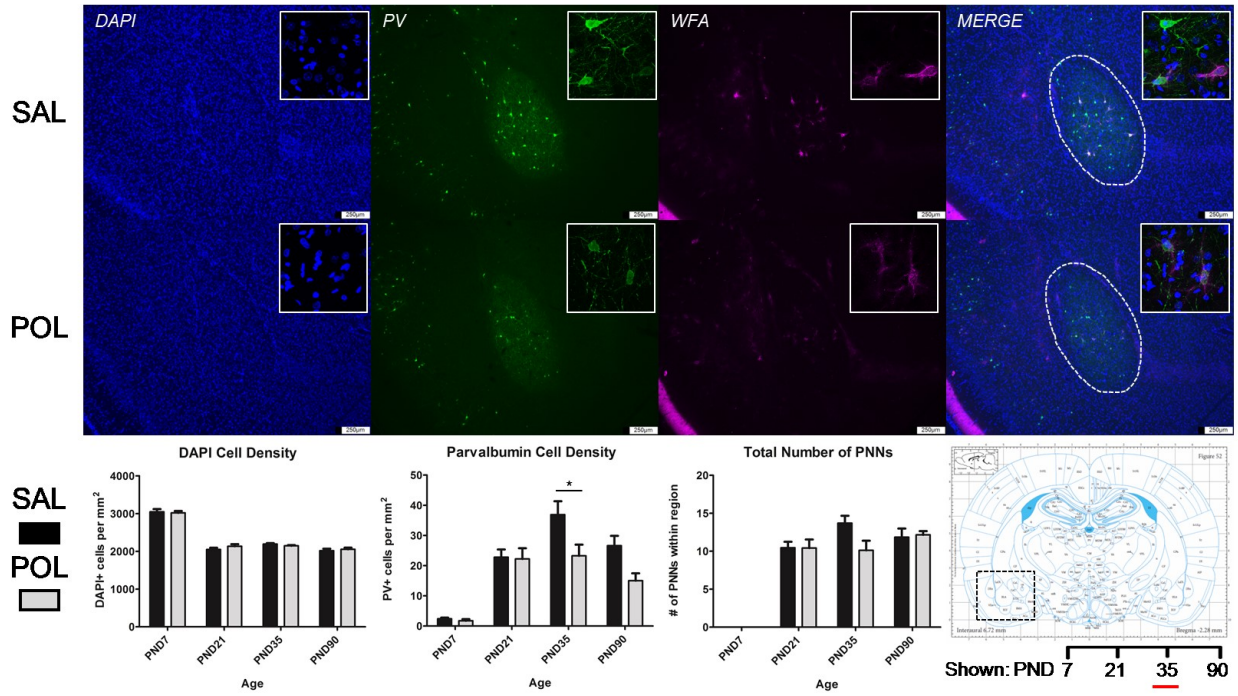

Figure 7. Perineuronal nets stained with WFA and parvalbumin interneurons in the basolateral amygdala (postnatal day 35 shown). DAPI cell density decreased from PND7 to PND21 where it stabilized into maturity (main effect of Age, $p < 0.0001$). PV+ cells were absent at PND7 but increased steadily till PND35 at which point they decreased at PND90 (main effect of Age, $p < 0.0001$). Across development, I observed a significant reduction of PV+ interneuron density in PolyI:C treated offspring (main effect of Treatment, $p < 0.01$; Age x Treatment, $p = 0.080$). This deficit in PolyI:C treated offspring was most pronounced in the PND35 cohort ($p < 0.05$). PNNs were absent in the PND7 cohort before forming at PND21 (main effect of Age, $p < 0.0001$). There was a slight but not significant reduction in PNN number in the PND35 cohort that might reflect the association of PNNs with PV+ interneurons which were reduced within this developmental period. The basolateral amygdala was identified using The Rat Brain in Stereotaxic Coordinates (Paxinos & Watson, 1986) as region BLA, between Bregma -2.12 mm to -2.80 mm. Black bars represent Saline treated offspring, light grey bars PolyI:C treated offspring. Insets are representative images from each condition. Scale bar represents 250 μm. *p<0.05, 2X2 ANOVA followed by *post hoc* Bonferroni t-tests. Data is mean ± SEM.

Parvalbumin Interneurons. Next I evaluated the density of PV+ interneurons within the same region across all cohorts. A two-way ANOVA revealed an effect of age on PV+ cell density within the basolateral amygdala, $F(3,45) = 33.72$, $p < 0.0001$. There was also a significant effect of treatment, $F(1,45) = 8.43$, $p < 0.01$. There was no interaction between treatment and age, $F(3,45) = 2.40$, $p = 0.080$. Post hoc comparisons revealed that there was a significant reduction in PV+ cell density at PND35, SAL (M= 26.61 ± 3.27) vs. POL (M= 16.89 ± 1.82), $t = 3.106$, $p < 0.05$. There were no significant differences between treatment groups at any of the developmental ages. Overall, PV+ cell density increased from infancy to childhood before decreasing slightly as adults. Within the PND35 cohort PolyI:C treated animals had a significantly reduced PV+ cell density.

DAPI Nuclear Stain. The density of DAPI+ positive cells was assessed using an automated counter. A two-way ANOVA revealed a significant effect of age, $F(3,45) = 204.70$, $p < 0.0001$. DAPI+ cell density decreased from infancy into adulthood. There was no significant effect of treatment, $F(1,45) = 0.11$, ns. There was no interaction between treatment and age, $F(3,45) = 0.76$, ns.

Microglia. Counts of the total number of microglia were assessed using an automated counter of IBA1+ cells (Fig. 8). A two-way ANOVA revealed a significant effect of age, $F(3,46) = 20.77$, $p < 0.0001$. Microglia density increased from infancy to early adolescence where it peaked before decreasing slightly into adulthood. There was no significant effect of treatment, $F(1,46) = 1.19$, ns. There was no interaction between treatment and age, $F(3,46) = 1.22$, ns.

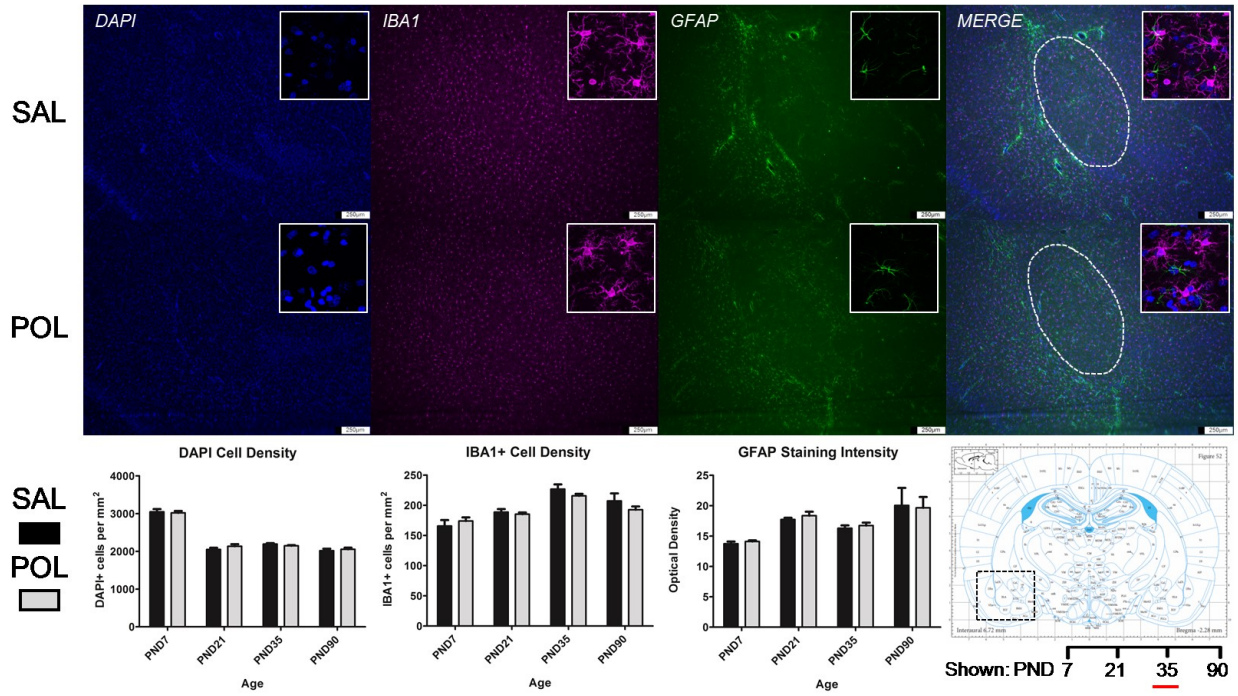

Figure 8. Microglia stained with IBA1 and astrocytes with GFAP in the basolateral amygdala (postnatal day 35 shown). DAPI cell density decreased from PND7 to PND21 where it stabilized into maturity (main effect of Age, $p < 0.0001$). Microglia density as labelled with IBA1 increase from PND7 to PND35 before dropping off slightly in PND90 (main effect of Age, $p < 0.0001$). Overall, GFAP staining intensity increased throughout postnatal development (main effect of Age, $p < 0.0001$). Neither PolyI:C treated animals or controls showed significant differences between either of these immune markers. The basolateral amygdala was identified using The Rat Brain in Stereotaxic Coordinates (Paxinos & Watson, 1986) as region BLA, between Bregma -2.12 mm to -2.80 mm. Black bars = Saline treated offspring, light grey bars = PolyI:C treated offspring. Insets are representative images from each condition. Scale bar represents 250 μm. *p<0.05, 2X2 ANOVA followed by *post hoc* Bonferroni t-tests. Data is mean ± SEM.

Astrocytes. To assess the degree of astrocytic activity throughout development, I examined the optical density of GFAP staining. A two-way ANOVA revealed a significant effect of age, $F(3,46) = 8.77$, $p = 0.0001$. Overall, GFAP immunoreactivity increased throughout postnatal development, with a slight dip during early adolescence. There was no significant effect of treatment, $F(1,46) = 0.09$, ns. There was no interaction between treatment and age, $F(3,46) = 0.07$, ns.

3.5 Dorsal Hippocampus: CA1 Region.

Perineuronal Nets. I examined the total number of PNNs present within the CA1 region of the dorsal hippocampus (Fig. 9). A two-way ANOVA revealed a significant effect of age on the number of PNNs, $F(3,45) = 7.88$, $p < 0.0001$. No PNNs were present in the PND7 cohort but appeared in there PND21 animals and persisted into maturity. There was no significant effect of treatment, $F(1,45) = 0.17$, ns. There was no interaction between treatment and age, $F(3,45) = 1.62$, ns.

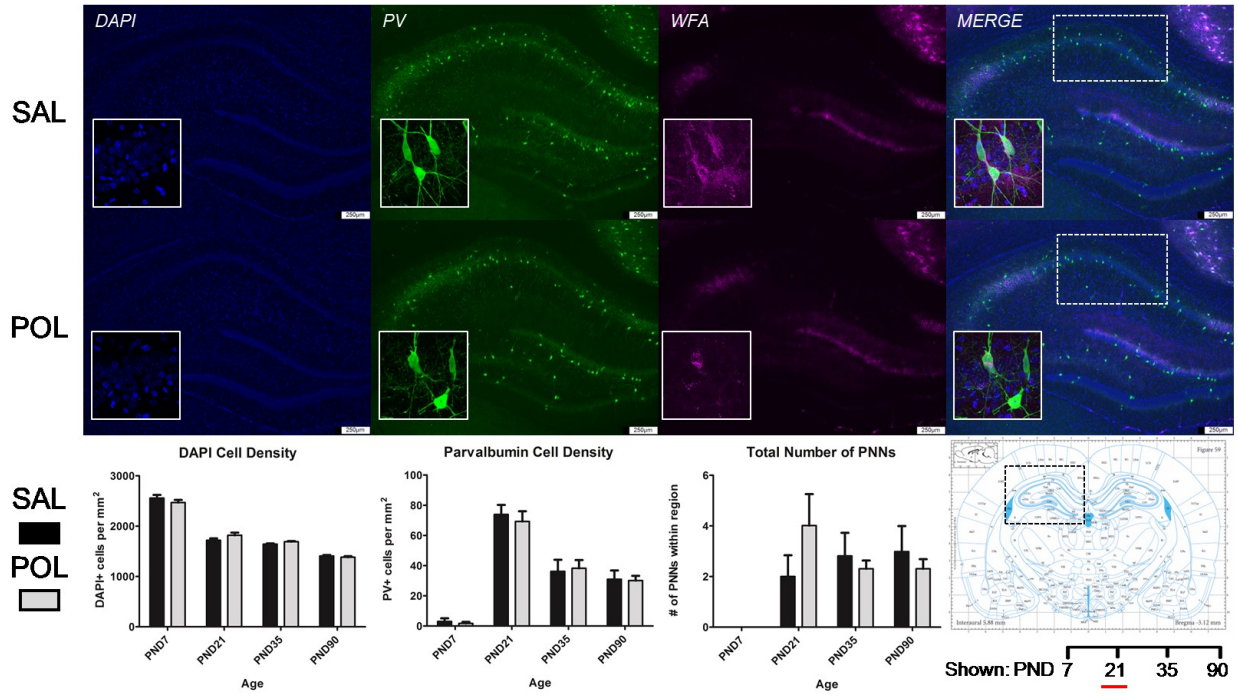

Figure 9. Perineuronal nets stained with WFA and parvalbumin interneurons in the CA1 region of the dorsal hippocampus (postnatal day 21 shown). DAPI cell density decreased across all developmental cohorts (main effect of Age, $p < 0.0001$). PV+ cell density peaked at PND21 before decreasing into maturity (main effect of Age, $p < 0.0001$). PNNs were absent at PND7 but appeared in the PND21 cohort and stabilized during adolescence into adulthood (main effect of Age, $p < 0.001$). The CA1 region of the dorsal hippocampus was identified using The Rat Brain in Stereotaxic Coordinates (Paxinos & Watson, 1986) as region CA1, between Bregma -2.80 mm to -3.30 mm. Black bars represent Saline treated offspring, light grey bars PolyI:C treated offspring. Insets are representative images from each condition. Scale bar represents 250 μm. *p<0.05, 2X2 ANOVA followed by *post hoc* Bonferroni t-tests. Data is mean ± SEM

Parvalbumin Interneurons. Next I evaluated the density of PV+ interneurons within the same region across all cohorts. A two-way ANOVA revealed an effect of age on PV+ cell density within CA1, $F(3,45) = 61.64$, $p < 0.0001$. There was no significant effect of treatment, $F(1,45) = 0.08$, ns. There was no interaction between treatment and age, $F(3,45) = 0.136$, ns. Overall, PV+ cell density was greatest in the PND21 cohort before decreasing at both PND35 and PND90.

DAPI Nuclear Stain. The density of DAPI+ positive cells was assessed using an automated counter. A two-way ANOVA revealed a significant effect of age, $F(3,45) = 286.7$, $p < 0.0001$. DAPI+ cell density decreased from infancy into adulthood. There was no significant effect of treatment, $F(1,45) = 0.10$, ns. There was no interaction between treatment and age, $F(3,45) = 2.14$, ns.

Microglia. Counts of the total number of microglia were assessed using an automated counter of IBA1+ cells (Fig. 10). A two-way ANOVA revealed a significant effect of age, $F(3,48) = 37.21$, $p < 0.0001$. Microglia density decreased across all developmental cohorts. There was no significant effect of treatment, $F(1,48) = 0.07$, ns. There was no interaction between treatment and age, $F(3,48) = 1.347$, ns.

Astrocytes. To assess the degree of astrocytic activity throughout development, I examined the optical density of GFAP staining. A two-way ANOVA revealed a significant effect of age, $F(3,48) = 18.61$, $p < 0.0001$. GFAP immunoreactivity increased from PND7 to PND21 before declining slightly into maturity. There was no significant effect of treatment, $F(1,48) = 0.109$, ns. There was however an interaction between treatment and age, $F(3,48) = 3.31$, $p < 0.05$. There were no significant differences between treatment groups at any of the developmental ages.

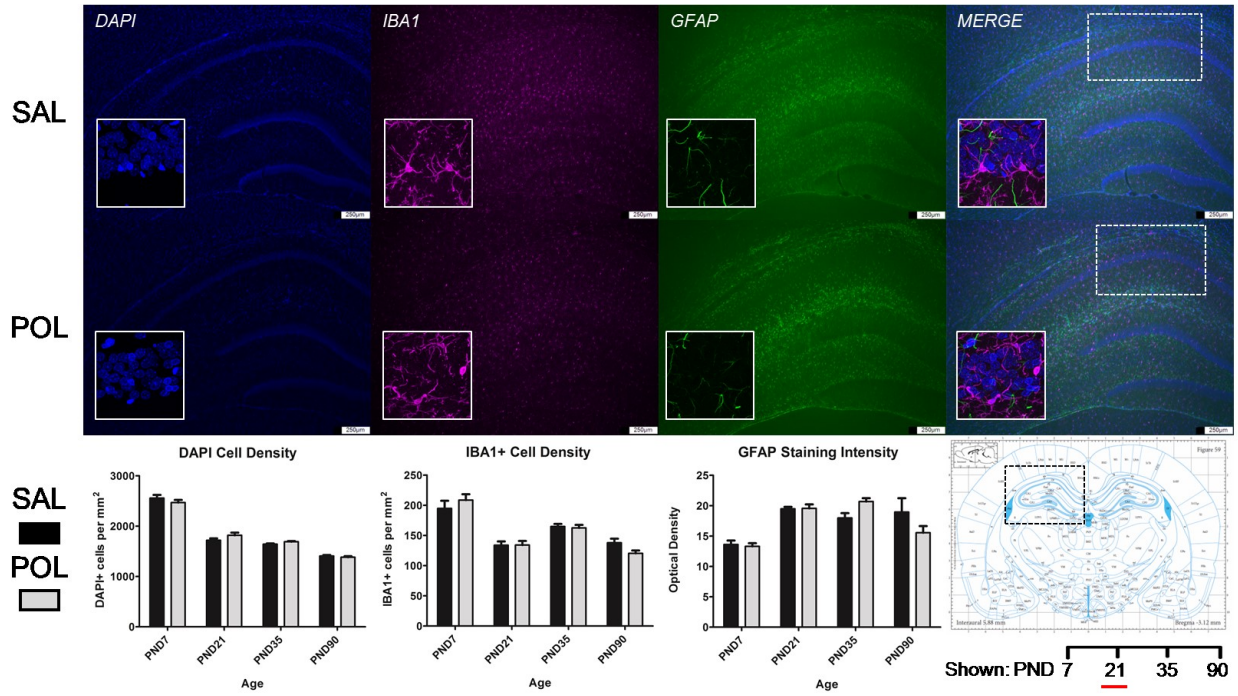

Figure 10. Microglia stained with IBA1 and astrocytes with GFAP in the CA1 region of the dorsal hippocampus (postnatal day 21 shown). DAPI cell density decreased across all developmental cohorts (main effect of Age, $p < 0.0001$). Microglial density as labelled with IBA1 was highest during the PND7 and PND35 with slight reductions in the PND21 and 90 cohorts (main effect of Age, $p < 0.0001$). GFAP increased steadily from PND7 to PND21 before dropping off slightly at PND90 (main effect of Age, $p < 0.0001$; Age x Treatment, $p < 0.05$). Neither PolyI:C treated animals or controls showed significant differences between either of these immune markers. The CA1 region of the dorsal hippocampus was identified using The Rat Brain in Stereotaxic Coordinates (Paxinos & Watson, 1986) as region CA1, between Bregma -2.80 mm to -3.30 mm. Black bars represent Saline treated offspring, light grey bars PolyI:C treated offspring. Insets are representative images from each condition. Scale bar represents 250 μm. *p<0.05, 2X2 ANOVA followed by *post hoc* Bonferroni t-tests. Data is mean ± SEM.

3.6 Dorsal Hippocampus: CA3 Region.

Perineuronal Nets. Within the CA3 region no PNNs were present. Instead, WFA staining appeared to label a dense staining pattern similar to that of the reticular thalamic nucleus (Fig. 11). As such, I measured the optical density of WFA staining within the area rather than PNN counts. A two-way ANOVA revealed a significant effect of age on the number of WFA optical density, $F(3,44) = 27.64$, $p < 0.0001$. There was no significant effect of treatment, $F(1,44) = 0.02$, ns. There was however an interaction between treatment and age, $F(3,44) = 4.66$, $p < 0.01$. Post hoc comparisons revealed a significant difference between PolyI:C and saline treated offspring in the PND90 cohort, SAL ($M = 12.79 \pm 1.92$) vs. POL ($M = 9.37 \pm 0.44$), $t = 3.13$, $p < 0.05$. There were no significant differences between treatment groups at any other developmental age.

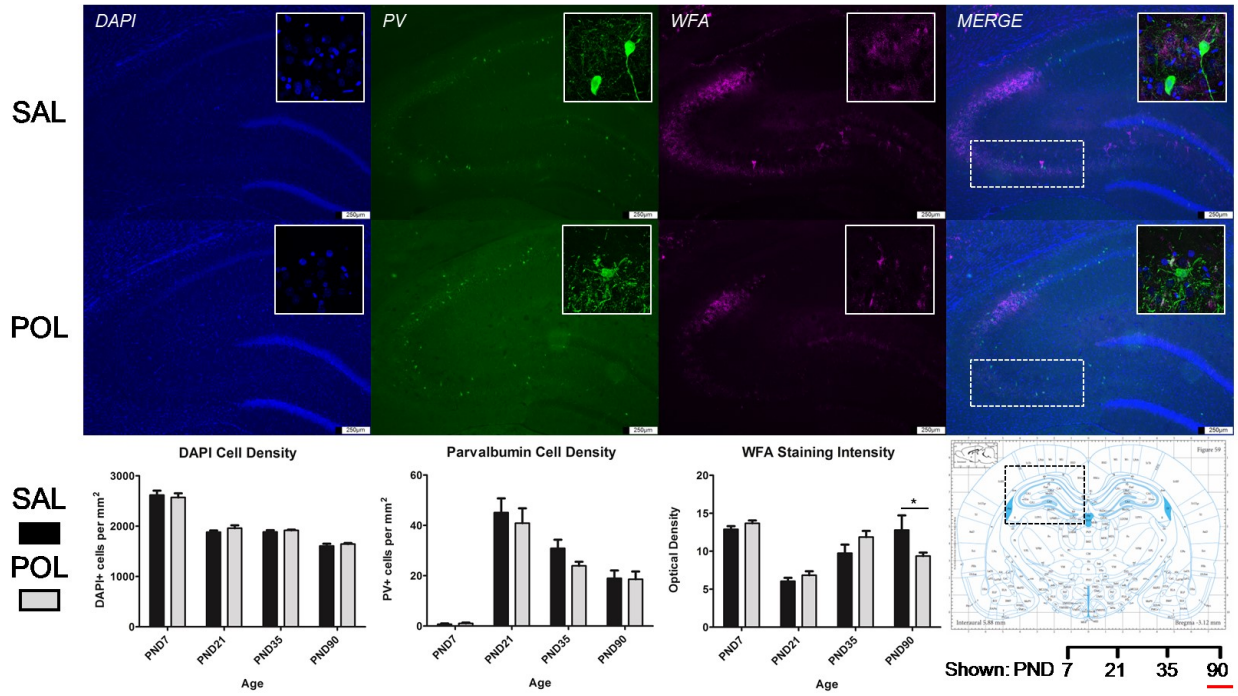

Figure 11. Parvalbumin interneurons and WFA immunoreactivity in the CA3 region of the dorsal hippocampus (postnatal day 90 shown). DAPI cell density decreased dramatically from PND7 to PND21 before a more slight decrease into maturity (main effect of Age, $p < 0.0001$). PV+ cell density was absent in PND7 before a large increase in density at PND21, after which it decreased in maturity (main effect of Age, $p < 0.0001$). CA3 also had no distinguishable PNNs but rather a dense lattice-like WFA staining pattern. The optical density of this staining pattern increased steadily from PND21 to PND90 (main effect of Age, $p < 0.0001$; Age x Treatment, $p < 0.01$). At PND90, the WFA optical density of the CA3 region was significantly reduced in PolyI:C treated offspring ($p < 0.05$). The CA3 region of the dorsal hippocampus was identified using The Rat Brain in Stereotaxic Coordinates (Paxinos & Watson, 1986) as region CA3, between Bregma -2.80 mm to -3.30 mm. Black bars represent Saline treated offspring, light grey bars PolyI:C treated offspring. Insets are representative images from each condition. Scale bar represents 250 μm. *p<0.05, 2X2 ANOVA followed by *post hoc* Bonferroni t-tests. Data is mean ± SEM.

Parvalbumin Interneurons. Next I evaluated the density of PV+ interneurons within the same region across all cohorts. A two-way ANOVA revealed an effect of age on PV+ cell density within CA1, $F(3,45) = 49.40$, $p < 0.0001$. There was no significant effect of treatment, $F(1,45) = 1.20$, ns. There was no interaction between treatment and age, $F(3,45) = 0.43$, ns. PV+ cell density was highest in the PND21 cohort and declined steadily after that.

DAPI Nuclear Stain. The density of DAPI+ positive cells was assessed using an automated counter. A two-way ANOVA revealed a significant effect of age, $F(3,45) = 123.20$, $p < 0.0001$. DAPI+ cell density decreased from infancy into adulthood. There was no significant effect of treatment, $F(1,45) = 0.45$, ns. There was no interaction between treatment and age, $F(3,45) = 0.51$, ns.

Microglia. Counts of the total number of microglia were assessed using an automated counter of IBA1+ cells (Fig. 12). A two-way ANOVA revealed a significant effect of age, $F(3,48) = 20.95$, $p < 0.0001$. Microglia density peaked bi-modally, being highest at the PND7 and PND35 cohorts with reduced density at PND21 and PND90. There was no significant effect of treatment, $F(1,48) = 2.10$, ns. There was no interaction between treatment and age, $F(3,48) = 1.08$, ns.

Astrocytes. To assess the degree of astrocytic activity throughout development, I examined the optical density of GFAP staining. A two-way ANOVA revealed a significant effect of age, $F(3,46) = 12.42$, $p < 0.0001$. GFAP immunoreactivity increased from PND7 to PND21 and decreased slightly from PND35 to PND90. There was no significant effect of treatment, $F(1,46) = 0.83$, ns. There was a trend towards a significant interaction between treatment and age on GFAP optical density, $F(3,46) = 2.73$, $p = 0.0546$. There were no significant differences between treatment groups at any age.

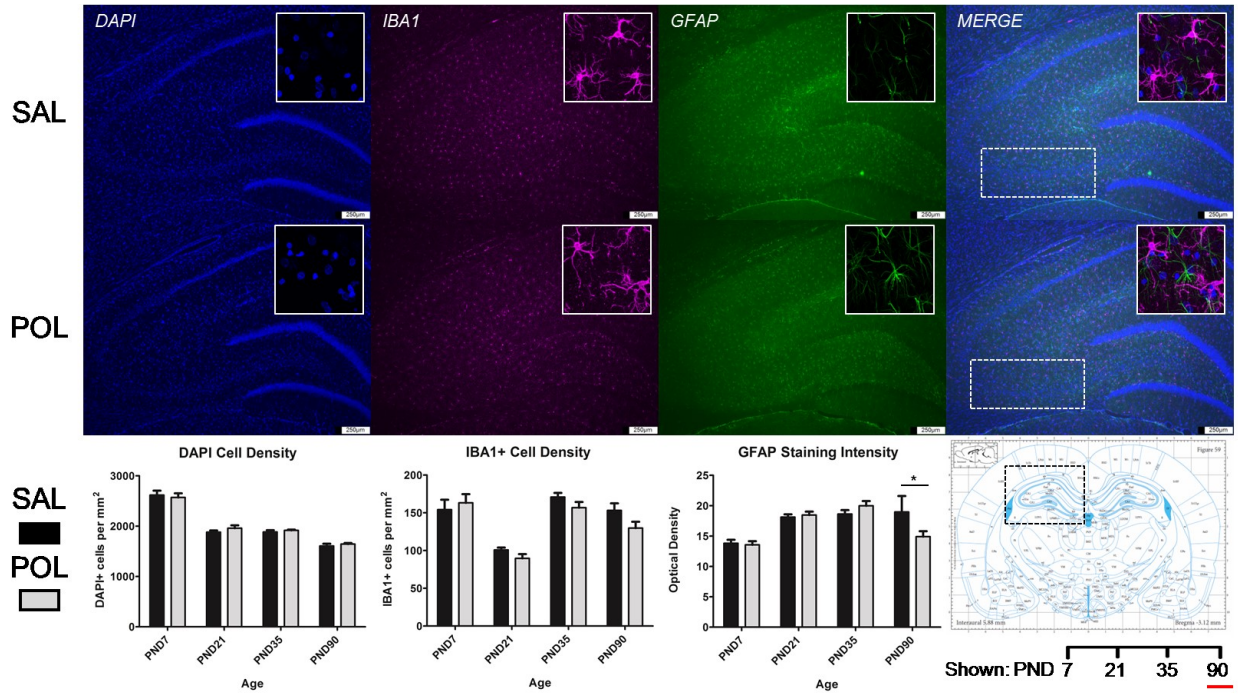

Figure 12. Microglia stained with IBA1 and astrocytes with GFAP in the CA3 region of the dorsal hippocampus (postnatal day 90 shown). DAPI cell density decreased across all developmental cohorts (main effect of Age, $p < 0.0001$). Microglial density as labelled with IBA1 was highest during the PND7 and PND35 with reductions in density in the PND21 and 90 cohorts (main effect of Age, $p < 0.0001$). GFAP increased from PND7 to PND21 where it remained relatively stable until PND90 (main effect of Age, $p < 0.0001$; Age x Treatment, $p = 0.055$). In the PND90 cohort, PolyI:C treated offspring had a significant reduction in GFAP staining intensity ($p < 0.05$). The CA3 region of the dorsal hippocampus was identified using The Rat Brain in Stereotaxic Coordinates (Paxinos & Watson, 1986) as region CA3, between Bregma -2.80 mm to -3.30 mm. Black bars represent Saline treated offspring, light grey bars PolyI:C treated offspring. Insets are representative images from each condition. Scale bar represents 250 µm. *p<0.05, 2X2 ANOVA followed by *post hoc* Bonferroni t-tests. Data is mean ± SEM.

3.7 Ventral Hippocampus: CA1 Region.

Perineuronal Nets. I examined the total number of PNNs present within the ventral portion of the CA1 region (Fig. 13). A two-way ANOVA revealed a significant effect of age on the number of PNNs, $F(3,47) = 254.50$, $p < 0.0001$. No PNNs were present in the PND7 cohort but appeared in there PND21 animals and increased slightly over the PND35 and P90 age groups. There was no significant effect of treatment, $F(1,47) = 0.58$, ns. There was no interaction between treatment and age, $F(3,47) = 2.03$, ns.

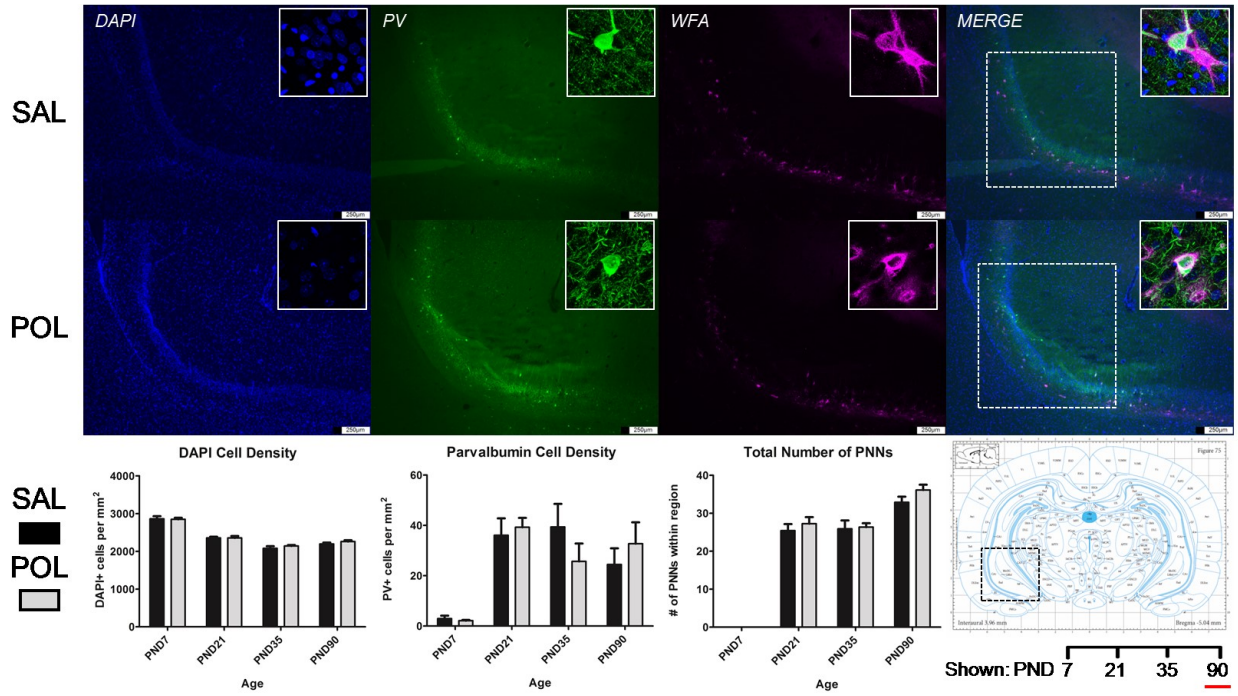

Figure 13. Perineuronal nets stained with WFA and parvalbumin interneurons in the CA1 region of the ventral hippocampus (postnatal day 90 shown). DAPI cell density decreased from PND7 to PND35 where it was relatively stable into maturity (main effect of Age, $p < 0.0001$). PV+ cells were absent in the PND7 cohort but present by PND21 after which it decrease very marginally into maturity (main effect of Age, $p < 0.0001$). PNNs were absent in PND7 but saw a large increase by PND21 and remained stable until a small increase at PND90 (main effect of Age, $p < 0.0001$). The CA1 region of the ventral hippocampus was identified using The Rat Brain in Stereotaxic Coordinates (Paxinos & Watson, 1986) as region CA1, between Bregma -4.80 mm to -5.80 mm. Black bars represent Saline treated offspring, light grey bars PolyI:C treated offspring. Insets are representative images from each condition. Scale bar represents 250 μm. *p<0.05, 2X2 ANOVA followed by *post hoc* Bonferroni t-tests. Data is mean ± SEM.

Parvalbumin Interneurons. Next I evaluated the density of PV+ interneurons within the same region across all cohorts. A two-way ANOVA revealed an effect of age on PV+ cell density within CA1, $F(3,47) = 11.33$, $p < 0.0001$. There was no significant effect of treatment, $F(1,47) = 0.03$, ns. There was no interaction between treatment and age, $F(3,47) = 0.91$, ns. PV+ cell density increased from PND7 to PND21 and was relatively stable thereafter.

DAPI Nuclear Stain. The density of DAPI+ positive cells was assessed using an automated counter. A two-way ANOVA revealed a significant effect of age, $F(3,47) = 114.10$, $p < 0.0001$. DAPI+ cell density decreased from PND7 to PND35 where it plateaued. There was no significant effect of treatment, $F(1,47) = 0.88$, ns. There was no interaction between treatment and age, $F(3,47) = 0.43$, ns.

Microglia. Counts of the total number of microglia were assessed using an automated counter of IBA1+ cells (Fig. 14). A two-way ANOVA revealed a significant effect of age, $F(3,47) = 36.66$, $p < 0.0001$. Microglia density spiked in the PND21 cohort but was relatively stable otherwise. There was no significant effect of treatment, $F(1,47) = 0.84$, ns. There was no interaction between treatment and age, $F(3,47) = 0.24$, ns.

Astrocytes. To assess the degree of astrocytic activity throughout development, I examined the optical density of GFAP staining. A two-way ANOVA revealed a significant effect of age, $F(3,47) = 56.29$, $p < 0.0001$. GFAP immunoreactivity increased across postnatal development. There was no significant effect of treatment, $F(1,47) = 1.82$, ns. There was no interaction between treatment and age, $F(3,47) = 0.66$, ns.

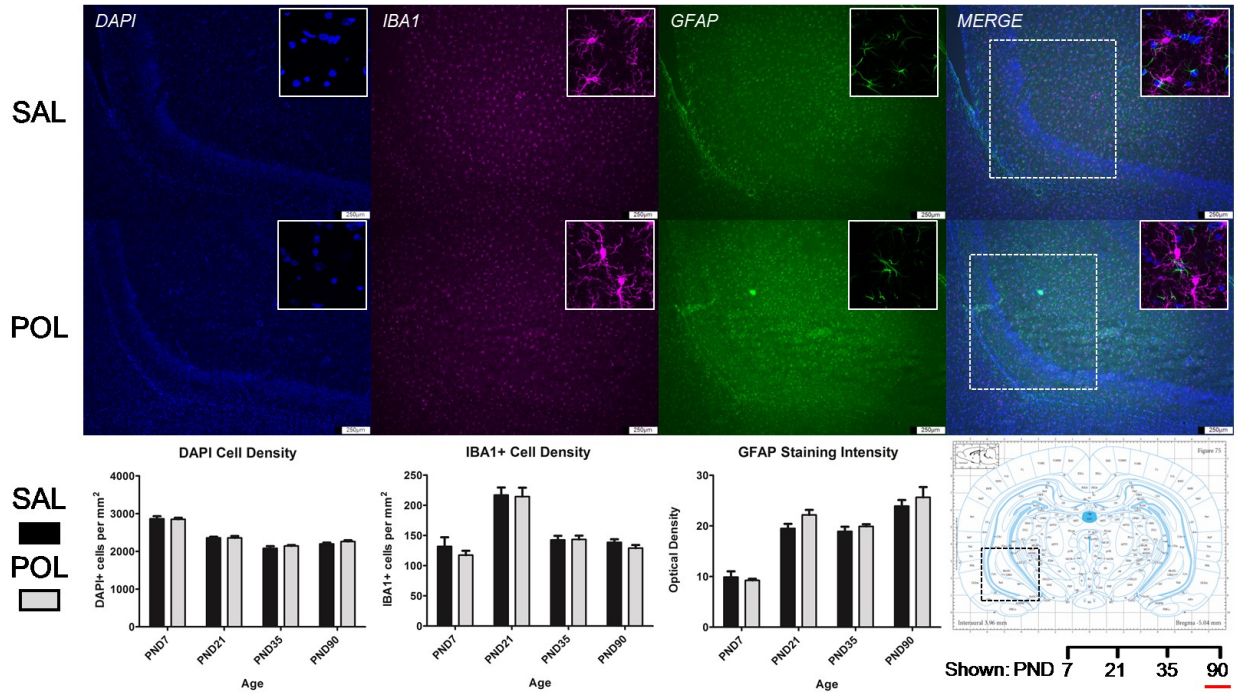

Figure 14. Microglia stained with IBA1 and astrocytes with GFAP in the CA1 region of the ventral hippocampus (postnatal day 90 shown). DAPI cell density decreased across all developmental cohorts (main effect of Age, $p < 0.0001$). Microglial density as labelled with IBA1 spiked during the PND21 cohort but was otherwise relatively stable otherwise (main effect of Age, $p < 0.0001$). GFAP staining intensity increased across postnatal development, being highest in the PND90 cohort (main effect of Age, $p < 0.0001$). Neither PolyI:C treated animals or controls showed significant differences between either of these immune markers. The CA1 region of the ventral hippocampus was identified using The Rat Brain in Stereotaxic Coordinates (Paxinos & Watson, 1986) as region CA1, between Bregma -4.80 mm to -5.80 mm. Black bars represent Saline treated offspring, light grey bars PolyI:C treated offspring. Insets are representative images from each condition. Scale bar represents 250 µm. *p<0.05, 2X2 ANOVA followed by *post hoc* Bonferroni t-tests. Data is mean ± SEM.

3.8 Ventral Hippocampus: CA3 Region.

Perineuronal Nets. Similar to in the dorsal CA3 region, no PNNs were present in the ventral CA3 (Fig. 15). Rather the WFA staining labelled a dense matrix pattern similar to that of the reticular thalamic nucleus. As such, I measured the optical density of WFA staining within the area rather than PNN counts. A two-way ANOVA revealed a significant effect of age on WFA optical density, $F(3,47) = 61.53$, $p < 0.0001$. There was also a significant effect of treatment, $F(1,47) = 6.32$, $p < 0.05$. There was an interaction between treatment and age, $F(3,47) = 2.95$, $p < 0.05$. Post hoc comparisons revealed a significant increase in WFA optical density of the CA3 region in PolyI:C as compared to saline treated offspring in the PND21 cohort, SAL ($M = 20.72 \pm 1.04$) vs. POL ($M = 28.44 \pm 1.90$), $t = 3.532$, $p < 0.01$.

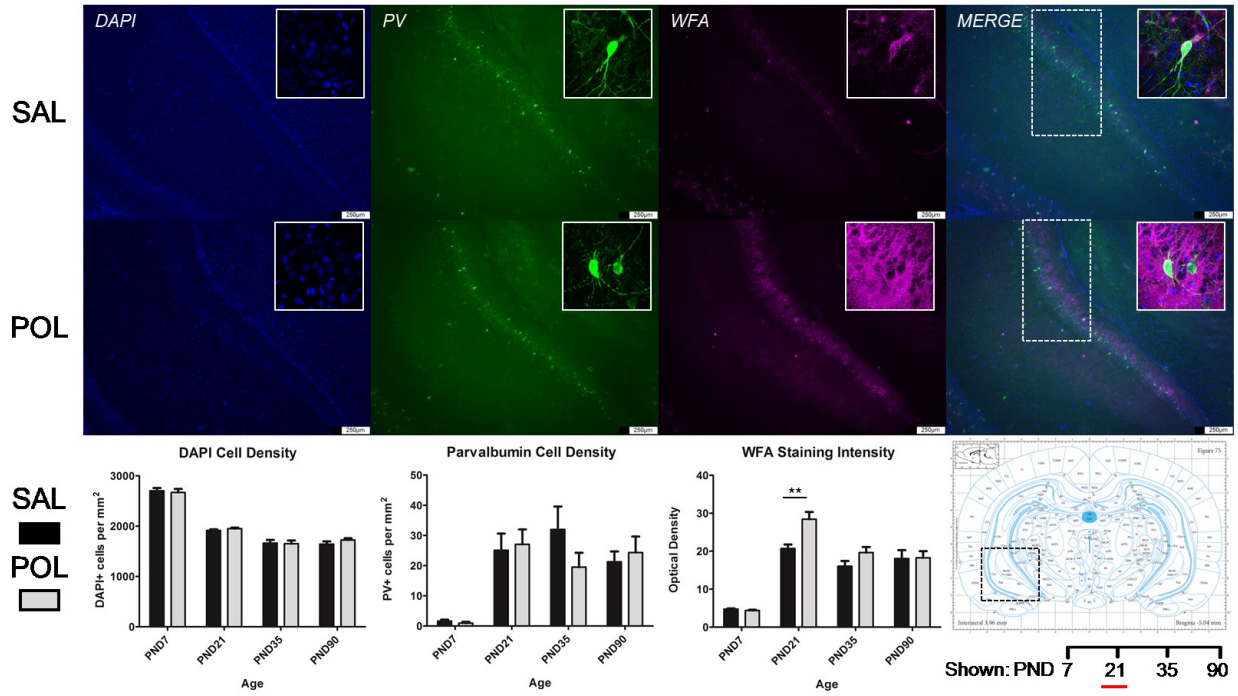

Figure 15. Parvalbumin interneurons and WFA immunoreactivity in the CA3 region of the dorsal hippocampus (postnatal day 21 shown). DAPI cell density decreased from PND7 to PND21 after which it decreased slightly into maturity (main effect of Age, $p < 0.0001$). PV+ cell density was absent in the PND7 cohort before an increase at PND21 (main effect of Age, $p < 0.0001$). CA3 also had no distinguishable PNNs but rather a dense lattice-like WFA staining pattern. The optical density of this staining pattern was absent at PND7 but increased dramatically at PND21 before leveling off in maturity (main effect of Age, $p < 0.0001$; Treatment, $p < 0.05$; Age x Treatment, $p < 0.05$). At PND21, PolyI:C treated animals has a singnificantly increased WFA optical density within CA3 as compared to controls ($p < 0.01$). The CA3 region of the ventral hippocampus was identified using The Rat Brain in Stereotaxic Coordinates (Paxinos & Watson, 1986) as region CA3, between Bregma -4.80 mm to -5.80 mm. Black bars represent Saline treated offspring, light grey bars PolyI:C treated offspring. Insets are representative images from each condition. Scale bar represents 250 μm. $^{**}p<0.01$, 2X2 ANOVA followed by *post hoc* Bonferroni t-tests. Data is mean ± SEM.

Parvalbumin Interneurons. Next I evaluated the density of PV+ interneurons within the same region across all cohorts. A two-way ANOVA revealed an effect of age on PV+ cell density within CA1, $F(3,47) = 12.62$, $p < 0.0001$. There was no significant effect of treatment, $F(1,47) = 0.34$, ns. There was no interaction between treatment and age, $F(3,47) = 1.01$, ns. PV+ cells were absent in PND7 and present in relatively steady numbers from PND21 to PND90.

DAPI Nuclear Stain. The density of DAPI+ positive cells was assessed using an automated counter. A two-way ANOVA revealed a significant effect of age, $F(3,47) = 147.20$, $p < 0.0001$. DAPI+ cell density decreased from infancy into adulthood. There was no significant effect of treatment, $F(1,47) = 0.21$, ns. There was no interaction between treatment and age, $F(3,47) = 0.42$, ns.

Microglia. Counts of the total number of microglia were assessed using an automated counter of IBA1+ cells (Fig. 16). A two-way ANOVA revealed a significant effect of age, $F(3,47) = 12.11$, $p < 0.0001$. Microglia density peaked bimodally, being highest at the PND7 and PND35 cohorts with reduced density at PND21 and PND90. There was no significant effect of treatment, $F(1,47) = 0.84$, ns. There was no interaction between treatment and age, $F(3,47) = 0.74$, ns.

Astrocytes. To assess the degree of astrocytic activity throughout development, I examined the optical density of GFAP staining. A two-way ANOVA revealed a significant effect of age, $F(3,47) = 98.42$, $p = 0.0001$. GFAP immunoreactivity plateaued between PND21 and PND35, but overall increased across all developmental cohorts. There was no significant effect of treatment, $F(1,47) = 0.33$, ns. There was no interaction between treatment and age on GFAP optical density, $F(3,47) = 1.40$, ns.

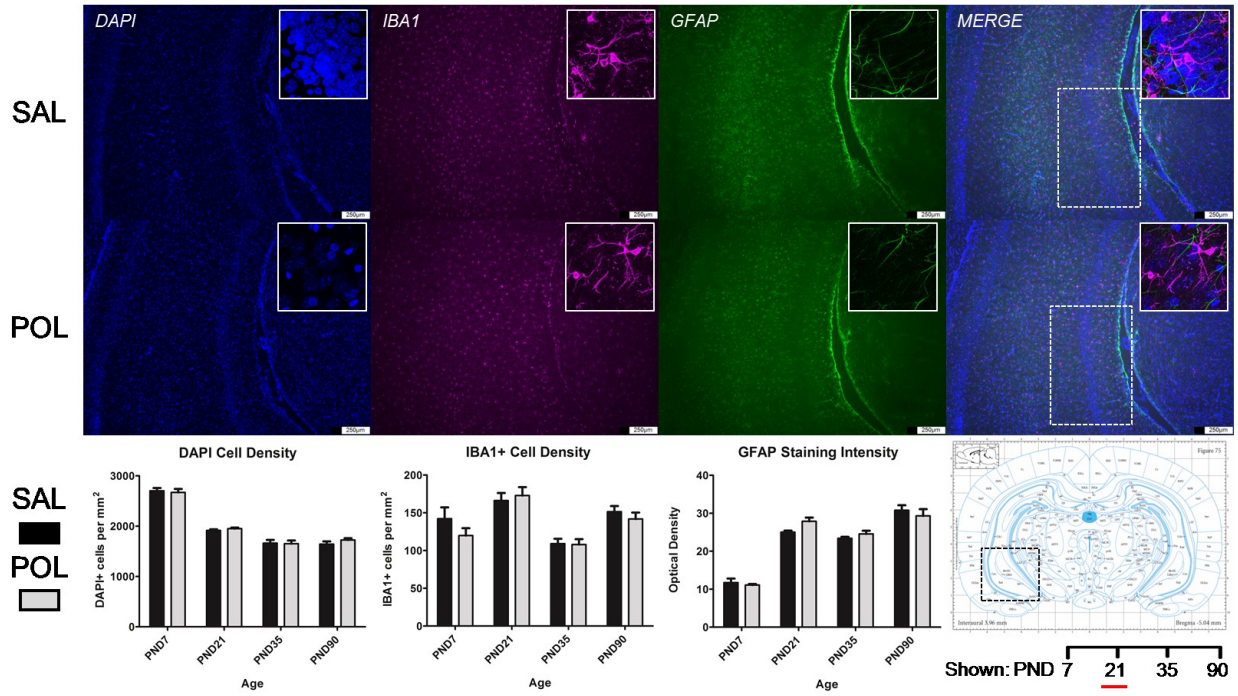

Figure 16. Microglia stained with IBA1 and astrocytes with GFAP in the CA3 region of the ventral hippocampus (postnatal day 21 shown). DAPI cell density decreased from PND7 to PND21 before stabilizing into maturity (main effect of Age, $p < 0.0001$). Microglial density as labelled with IBA1 peaked in the PND21 cohort before decreasing at PND35 and then a slight increase again at PND90 (main effect of Age, $p < 0.0001$). Overall, GFAP staining intensity increased across postnatal development peaking in the PND90 cohort (main effect of Age, $p < 0.0001$). The CA3 region of the ventral hippocampus was identified using The Rat Brain in Stereotaxic Coordinates (Paxinos & Watson, 1986) as region CA3, between Bregma -4.80 mm to -5.80 mm. Black bars represent Saline treated offspring, light grey bars PolyI:C treated offspring. Insets are representative images from each condition. Scale bar represents 250 μm. *p<0.05, 2X2 ANOVA followed by *post hoc* Bonferroni t-tests. Data is mean ± SEM.

3.9 Primary Auditory Cortex. I targeted the primary auditory cortex based on previous studies in humans showing genetic changes in genes associated with PNN development and maintenance in SCZ patients (Pietersen et al., 2014). Furthermore, the primary auditory cortex is of interest to SCZ as the primary hallucination type experienced by SCZ patients is auditory in nature (Thomas et al., 2007). SCZ patients have also been shown consistently to have deficits in verbal declarative memory, which have been associated with the primary auditory cortex (Cirillo & Seidman, 2003).

Perineuronal Nets. I examined the total number of PNNs present within the primary auditory cortex (Fig. 17). Similar to other regions, PNNs increased throughout development. A two-way ANOVA revealed a significant effect of age, $F(3,45) = 240.30$, $p < 0.0001$. There was no significant effect of age, $F(1,45) = 1.04$, ns. There was no interaction between treatment and age, $F(3,45) = 0.92$, ns.

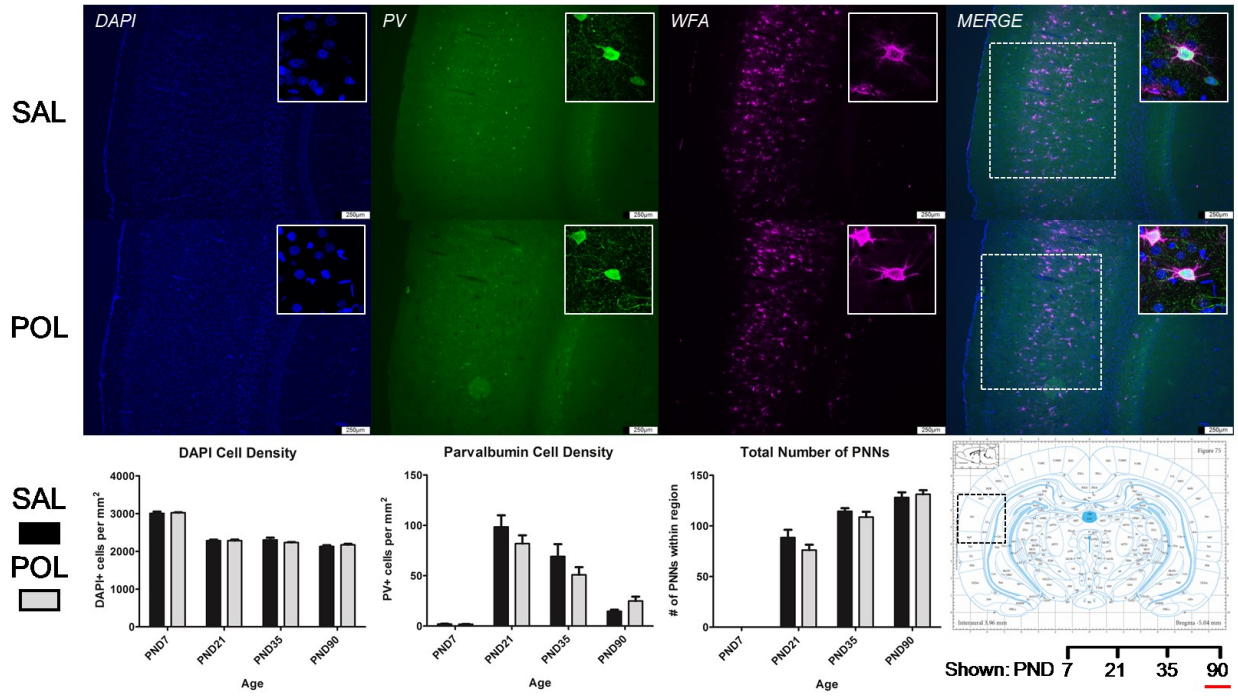

Figure 17. Perineuronal nets stained with WFA and parvalbumin interneurons in the primary auditory cortex (postnatal day 90 shown). DAPI cell density decreased from PND7 to PND21 where it was relatively stable into maturity (main effect of Age, $p < 0.0001$). PV+ cell density was highest in the PND21 cohort before decreasing steadily into maturity (main effect of Age, $p < 0.0001$). PNNs were absent in the PND7 cohort but appeared at PND21 after which they steadily increased across postnatal development (main effect of Age, $p < 0.0001$). The primary auditory cortex was identified using The Rat Brain in Stereotaxic Coordinates (Paxinos & Watson, 1986) as region CA1, between Bregma -4.16 mm to -5.20 mm. Black bars represent Saline treated offspring, light grey bars PolyI:C treated offspring. Insets are representative images from each condition. Scale bar represents 250 μm. *p<0.05, 2X2 ANOVA followed by *post hoc* Bonferroni t-tests. Data is mean ± SEM.

Parvalbumin Interneurons. I evaluated the density of PV+ interneurons within the primary auditory cortex across all cohorts. A two-way ANOVA revealed an effect of age on PV+ cell density, $F(3,45) = 57.90$, $p < 0.0001$. PV+ cell density increased from infancy to childhood and decreased during adolescence. There was no significant effect of treatment, $F(1,45) = 1.38$, ns. There was also no interaction between treatment and age, $F(3,45) = 1.71$, ns.

DAPI Nuclear Stain. Cellular density of DAPI+ positive cells was assessed using an automated counter. A two-way ANOVA revealed a significant effect of age, $F(3,45) = 345.10$, $p < 0.0001$. The density of DAPI+ cells decreased with age. There was no significant effect of treatment, $F(1,45) = 0.007$, ns. There was no interaction between treatment and age, $F(3,45) = 1.30$, ns.

Microglia. Counts of the total number of microglia were assessed using an automated counter of IBA1+ cells (Fig. 18). A two-way ANOVA revealed a significant effect of age, $F(3,47) = 65.32$, $p < 0.0001$. Microglia density increased during childhood before it plateaued into maturity. There was no significant effect of treatment, $F(1,47) = 0.24$, ns. There was however an interaction between treatment and age, $F(3,47) = 3.10$, $p < 0.05$. Post hoc Bonferroni t-tests showed that there was no significant effect of treatment within any cohort.

Astrocytes. To assess the degree of astrocytic activity throughout development, I examined the optical density of GFAP staining. A two-way ANOVA revealed a significant effect of age, $F(3,46) = 153.4$, $p < 0.0001$. GFAP immunoreactivity peaked during childhood and adolescence before decreasing into adulthood. There was no significant effect of treatment condition, $F(1,46) = 0.717$, ns. There was no interaction between treatment and age, $F(3,46) = 1.521$, ns.

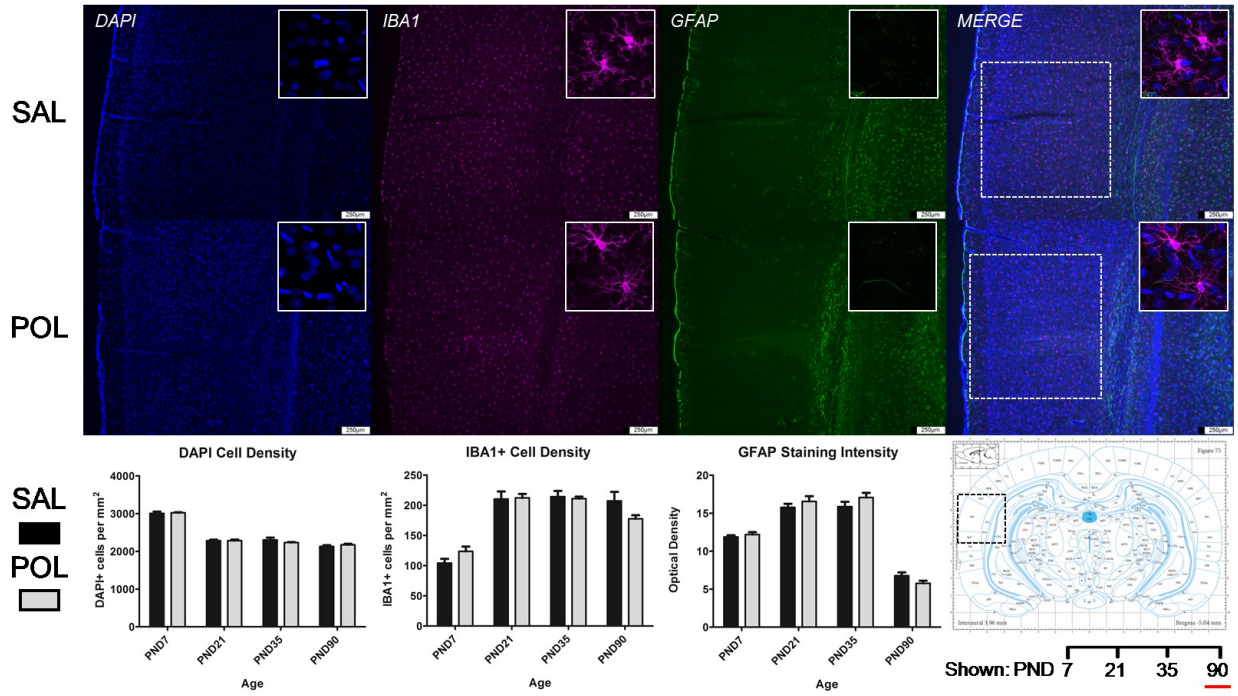

Figure 18. Microglia stained with IBA1 and astrocytes with GFAP in the primary auditory cortex (postnatal day 90 shown). DAPI cell density decreased from PND7 to PND21 where it was relatively stable into maturity (main effect of Age, $p < 0.0001$). Microglial density as labelled with IBA1 was highest and stable from PND21 to PND35 before decreasing at PND90, which was slightly more pronounced in PolyI:C treated animals (main effect of Age, $p < 0.0001$; Age x Treatment, $p < 0.05$). GFAP staining intensity increased from PND7 to PND21 before decreasing dramatically at PND90 (main effect of Age, $p < 0.0001$). The primary auditory cortex was identified using The Rat Brain in Stereotaxic Coordinates (Paxinos & Watson, 1986) as region CA1, between Bregma -4.16 mm to -5.20 mm. Black bars represent Saline treated offspring, light grey bars PolyI:C treated offspring. Insets are representative images from each condition. Scale bar represents 250 µm. *p<0.05, 2X2 ANOVA followed by *post hoc* Bonferroni t-tests. Data is mean ± SEM.

4. Discussion

4.1 The Present Study

In the present study I sought to examine whether the PNN deficits that have been observed in SCZ patient's brains post-mortem were also present in the PolyI:C model of SCZ. This model has been extensively studied and been shown to share a number of the behavioural and anatomical features of SCZ, but PNNs had not yet been examined. I evaluated PNNs, PV+ interneurons, microglia, astrocytes, as well as total cellular density as labelled by DAPI nuclear staining across development from infancy to adulthood (see summary, Table 2).

Table 2. Summary of results from regions of interest for the present study.

Brain Region Examined	Results	Human Anatomical Correlate	PNN & PV in Human SCZ Patients
Frontal Association Cortex	**Perineuronal net deficits emerging in adolescence**	Dorsal Prefrontal Cortex	**Perineuronal net deficits in the dorsolateral prefrontal cortex** Decreased PV+ cell density
Prelimbic Cortex	**Perineuronal net deficits emerging in adolescence**	Medial Prefrontal Cortex	None examined
Reticular Thalamic Nucleus	Reduced PV+ cell density in infancy	Reticular Thalamic Nucleus	None examined
Amygdala	Reduced PV+ cell density across development	Amygdala	**Perineuronal net deficits in subnuclei of the amygdala**
Primary Auditory Cortex	No observed deficits	Superior Temporal Cortex	Significant changes to genes associated with PNN components & degrading enzymes
Dorsal Hippocampus	Reduced WFA & GFAP staining in CA3 region of adult rats Increased WFA staining in CA3 region of childhood rats	Dorsal Hippocampus	Decreased PV+ cell density
Ventral Hippocampus		Ventral Hippocampus	

4.2 Perineuronal Net Deficits

The observation that PNNs are reduced in the prefrontal cortex could contribute to a number of pathological processes associated with SCZ. Of particular interest is the role of PNNs in critical periods, where they have been associated with the closure of these heightened windows of plasticity (Hensch, 2005; Takesian & Hensch, 2013). PNN deficits in adulthood within these areas could represent a failure to progress fully through associated critical periods. PNNs are known to stabilize synapses at the closure of the critical period and their failure to form could leave functional synapses vulnerable to degradation. This mechanism could explain spine density reductions seen in SCZ patients in regions associated with PNN loss (Moyer et al., 2014). PNNs are also known to play important roles in ion homeostasis around highly active PV+ interneurons (Brückner et al., 1993, 1996; Hartig et al., 1990). Disruption of ion homeostasis around these highly metabolically active interneurons could result in changes in their electrophysiological activity. The fast-spiking nature of PV+ interneurons has shown to be essential to the generation of gamma oscillatory activity, which is perturbed in electrophysiological recordings from SCZ patients from multiple regions, including the dorsolateral prefrontal cortex (Carter et al., 1998; Manoach et al., 1999; Cho et al., 2006; Basar-Eroglu et al., 2007; Dityatev et al., 2007; Lewis & Gonzalez-Burgos, 2008; Spencer et al., 2008; Farzan et al., 2010; Uhlhaas & Singer, 2010; Woo et al., 2010; Sun et al., 2011; Kirihara et al., 2012; Grutzner et al., 2013). While our model was able to replicate the clinical studies showing deficits in PNNs in the PFC, I did not however see the same effects in the amygdala or superior temporal cortex as has been shown in humans (Pietersen et al., 2014; Pantazopolous et al., 2010; 2015).

Interestingly, I identified that the reticular thalamic nucleus and CA3 region of the hippocampus while not having distinguishable PNNs did appear to have a dense WFA staining pattern. Presumably, this represents WFAs affinity for the N-acetylgalactosamine linkages to galactose on chondroitin sulfate proteoglycans that aggregate into PNNs, but in a more dense and extensive form. Consistent with that hypothesis I found that the WFA staining pattern did co-localize with labelling of the chondroitin sulfate proteoglycan isoform aggrecan (data not shown). This pattern was diminished in the CA3 region of the dorsal hippocampus in adult PolyI:C treated offspring as compared to saline controls. Conversely, this same staining pattern in the CA3 region of the ventral hippocampus was increased in PolyI:C treated animals during childhood. The exact contribution of these changes are hard to discern without a better understanding of the role of the dense WFA staining pattern observed. However, the hippocampus has shown to be particularly affected by prenatal treatment with PolyI:C and preliminary findings of a disturbed ECM within this region would be consistent with other ongoing pathological processes in this area (Dickerson et al., 2014; Giovanoli et al., 2014; Patrich et al., 2015). Furthermore, the dorsal and ventral hippocampus are both known to contribute to a number of behaviours and cognitive processed that comprise the SCZ phenotype (McCarley et al., 1993; Saykin et al., 1994; 1999; Keefe et al., 1997; Heinrichs & Zakzanis, 1998; Stone et al., 1998; Dickinson et al., 2004; Neuchterlein et al., 2004; Weiss et al., 2004; Ranganath et al., 2008). Direct disruption of PNNs in the ventral hippocampus with ChABC has previously shown to disturb hippocampal activity, enhance dopaminergic signalling in the prefrontal cortex, and augment locomotor responses to amphetamines (Shah & Lodge, 2013).

4.3 Parvalbumin Interneuron Deficits

We also examined PV+ interneurons which have been extensively studied in SCZ patients and shown to be disturbed (Lewis et al., 2012; Gonzalez-Burgos et al., 2015). I found that PV+ interneuron density was stunted in PolyI:C treated animals throughout development in basolateral amygdala. There was also a trend towards a significant reduction across development in the frontal association cortex which has been previously reported in human SCZ patient's brains post-mortem (Beasley & Reynolds, 1997). The frontal association cortex is known to have reciprocal connections with the basolateral amygdala that are integral to associative learning, particularly with respect to fear learning and memory (Nakayama et al., 2015). The functional relationship between these two areas could be reflected in their like-deficits, where PV+ interneuron seemed to be most affected during early adolescence. PolyI:C affected animals are known to have a variety of deficits in fear processing, however many of these do not emerge until later adolescence and early adulthood (Ibi et al., 2010; Vorhees et al., 2015). In future studies it would be of interest to evaluate not only PV+ cell density but also PV+ expression as several studies have identified stable PV+ cell densities with changes in both PV+ protein and mRNA as well as reduced GAD67 on PV+ interneurons (Hashimoto et al., 2003; Mellios et al., 2009; Fung et al., 2010; Curley & Lewis, 2012; Volk et al., 2012; Glausier et al., 2014).

In addition to the deficits in PV+ interneurons I observed in the basolateral amygdala and frontal association cortex, I also found a profound deficit in reticular thalamic nucleus of PolyI:C treated animals during infancy. This striking deficit could be integral to the etiogenesis of later pathological features of PolyI:C affected animals. The thalamus is part of the fundamental sensory processing stream that via thalamacortical connections relays most of the bodies sensory signalling to the cortex. While the deficit in the reticular thalamic nucleus was only transiently present during infancy, it could feasibly disrupt the ongoing maturation of a number of intra-

thalamic and thalamocortical projections which are essential to cortical networks. As the reticular thalamic nucleus itself has no cortical input or output but rather modulates the function of other regions of the thalamus, it would be of interest to examine the consequences of this early PV+ deficit on the development of other thalamic nuclei (Guillery & Harting, 2003; Ferrarelli et al., 2011; Pratt & Morris, 2015). The reticular thalamic nucleus has been shown to be particularly sensitive to psychomimetic drugs and is thought to be important to sensorimotor gating, both of which are disturbed in PolyI:C and SCZ (Braff et al., 1978; Cochran et al., 2003; Krause et al., 2003; Troyano-Rodriguez et al., 2014). However these deficits have not been shown to emerge until adolescence in PolyI:C affected animals, well after I saw PV+ density had normalized.

4.4 Immune Cells

My preliminary examination of microglia and astrocytes revealed that there does not appear to be widespread ongoing inflammatory processes in PolyI:C treated offspring compared to controls. Most notably, while I did observe some minor differences in astrocytic reactivity between conditions in the dorsal hippocampus (CA3) these changes were not associated with regions of PNN and PV+ disturbances. Outside of neurons themselves, astrocytes are known to be the major secretors of PNN components including chondroitin sulfate proteoglycans. Consistent with this, astrocytic staining was sparsely present during infancy but increased throughout development very similarly to the formation of PNNs. While astrocytes are the primary secretors of ECM components, microglia are the primary secretors of the enzymes which degrade the ECM (Gotschall & Deb, 1996; Faissner et al., 2010; Klausmeyer et al., 2011; Weise et al., 2012). These include enzymes like the matrix metalloproteinases (MMPs) and ADAMTSs (a disintegrin with a thrombospondin motif). I however found no signs of ongoing

microglial dysfunction throughout development, at least in terms of cellular density. This is consistent with several other studies that examined microglia after prenatal PolyI:C treatment (Giovanoli et al., 2015; Smolders et al., 2015). The lack of ongoing inflammatory processes suggests that the effects I observed on PNNs in the prefrontal cortex and PV+ interneurons in the BLA and reticular thalamic nucleus are the consequence of disturbed developmental trajectories rather than ongoing immune dysfunction as a result of prenatal infection. However, it should be noted that cell density alone is not a sensitive measure to the full scope of microglia's role in CNS maintenance. It is entirely possible that the functional attributes and secretion of ECM degrading enzymes by microglia could be dramatically altered despite no changes in their density. It has previously been shown that MMP-9 is elevated in the brains of SCZ patients and mutations in the gene associated with MMP-16 was recently identified to confer heightened SCZ risk in a genome-wide association scan (Domenici et al., 2010; Yamamori et al., 2013; Pietersen et al., 2014; Devanarayanan et al., 2015). The relationship between microglia and the ECM, PNNs in particular, remains an intriguing avenue for future research.

4.5 Pathological Mechanisms

While this study confirms a loss of PNNs in the prefrontal cortex of offspring exposed to maternal immune activation, I was unable to provide insight towards a mechanism by which this occurs. With no readily observable changes to microglia and astrocytes, the process by which PV+ and PNNs are disturbed as a result of prenatal infection are still a matter of speculation. Previously, two leading hypotheses have been proposed (Beretta et al., 2015). Firstly, PNN deficits could be the result of disruption or a lack of generation of PNN components like CSPGs. Decreases in PNNs in the amygdala of SCZ patients has been associated with reduced levels of CSPG expressing astrocytes within the same area (Pantazopoulos et al., 2015). As astrocytes are

the primary source of CSPG synthesis this could represent a potential mechanism by which PNNs fail to form (John et al., 2006; Faissner et al., 2010; Wiese et al., 2012). Additionally, studies have identified several genetic vulnerabilities in SCZ for genes which contribute to CSGP synthesis, including PTPRZ1 and neurocan (Buxbaum et al., 2008; Muhleisen et al., 2012; Ripke & Schizophrenia Working Group of the Psychiatric Genomics, 2014). Secondly, PNN deficits could be the result of overactive enzymatic activity perpetually degrading these structures. A growing body of evidence suggests that the ECM is continuously being remodeled even into adulthood (Frischknect & Gundelfinger, 2012). Increases in expression of MMPs which degrade the ECM have been shown to occur in the prefrontal cortex, amygdala, and hippocampus during contextual fear learning tasks (Brown et al., 2009; Ganguly et al., 2013). Furthermore, inhibition of MMPs has been shown to disturb the reconsolidation of fear memories and disturb spatial memory and avoidance learning (Nagy et al., 2007; Wright et al., 2007). It was recently shown that the superior temporal cortex of SCZ patients had altered mRNA expression of specific MMPs and ADAMTSs (Pietersen et al., 2014). Furthermore, a variety of genetic studies have identified several genes encoding for ADAMTSs and MMPs that may confer a heightened vulnerably for SCZ (Dow et al., 2011; Ripke et al., 2011; Besplova et al., 2013; McGrath et al., 2013). Heightened levels of these ECM degrading enzymes could explain the deficits observed in adult SCZ patients.

Conclusion

While my data cannot provide further support for either mechanism by which PNNs are lost, my data does strengthen a growing body of support in using the PolyI:C model to examine SCZ. I have shown that the PolyI:C model shares the prefrontal cortex PNN disturbances that have been seen in SCZ patient's brains post-mortem. Furthermore, I have shown that these

deficits do not emerge until during adolescence similar to when both PolyI:C animals and SCZ patients symptoms will typically manifest. This shared pathological feature not only adds to the growing list of shared features of the model and the disease, but also provides an intriguing platform for future investigation. I support the use of the PolyI:C model for further inquiry into the mechanism by which PNNs come to be disturbed and the consequences of those disturbances. The model affords a unique opportunity to examine the relationships between the ECM, prenatal infections, and behaviour. Future studies could include a more directed manipulation of PNNs by use of chondroitinase ABC in regions of interest like the prefrontal cortex. This would prove valuable in isolating the consequences of PNN disturbances alone, outside of the confounding effects of prenatal infection. With a better understanding of PNN's functional role in the prefrontal cortex and the means by which they are both maintained and or disturbed, I can then evaluate therapeutic strategies to prevent or compensate for their loss in SCZ.

References

Achim, A. M., Bertrand, M. C., Sutton, H., Montoya, A., Czechowska, Y., Malla, A. K., Joober, R., Pruessner, J.C., & Lepage, M. (2007). Selective abnormal modulation of hippocampal activity during memory formation in first-episode psychosis. *Archives of General Psychiatry, 64*(9), 999-1014.

Alexopoulou, L., Holt, A.C., Medzhitov, R., & Flavell, R.A. (2001). Recognition of doublestranded RNA and activation of NF-kB by toll-like receptor 3. *Nature, 413*, 732–738.

Alpár, A., Gärtner, U., Härtig, W., & Brückner, G. (2006). Distribution of pyramidal cells associated with perineuronal nets in the neocortex of rat. *Brain research*, *1120*(1), 13-22.

Anomal, R., de Villers-Sidani, E., Merzenich, M. M., & Panizzutti, R. (2013). Manipulation of BDNF signaling modifies the experience-dependent plasticity induced by pure tone exposure during the critical period in the primary auditory cortex. *PLoS On*e, e64208.

Ayuso-Mateos, J. L. (2002). Global Burden of schizophrenia in the year 2000-Version 1 Estimates. *World health organization*.

Balmer, T.S., Carels, V.M., Frisch, J.L., & Nick, T.A. (2009). Modulation of perineuronal nets and parvalbumin with developmental song learning. *Journal of Neuroscience, 29*(41), 12878-12885.

Basar-Eroglu, C., Brand, A., Hildebrandt, H., Karolina Kedzior, K., Mathes, B., & Schmiedt, C. (2007). Working memory related gamma oscillations in schizophrenia patients. *International Journal of Psychophysiology, 64*, 39-45.

Bavelier, D., Levi, D. M., Li, R. W., Dan, Y., & Hensch, T. K. (2010). Removing brakes on adult brain plasticity: from molecular to behavioral interventions. *The Journal of neuroscience*, *30*(45), 14964-14971.

Bayer, T. A., Buslei, R., Havas, L., & Falkai, P. (1999). Evidence for activation of microglia in patients with psychiatric illnesses. *Neuroscience letters*, *271*(2), 126-128.

Beasley, C. L., & Reynolds, G. P. (1997). Parvalbumin-immunoreactive neurons are reduced in the prefrontal cortex of schizophrenics. *Schizophrenia research*, *24*(3), 349-355.

Becker, T., Elmer, K., Schneider, F., Schneider, M., Grodd, W., Bartels, M., Heckers, S., & Beckmann, H. (1996). Confirmation of reduced temporal limbic structure volume on magnetic resonance imaging in male patients with schizophrenia. *Psychiatry Research: Neuroimaging*, *67*(2), 135-143.

Benes, F. M., Sorensen, I., & Bird, E. D. (1991). Reduced neuronal size in posterior hippocampus of schizophrenic patients. *Schizophrenia bulletin*, *17*(4), 597.

Benes, F. M., Khan, Y., Vincent, S. L., & Wickramasinghe, R. (1996). Differences in the subregional and cellular distribution of GABAA receptor binding in the hippocampal formation of schizophrenic brain. *Synapse*, *22*(4), 338-349.

Benes, F.M., Vincent, S.L., Marie, A., & Khan, Y. (1996). Up-regulation of GABAa receptor binding on neurons of the prefrontal cortex in schizophrenic subjects. *Neuroscience, 75*(4), 1021-1031. doi: doi:10.1016/0306-4522(96)00328-4

Berardi, N., Pizzorusso, T., Ratto, G.M., & Maffei, L. 2003. Molecular basis of plasticity in the visual cortex. *Trends in Neurosciences, 26*(7), 369-78.

Berretta, S., Pantazopoulos, H., Markota, M., Brown, C., & Batzianouli, E. T. (2015). Losing the sugar coating: Potential impact of perineuronal net abnormalities on interneurons in schizophrenia. *Schizophrenia research*.

Bespalova, I. N., Angelo, G. W., Ritter, B. P., Hunter, J., Reyes-Rabanillo, M. L., Siever, L. J., & Silverman, J. M. (2012). Genetic variations in the ADAMTS12 gene are associated with schizophrenia in Puerto Rican patients of Spanish descent. *Neuromolecular medicine*, *14*(1), 53-64.

Beurdeley, M., Spatazza, J., Lee, H.H.C., Sugiyama, S., Bernard, C., Di Nardo, A.A., Hensch, T., & Prochiantz, A. (2012). Otx2 binding to perineuronal nets persistently regulates plasticity in the mature visual cortex. *Journal of Neuroscience, 32*(27), 9429-9437.

Bilder, R.M., Bogerts, B., Ashtari, M., Wu, H., Alvir, J.M., Jody, D., Reiter, G., Bell, L., & Leiberman, J.A. (1995). Anterior hippocampal volume reductions predict frontal lobe dysfunction in first episode schizophrenia. *Schizophrenia Research, 17*(1), 47-58.

Birrell, J. M., & Brown, V. J. (2000). Medial frontal cortex mediates perceptual attentional set shifting in the rat. *The Journal of Neuroscience*, *20*(11), 4320-4324.

Bitanihirwe, B. K., Peleg-Raibstein, D., Mouttet, F., Feldon, J., & Meyer, U. (2010). Late prenatal immune activation in mice leads to behavioral and neurochemical abnormalities relevant to the negative symptoms of schizophrenia. *Neuropsychopharmacology*, *35*(12), 2462-2478.

Bochner, D. N., Sapp, R. W., Adelson, J. D., Zhang, S., Lee, H., Djurisic, M., Syken, J., Dan, Y., & Shatz, C. J. (2014). Blocking PirB up-regulates spines and functional synapses to unlock visual cortical plasticity and facilitate recovery from amblyopia. *Science translational medicine*, *6*(258), 258ra140-258ra140.

Bogerts B., Ashtari M., Degreef G., Alvir J.M., Bilder R.M., Lieberman J.A. (1990). Reduced temporal limbic structure volumes on magnetic resonance images in first episode schizophrenia. *Psychiatry Research, 35*, 1–13.

Braff, D., Stone, C., Callaway, E., Geyer, M., Glick, I., & Bali, L. (1978). Prestimulus effects on human startle reflex in normals and schizophrenics.*Psychophysiology*, *15*(4), 339-343.

Brown, A.S. (2012). Epidemiologic studies of exposure to prenatal infection and risk of schizophrenia and autism. *Developmental Neurobiology, 72*(10), 1272-1276. doi: 10.1002/dneu.22024

Brown, A.S., & Derkits, E.J. (2010). Prenatal infection and schizophrenia: a review of epidemiologic and translation studies. *American Journal of Psychiatry, 167*(3), 261-280. doi: 10.1176/appi.ajp.2009.09030361

Brown, A. S., & Patterson, P. H. (2011). Maternal infection and schizophrenia: implications for prevention. *Schizophrenia bulletin*, *37*(2), 284-290.

Brown, T. E., Wilson, A. R., Cocking, D. L., & Sorg, B. A. (2009). Inhibition of matrix metalloproteinase activity disrupts reconsolidation but not consolidation of a fear memory. *Neurobiology of learning and memory*, *91*(1), 66-72.

Brückner, G., Brauer, K., Härtig W, Wolff JR, Rickmann MJ, Derouiche A, Delpech B, Girard N, Oertel WH, & Reichenbach A. (1993). Perineuronal nets provide a polyanionic, glia-associated form of microenvironment around certain neurons in many parts of the rat brain. *Glia, 8*(3), 183-200.

Brückner, G., Bringmann, A., Koppe, G., Hartig, W., & Brauer, K. (1996a). In vivo and in vitro labelling of perineuronal nets in the rat brain. *Brain Research, 720*, 84-92.

Brückner, G., Grosche, J. Schmidt, S., Härtig W, Margolis, R.U., Delpech, B., Seidenbercher, C.I., Czaniera, R., & Schachner, M. (2000). Postnatal Development of Perineuronal Nets in Wild-Type Mice and in a Mutant Deficient in Tenascin-R. *The Journal of Comparative Neurology, 428*, 616-629.

Brennaman, L.H., Kochlamazashvili, G., Stoenica, L., Nonneman, R.J., Moy, S.S., Schachner, M., Dityatev, A., Maness, P.F. (2011).Transgenic mice overexpressing the extracellular domain of NCAM are impaired in working memory and cortical plasticity. *Neurobiology of Disease, 43*, 372–378.

Butler, P.D., Susser, E.S., Brown, A.S., Kaufmann, C.A., & Gorman, J.M. (1994). Prenatal nutritional deprivation as a risk factor for schizophrenia: preclinical evidence. *Neuropsychopharmacology, 11*(4), 227-235.

Buxbaum, J. D., Georgieva, L., Young, J. J., Plescia, C., Kajiwara, Y., Jiang, Y., Moskvina, V., Norton, N., Peirce, T., Williams, H., Craddock, N.J., Carroll, L., Gorfas, G., Davis, K.L., Owen, M.J., Harroch, S., Sakurai, T., & O'Donovan, M. C. (2008). Molecular dissection of NRG1-ERBB4 signaling implicates PTPRZ1 as a potential schizophrenia susceptibility gene. *Molecular psychiatry*, *13*(2), 162-172.

Cabelli, R. J., Shelton, D. L., Segal, R. A., & Shatz, C. J. (1997). Blockade of endogenous ligands of trkB inhibits formation of ocular dominance columns. *Neuron*, *19*(1), 63-76.

Cabungcal, J. H., Counotte, D. S., Lewis, E. M., Tejeda, H. A., Piantadosi, P., Pollock, C., Calhoon, G., Sullivan, E.M., Presgraves, E.., Kil, J., Hong, L.H., Cuenod, M., Do, K.Q.,

& O'Donnell, P. (2014). Juvenile antioxidant treatment prevents adult deficits in a developmental model of schizophrenia. *Neuron*, *83*(5), 1073-1084.

Cahill, M.E., Xie, Z., Day, M., Photowala, H., Barbolina, M.V., Miller, C.A., Weiss, C. Radulovic, J., Sweatt, J.D., Disterhoft, J.F., Surmeier, D.J., & Penzes, P. (2009). Kalirin regulates cortical spine morphogenesis and disease-related behavioral phenotypes *Proceedings of the National Academy of Sciences USA, 106*, 13058–13063.

Caldwell, C.B., & Gottesman, I.I. (1990). Schizophrenics kill themselves too: A review of risk factors for suicide. *Schizophrenia Bulletin, 16*(4), 571-589

Cardin, J. A., Carlén, M., Meletis, K., Knoblich, U., Zhang, F., Deisseroth, K., Tsai, L.H., & Moore, C. I. (2009). Driving fast-spiking cells induces gamma rhythm and controls sensory responses. *Nature*, *459*(7247), 663-667.

Carter, C. S., Perlstein, W., Ganguli, R., Brar, J., Mintun, M., & Cohen, J. D. (1998). Functional hypofrontality and working memory dysfunction in schizophrenia. *American Journal of Psychiatry, 155*(9), 1285-7.

Carter, C. S., Perlstein, W., Ganguli, R., Brar, J., Mintun, M., & Cohen, J. D. (2014). Functional hypofrontality and working memory dysfunction in schizophrenia. *American Journal of Psychiatry, 155*(9), 1285-1287.

Carulli, D., Rhodes, K. E., & Fawcett, J. W. (2007). Upregulation of aggrecan, link protein 1, and hyaluronan synthases during formation of perineuronal nets in the rat cerebellum. *Journal of Comparative Neurology*, *501*(1), 83-94.

Carulli, D., Pizzorusso, T., Kwok, J.C., Putignano, E., Poli, A., Forostyak, S., Andrews, M.R., Deepa, S.S., Glant, T.T., & Fawcett, J.W. (2010). Animals lacking link protein have attenuated perineuronal nets and persistent plasticity. *Brain*, *133*(8), 2331-47. doi: 10.1093/brain/awq145

Celio, M. R. (1990). Calbindin D-28k and parvalbumin in the rat nervous system. *Neuroscience*, *35*(2), 375-475.

Celio, M.R., & Blumcke, I. (1994). Perieneuronal nets – a specialized form of extracellular matrix in the adult nervous system. *Brain Research Review, 19*(1), 128-145.

Cho, R.Y., Konecky, R.O., & Carter, C.S. (2006). Impairments in frontal cortical (gamma) synchrony and cognitive control in schizophrenia. *Proceedings of the National Academy of Sciences USA*, *103*, 19878-19883.

Cirillo, M. A., & Seidman, L. J. (2003). Verbal declarative memory dysfunction in schizophrenia: from clinical assessment to genetics and brain mechanisms. *Neuropsychology review*, *13*(2), 43-77.

Cochran, S. M., Kennedy, M., McKerchar, C. E., Steward, L. J., Pratt, J. A., & Morris, B. J. (2003). Induction of metabolic hypofunction and neurochemical deficits after chronic

intermittent exposure to phencyclidine: differential modulation by antipsychotic drugs. *Neuropsychopharmacology*, *28*(2), 265-275.

Cohen N, & Eichenbaum H: Memory, Amnesia, and the Hippocampal System. Cambridge, Mass, MIT Press, 1993

Cowan, R. L., Wilson, C. J., Emson, P. C., & Heizmann, C. W. (1990). Parvalbumin-containing GABAergic interneurons in the rat neostriatum. *Journal of comparative neurology*, *302*(2), 197-205.

Crump, C., Winkleby, M.A., Sundquist, K., & Sundquist, J. (2013). Comorbidities and mortality in person with Schizophrenia: A Swedish National Cohort Study. *American Journal of Psychiatry*, 170, 324-333. doi: 10.1176/appi.ajp.2012.12050599

Curley, A. A., Arion, D., Volk, D. W., Asafu-Adjei, J. K., Sampson, A. R., Fish, K. N., & Lewis, D. A. (2011). Cortical deficits of glutamic acid decarboxylase 67 expression in schizophrenia: clinical, protein, and cell type-specific features. *American Journal of Psychiatry*, *168*(9), 921-929.

Curley, A. A., & Lewis, D. A. (2012). Cortical basket cell dysfunction in schizophrenia. *The Journal of physiology*, *590*(4), 715-724.

Davidson, R. J. (2002). Anxiety and affective style: role of prefrontal cortex and amygdala. *Biological psychiatry*, *51*(1), 68-80.

Davis, M. (1992). The role of the amygdala in fear and anxiety. *Annual review of neuroscience*, *15*(1), 353-375.

Dalley, J. W., Cardinal, R. N., & Robbins, T. W. (2004). Prefrontal executive and cognitive functions in rodents: neural and neurochemical substrates.*Neuroscience & Biobehavioral Reviews*, *28*(7), 771-784.

Del Rio, J. A., De Lecea, L., Ferrer, I. & Soriano, E. (1994). The development of parvalbumin-immunoreactivity in the neocortex of the mouse. *Developmental Brain Research, 81*, 247–259.

Devanarayanan, S., Nandeesha, H., Kattimani, S., & Sarkar, S. (2015). Relationship between matrix metalloproteinase-9 and oxidative stress in drug-free male schizophrenia: a case control study. *Clinical Chemistry and Laboratory Medicine (CCLM)*.

Dickenhesher, T.L., Baldwin, K.T., Mironova, Y.A., et al. (2012). NgR1 and NgR3 are receptors for chondroitin sulfate proteoglycans. *Nature Neuroscience, 15*, 703-712.

Dickinson D., Iannone V.N., Wilk C.M., & Gold J.M. (2004). General and specific cognitive deficits in schizophrenia. *Biological Psychiatry*, *55*, 826–833.

Dickerson, D. D., Overeem, K. A., Wolff, A. R., Williams, J. M., Abraham, W. C., & Bilkey, D. K. (2014). Association of aberrant neural synchrony and altered GAD67 expression

following exposure to maternal immune activation, a risk factor for schizophrenia. *Translational psychiatry*, *4*(7), e418.

Dityatev, A., Bruckner, G., Dityateva, G., Grosche, J., Kleene, R., & Schachner, M. (2007). Activity-dependent formation and functions of chondroitin sulphate-rich extracellular matrix of perineuronal nets. *Developmental Neurobiology, 67*(5), 570-588.

Do, K. Q., Cuenod, M., & Hensch, T. K. (2015). Targeting oxidative stress and aberrant critical period plasticity in the developmental trajectory to schizophrenia. *Schizophrenia bulletin*, sbv065.

Domenici, E., Willé, D. R., Tozzi, F., Prokopenko, I., Miller, S., McKeown, A., ... & Muglia, P. (2010). Plasma protein biomarkers for depression and schizophrenia by multi analyte profiling of case-control collections. *PLoS one*,*5*(2), e9166.

Dow, D. J., Huxley-Jones, J., Hall, J. M., Francks, C., Maycox, P. R., Kew, J. N., ... & Barnes, M. R. (2011). ADAMTSL3 as a candidate gene for schizophrenia: Gene sequencing and ultra-high density association analysis by imputation. *Schizophrenia research*, *127*(1), 28-34.

Fagiolini, M., Hensch, T.K. (2000). Inhibitory threshold for critical period activation in primary visual cortex. *Nature, 404*(6774), 183–186

Fagiolini, M., Fritschy, J.M., Low, K., Mohler, H., Rudolph, U., Hensch, T.K. (2004). Specific GABA-A circuits for visual cortical plasticity. *Science 303*, 1681–1683.

Faissner, A., Pyka, M., Geissler, M., Sobik, T., Frischknecht, R., Gundelfinger, E. D., & Seidenbecher, C. (2010). Contributions of astrocytes to synapse formation and maturation—potential functions of the perisynaptic extracellular matrix. *Brain research reviews*, *63*(1), 26-38.

Farzan, F. Barr, M.S., Levinson, A.J., Chen, R., Wong, W., Fitzgerald, P.B., & Daskalakis, Z.J. (2010). Evidence for gamma inhibition deficits in the dorsolateral prefrontal cortex of patients with schizophrenia. *Brain*, *133*, 1505-1514.

Fawcett, J. (2009). Molecular control of brain plasticity and repair. *Progress in brain research*, *175*, 501-509.

Ferrarelli, F., Massimini, M., Peterson, M. J., Riedner, B. A., Lazar, M., Murphy, M. J., ... & Tononi, G. (2008). Reduced evoked gamma oscillations in the frontal cortex in schizophrenia patients: a TMS/EEG study. *The American journal of psychiatry*, *165*(8), 996-1005.

Ferrarelli, F., Peterson, M. J., Sarasso, S., Riedner, B. A., Murphy, M. J., Benca, R. M., Bria, P., Kalin, N.H., & Tononi, G. (2010). Thalamic dysfunction in schizophrenia suggested by whole-night deficits in slow and fast spindles. *American Journal of Psychiatry*, *167*(11), 1339-1348.

Ferrarelli, F., & Tononi, G. (2011). The thalamic reticular nucleus and schizophrenia. *Schizophrenia Bulletin*, 37, 306-315.

FitzGibbon, T., Solomon, S.G., & Goodchild, A.K. (2000). Distribution of calbindin, parvalbumin, and calrentin immunoreactivity in the reticular thalamic nucleus of the marmoset: evidence from a medial leafleft of incertal neurons. *Experimental Neurology, 164*, 371-383.

Fortier, M.E., Kent, S., Ashdown, H., Poole, S., Boksa, P., & Luheshi, G.N. (2004). The viral mimic, polyinosinic:polycytodilic acid, induces fever in rats via an interleukin-1-dependent mechanism. *American Journal of Phsyiology: Regulatory, Integrative and Comparative Physiology*, *287*, 759-66.

Fox, K., & Caterson, B. 2002. Freeing the Brain from the Perineuronal Net. *Science*, *5596*(8), 1187-1189. doi: 10.1126/science.1079224

Frischknecht, R., & Gundelfinger, E. D. (2012). The brain's extracellular matrix and its role in synaptic plasticity. In *Synaptic Plasticity* (pp. 153-171). Springer Vienna.

Fung, S.J., Webster, M.J., Sivagnanasundaram, S., Duncan, C., Elashoff, M., and Weickert, C.S. (2010). Expression of interneuron markers in the dorsolateral prefrontal cortex of the developing human and in schizophrenia. *American Journal of Psychiatry, 169*, 1082-1091.

Gaddum, J. H., & Hameed, K. A. (1954). Drugs which antagonize 5-hydroxytryptamine. *British journal of pharmacology and chemotherapy*, *9*(2), 240-248.

Galtrey, C.M., & Fawcett, J.W. (2007). The role of chondroitin sulphate proteoglycans in regeneration and plasticity in the central nervous system. *Brain Research Review*, *54*(1), 1-18.

Ganguli, R., Yang, Z., Shurin, G., Chengappa, R., Brar, J.S., Gubbi, A.V., & Rabin, B.S. (1994). Serum interleukin-6 concentration in schizophrenia: elevation associated with duration of illness. *Psychiatry Research, 51*, 1-10.

Ganguly, K., Rejmak, E., Mikosz, M., Nikolaev, E., Knapska, E., & Kaczmarek, L. (2013). Matrix metalloproteinase (MMP) 9 transcription in mouse brain induced by fear learning. *Journal of Biological Chemistry*, *288*(29), 20978-20991.

Garey, L. (2010). When cortical development goes wrong: schizophrenia as a neurodevelopmental disorder of microcircuits. *Journal of Anatomy*, *217*, 324-333.

Garey, L.J., Ong, W.Y., Patel, T.S., Kanani, M., Davis, A., Mortimer, A.M., Barnes, T.R.E., Hirsch, S.R. (1998). Reduced dendritic spine density on cerebral cortical pyramidal neurons in schizophrenia. *Journal of Neurology, Neurosurgery, & Psychiatry, 65*, 446–453.

Glantz, L. A., & Lewis, D. A. (2000). Decreased dendritic spine density on prefrontal cortical pyramidal neurons in schizophrenia. *Archives of general psychiatry*, *57*(1), 65-73.

Glausier, J.R., Fish, K.N., & Lewis, D.A. (2014). Altered parvalbumin basket cell inputs in the dorsolateral prefrontal cortex of schizophrenia. *American Journal of Psychiatry, 19*, 30-36.

Gilmore, J.H., Jarskog, L.F., & Vadlamudi, S. (2005). Maternal poly I:C exposure during pregnancy regulates TNF alpha, BDNF, and NGF expression in neonatal brain and the maternal-fetal unit of the rat brain. *Journal of Neuroimmunology, 159*, 106-112.

Giovanoli, S., Weber, L., & Meyer, U. (2014). Single and combined effects of prenatal immune activation and peripubertal stress on parvalbumin and reelin expression in the hippocampal formation. *Brain, behavior, and immunity*, *40*, 48-54.

Giovanoli, S., Weber-Stadlbauer, U., Schedlowski, M., Meyer, U., & Engler, H. (2015). Prenatal immune activation causes hippocampal synaptic deficits in the absence of overt microglia anomalies. *Brain, Behavior, and Immunity* (in press).

Giurado, R., Perez-Rando, M., Sanchez-Matarredona, D., Castren, E., & Nacher, J. (2014). Chronic fluoxetine treatment alters the structure, connectivity and plasticity of cortical interneurons. *International Journal of Neuropsychopharmacology, 17*(10), 1635-1646. doi: 10.1017/S1461145714000406

Gogolla, N., Caroni, P., Lüthi, A., & Herry, C. (2009). Perineuronal nets protect fear memories from erasure. *Science, 325*(5945), 1258-61. doi: 10.1126/science

Goldman-Rakic, P. S. (1994). Working memory dysfunction in schizophrenia. *The Journal of neuropsychiatry and clinical neurosciences*.

Gonzalez-Burgos, G., Hashimoto, T., & Lewis, D. A. (2010). Alterations of cortical GABA neurons and network oscillations in schizophrenia. *Current psychiatry reports*, *12*(4), 335-344.

Gottschall, P. E., & Deb, S. (1996). Regulation of matrix metalloproteinase expression in astrocytes, microglia and neurons. *Neuroimmunomodulation*, *3*(2-3), 69-75.

Grutzner, C., Wibral, M., Sun. L., Rivolta, D.m Singer, W., Maurer, K., & Uhlhaas, P.J. (2013). Deficits in high-(>60Hz) gamma-band oscillations during visual processing in schizophrenia. *Frontiers of Human Neuroscience*, *7*, 88.

Guidotti, A., Auta, J., Davis, J.M., Gerevini, V.D., Dwivedi, Y., Grayson, D.R., Impagnatiello, F., Pandey, G., Pesold, C., Sharma, R., Uzunov, D., & Costa, E. (2000). Decrease in reelin and glutamic acid decarboxylase 67 (GAD67) expression in schizophrenia and bipolar disorder. *Archives of General Psychiatry, 57*, 1061-1069.

Guillery, R.W., & Harting, J.K. (2003). Structure and connections of the thalamic reticular nucleus: advancing views over half a century. *Journal of Comparative Neurology*, 463, 360-371.

Guillozet-Bongaarts, A. L., Hyde, T. M., Dalley, R. A., Hawrylycz, M. J., Henry, A., Hof, P.R., Hohmann, J., Jones, A.R., Kuan, C.L., Royall, J., Shen, E., Swanson, B., Zeng, H., &

Kleinman, J. E. (2014). Altered gene expression in the dorsolateral prefrontal cortex of individuals with schizophrenia. *Molecular psychiatry*, *19*(4), 478-485.

Hains, A.B., Vu, M.A., Maciejewski, P.K., van Dyck, C.H., Gottron, M., & Arnsten, A.F. (2009). Inhibition of protein kinase C signaling protects prefrontal cortex dendritic spines and cognition from the effects of chronic stress. *Proceedings of the National Academy of Sciences USA*, 106, 17957–17962.

Hartig, W. Singer, A., Grosche, J., Brauer, K., Ottersen, O.P.,& Bruckner, G. 2001. Perienruonal nets in the rat medial nucleus of the trapezoid body surround neurons immunoreactive for various amine acids, calcium-binding proteins and the potassium channel subunit Kv3.1b. *Brain Research*, *899*(1-2), 123-133.

Hashimoto, T., Volk, D.W., Eggan, S.M., Mirnics, K., Pierri, J.N., Sun, Z., Sampson, S.R., & Lewis, D.A. (2003). Gene expression deficits in a subclass of GABA neurons in the prefrontal cortex of subjects with schizophrenia. *Journal of Neuroscience, 23*, 6315-6326.

Hama, T., Kushima, Y., Miyamoto, M., Kubota, M., Takei, N., & Hatakana, H. (1991). Interleukin-6 improves the survival of mesencephalic catecholaminergic and septal cholinergic neurons from postnatal, two-week old rats in cultures. *Neuroscience, 40*, 445-452.

Hanover, J. L., Huang, Z. J., Tonegawa, S., & Stryker, M. P. (1999). Brain-derived neurotrophic factor overexpression induces precocious critical period in mouse visual cortex. *The Journal of neuroscience: the official journal of the Society for Neuroscience*, *19*(22), RC40.

Hebb, D.O. (1945). Man's Frontal Lobes: A critical review. *Archives of Neurology and Psychiatry, 54*(1), 10-24.

Heckers, S., Rauch, S., Goff, D., Savage, C., Schacter, D., Fischman, A., & Alpert, N. (1998). Impaired recruitment of the hippocampus during conscious recollection in schizophrenia. *Nature neuroscience*, *1*(4), 318-323.

Heinrichs R.W., & Zakzanis K.K. (1998). Neurocognitive deficit in schizophrenia: a quantitative review of the evidence. *Neuropsychology, 12*, 426–445.

Hensch, T.K., Fagiolini, M., Mataga, N., Stryker, M.P., Baekkeskov, S., Kash, S.F. (1998). Local GABA circuit control of experience-dependent plasticity in developing visual cortex. *Science, 282*, 1504–1508.

Hensch, T. K. (2005). Critical period plasticity in local cortical circuits. *Nature Reviews Neuroscience*, *6*(11), 877-888.

Hockfield, S., Kalb, R.G., Zaremba, S., & Fryer, H. (1990). Expression of neural proteoglycans correlates with the acquisition of mature neuronal properties in the mammalian brain. *Cold Spring Harbor Symposium on Quantitative Biology, 55*, 505-514.

Hor, K., & Taylor, M. (2010). Suicide and schizophrenia: a systematic review of rates and risk factors. *Journal of Psychopharmacology*, 24, 81-90.

Howland, J.G., Cazakoff, B.N., & Zhang, Y. (2012). Altered object-in-place recognition memory, prepulse inhibition, and locomotor activity in the offspring of rats exposed to a viral mimetic during pregnancy. *Journal of Neuroscience*, *201*, 184-198.

Hu, H., Gan, J., & Jonas, P. (2014). Fast-spiking, parvalbumin+ GABAergic interneurons: From cellular design to microcircuit function. *Science*, *345*(6196), 1255263.

Huang, Z. J., Kirkwood, A., Pizzorusso, T., Porciatti, V., Morales, B., Bear, M. F., Maffei, L., & Tonegawa, S. (1999). BDNF regulates the maturation of inhibition and the critical period of plasticity in mouse visual cortex. *Cell*, *98*(6), 739-755.

Ibi, D., Nagai, T., Koike, H., Kitahara, Y., Mizoguchi, H., Niwa, M., Jaaro-Peled, H., Nitta, A., Yoneda, Y., Nabeshima, T., Sawa, A., & Yamada, K. (2010). Combined effect of neonatal immune activation and mutant DISC1 on phenotypic changes in adulthood. *Behavioural brain research*, *206*(1), 32-37.

Iwai, Y., Fagiolini, M., Obata, K., Hensch, T.K. (2003). Rapid critical period induction by tonic inhibition in visual cortex. *Journal of Neuroscience, 23*(17), 6695–6702.

Javitt, D. C. (2012). Twenty-five years of glutamate in schizophrenia: are we there yet?. *Schizophrenia bulletin*, *38*(5), 911-913.

Jessen F., Scheef L., Germeshausen L., Tawo Y., Kockler M., Kuhn K-U., Maier W., Schild H.H., & Heun R. (2003). Reduced hippocampal activation during encoding and recognition of words in schizophrenia patients. *American Journal of Psychiatry*, *160*, 1305–1312.

John, N., Krügel, H., Frischknecht, R., Smalla, K.H., Schultz, C., Kreutz, M.R., Gundelfinger, E.D., & Seidenbecher, C. I. (2006). Brevican-containing perineuronal nets of extracellular matrix in dissociated hippocampal primary cultures. *Molecular and Cellular Neuroscience*, *31*(4), 774-784.

Jones, P (1997). The early origins of schizophrenia. *British medical bulletin, 53*(1), 135-155.

Karpova, N. N., Pickenhagen, A., Lindholm, J., Tiraboschi, E., Kulesskaya, N., Ágústsdóttir, A., Antila, H., Popova, D., Akamine, Y., Sullivan, R., Hen, R., Drew, L.J., & Castrén, E. (2011). Fear erasure in mice requires synergy between antidepressant drugs and extinction training. *Science*, *334*(6063), 1731-1734.

Keefe, R.S.E., Silverman, J.M., Mohs, R.C., Siever, L.J., Harvey, P.D., Friedman, L., Roitman S.E.L., DuPre, R.L., Smith, C.J., Schmeidler, J., & Davis, K.L. (1997). Eye tracking, attention, and schizotypal symptoms in nonpsychotic relatives of patients with schizophrenia. *Archives of General Psychiatry, 54*(2), 169-176.

Kim, J.S., Kornhuber, H.H., Schmid-Burgk, W., & Holzmuller, B. (1980). Low cerebrospinal fluid glutamate in schizophrenic patients and a new hypothesis of schizophrenia. *Neuroscience Letters, 20*(3), 379-382.

Kirihara, K., Rissling, A.J., Swerdlow, N.R., Braff, D.L., & Light, G.A., (2012). Hierarchical organization of gamma and theta oscillatory dynamics in schizophrenia. *Biological Psychiatry*, *71*, 873-880.

Klausmeyer, A., Conrad, R., Faissner, A., & Wiese, S. (2011). Influence of glial-derived matrix molecules, especially chondroitin sulfates, on neurite growth and survival of cultured mouse embryonic motoneurons. *Journal of neuroscience research*, *89*(2), 127-141.

Klosterkötter, J., Hellmich, M., Steinmeyer, EM., Schultze-Lutter, F. (2001). Diagnosing Schizophrenia in the Initial Prodromal Phase. *Archives of General Psychiatry, 58*(2), 158-164. doi:10.1001/archpsyc.58.2.158.

Kolomeets, N. S., Orlovskaya, D. D., Rachmanova, V. I., & Uranova, N. A. (2005). Ultrastructural alterations in hippocampal mossy fiber synapses in schizophrenia: a postmortem morphometric study. *Synapse*, *57*(1), 47-55.

Konopaske, Glenn T., et al. (2014). Prefrontal cortical dendritic spine pathology in schizophrenia and bipolar disorder. *Journal of American Medical Association Psychiatry*, *71*(12), 1323-1331.

Koppe, G., Bruckner, G., Hartig, W., Delpech, B., & Bigl, V. (1997). Characterization of proteoglycan-containing perineuronal nets by enzymatic treatments of rat brain sections. *The Histochemical journal*, *29*(1), 11-20.

Krause, M., Hoffmann, W. E., & Hajós, M. (2003). Auditory sensory gating in hippocampus and reticular thalamic neurons in anesthetized rats. *Biological psychiatry*, *53*(3), 244-253.

Kwok, J. C., Carulli, D., & Fawcett, J. W. (2010). In vitro modeling of perineuronal nets: hyaluronan synthase and link protein are necessary for their formation and integrity. *Journal of neurochemistry*, *114*(5), 1447-1459.

Laursen, T.M., Munk-Olsen, T., & Vestergaard, M. (2012). Life expectancy and cardiovascular mortality in person with schizophrenia. *Current Opinion in Psychiatry, 25*(2), 83-88. doi: 10.1097/YCO.0b013e32835035ca

Lawrie, S. M., & Abukmeil, S. S. (1998). Brain abnormality in schizophrenia. A systematic and quantitative review of volumetric magnetic resonance imaging studies. *The British Journal of Psychiatry*, *172*(2), 110-120.

Lewis, D.A., & Gonzalez-Burgos, G. (2008). Neuroplasticity of neocortical circuits in schizophrenia. *Neuropsychopharmacology*, *33*(1), 141-165.

Lewis, D.A., Hashimoto, T., & Volk, D.W. 2005. Cortical inhibitory neurons and schizophrenia. *Nature Reviews Neuroscience*, 6(4), 312-24.

Lewis, D.A., Curley, A.A., Glausier, J.R., & Volk, D.W. (2012). Cortical parvalbumin interneurons and cognitive dysfunction in schizophrenia. *Trends in Neurosciences, 35*(1), 57-67. doi: 10.1016/j.tins.2011.10.004

Li, W.Y., Chang, Y.C., Lee, L.J., & Lee, L.J. (2014). Prenatal infection affects the neuronal architecture and cognitive function in adult mice. *Developmental Neuroscience, 36*(5), 359-70. doi: 10.1159/000362383.

Lieberman, J. A., Perkins, D., Belger, A., Chakos, M., Jarskog, F., Boteva, K., & Gilmore, J. (2001). The early stages of schizophrenia: speculations on pathogenesis, pathophysiology, and therapeutic approaches. *Biological psychiatry*, *50*(11), 884-897.

Lin, A., Kenis, G., Bignotti, S., Tura, G.J.B., De Jong, R., Bosmans, E., Pioli, R., Altamura, C., Sharpe, S., & Maes, M. (1998). The inflammatory response system in treatment-resistant schizophrenia: increased serum interleukin-6. *Schizophrenia Research, 32*, 9-15.

Lindström, L. H., Gefvert, O., Hagberg, G., Lundberg, T., Bergström, M., Hartvig, P., & Långström, B. (1999). Increased dopamine synthesis rate in medial prefrontal cortex and striatum in schizophrenia indicated by L-(β-11 C) DOPA and PET. *Biological psychiatry*, *46*(5), 681-688.

Liston, M.M. Miller, D.S. Goldwater, J.J. Radley, A.B. Rocher, P.R. Hof, J.H. & Morrison, B.S. (2006). Stress-induced alterations in prefrontal cortical dendritic morphology predict selective impairments in perceptual attentional set-shifting. *Journal of Neuroscience, 26*, 7870–7874.

Liu, H., Gao, P.F., Xu, H.W., Liu, M.M., Yu, T., Yao, J.P., & Yin, Z.Q. (2013). Perineuronal nets increase inhibitory GABAergic currents during critical period in rats. *International Journal of Opthamology, 6*(2), 120-125. doi: 10.3980/j.issn.2222-3959.2013.02.02.

Lumey, L.H., Stein, A.D., & Susser, E. (2011). Prenatal famine and adult health. *Annual Review of Public Health*, 32, 237-262. doi: 10.1146/annurev-publhealth-031210-101230

Machado, C.J., Whitaker, A.M., Smith, S.E., Patterson, P.H., & Bauman, M.D (2015). Maternal immune activation in nonhuman primates alters social attention in juvenile offspring. *Biological Psychiatry, 77*(9), 823-32. doi: 10.1016/j.biopsych.2014.07.035

Maeda, A., & Sobel, R. A. (1996). Matrix metalloproteinases in the normal human central nervous system, microglial nodules, and multiple sclerosis lesions. *Journal of Neuropathology & Experimental Neurology*, *55*(3), 300-309.

Maes, M., Bosmans, E., Calabrese, J., Smith, R., & Meltzer, H.Y. (1995). Interleukin-2 and interleukin-6 in schizophrenia and mania: effects of neuroleptics and mood stabilizers. *Journal of Psychiatry Research*, *29*, 141-152.

Malla, A.K., & Norman, R.M (1994). Prodromal symptoms in schizophrenia. *The British Journal of Psychiatry* 164(4), 487-493.

Manoach, D. S., Press, D. Z., Thangaraj, V., Searl, M. M., Goff, D. C., Halpern, E., Saper, C.B., & Warach, S. (1999). Schizophrenic subjects activate dorsolateral prefrontal cortex during a working memory task, as measured by fMRI. *Biological psychiatry*, *45*(9), 1128-1137.

Margari, F., Petruzzelli, M. G., Lecce, P. A., Todarello, O., De Giacomo, A., Lucarelli, E., Martinelli, D., & Margari, L. (2011). Familial liability, obstetric complications and childhood development abnormalities in early onset schizophrenia: a case control study. *BMC psychiatry*, *11*(1), 60.

Matute, C., Melone, M., Vallejo-Illarramendi, A., & Conti, F. (2005). Increased expression of the astrocytic glutamate transporter GLT-1 in the prefrontal cortex of schizophrenics. *Glia*, *49*(3), 451-455.

Maffei, A., Lambo, M. E., & Turrigiano, G. G. (2010). Critical Period for Inhibitory Plasticity in RodentBinocular V1. *The Journal of Neuroscience*, *30*(9), 3304-3309.

Mauney, S.A., Athanas, K.M., Pantazopoulos, H., Shaskan, N., Passeri, E., Beretta, S., & Woo, T.U. (2013). Developmental pattern of perineuronal nets in the human prefrontal cortex and their deficit in schizophrenia. *Biological Psychiatry, 74*(6), 427-35. doi: 10.1016/j.biopsych.2013.05.007

McCarley, R. W., Shenton, M. E., O'Donnell, B. F., Faux, S. F., Kikinis, R., Nestor, P. G., & Jolesz, F. A. (1993). Auditory P300 abnormalities and left posterior superior temporal gyrus volume reduction in schizophrenia. *Archives of General Psychiatry*, *50*(3), 190-197.

McGlashan, T. H., & Hoffman, R. E. (2000). Schizophrenia as a disorder of developmentally reduced synaptic connectivity. *Archives of General Psychiatry*, *57*(7), 637-648.

McClelland J,L., McNaughton B.L., & O'Reilly R.C. (1995). Why there are complementary learning systems in the hippocampus and neocortex: insights from the successes and failures of connectionist models of learning and memory. *Psychological Review*, *102*, 419–457

McGrath, L.M., Cornelis, M.C., Lee, P.H., Robinson, E.B., Duncan, L.E., Barnett, J.H., Huang, J., Gerber, G., Sklar, P., Sullivan, P., Perlis, R.H., & Smoller, J. W. (2013). Genetic predictors of risk and resilience in psychiatric disorders: A cross-disorder genome-wide association study of functional impairment in major depressive disorder, bipolar disorder, and schizophrenia. *American Journal of Medical Genetics Part B: Neuropsychiatric Genetics*, *162*(8), 779-788.

McRae, P. A., Rocco, M. M., Kelly, G., Brumberg, J. C., & Matthews, R. T. (2007). Sensory deprivation alters aggrecan and perineuronal net expression in the mouse barrel cortex. *The Journal of neuroscience*, *27*(20), 5405-5413.

Mellios, N., Huang, H.S., Baker, S.P., Galdzicka, M., Ginns, E., & Akbarian, S. (2009). Molecular determinants of dysregulated GABAergic gene expression in the prefrontal cortex of subjects with schizophrenia. *Biological Psychiatry, 65*, 1006-1014.

Meyer U., Feldon J., & Fatemi S.H (2009). In-vivo rodent models for the experimental investigation of prenatal immune activation effects in neurodevelopmental brain disorders. *Neuroscience and Biobehavioural Review, 33*(7):1061-79.

Meyer, U., Spoerri, E., Yee, B. K., Schwarz, M. J., & Feldon, J. (2010). Evaluating early preventive antipsychotic and antidepressant drug treatment in an infection-based neurodevelopmental mouse model of schizophrenia. *Schizophrenia bulletin*, *36*(3), 607-623.

Meyer, U., & Feldon, J. (2012). To poly (I: C) or not to poly (I: C): advancing preclinical schizophrenia research through the use of prenatal immune activation models. *Neuropharmacology*, *62*(3), 1308-1321.

Meyer, U. (2014). Prenatal poly (I: C) exposure and other developmental immune activation models in rodent systems. *Biological psychiatry*, *75*(4), 307-315.

Miles, CP. (1977). Conditions predisposing to suicide: a review. *Journal of Nervous and Mental Disease*, 164(4), 231-246.

Miner, L. A. H., Ostrander, M., & Sarter, M. (1997). Effects of ibotenic acid-induced loss of neurons in the medial prefrontal cortex of rats on behavioral vigilance: evidence for executive dysfunction. *Journal of Psychopharmacology*, *11*(2), 169-178.

Morawski, M. Alpár A, Brückner G, Fiedler A, Jäger C, Gati G, Stieler JT, Arendt T. (2009). Chondroitin sulphate proteoglycan-based extracellular matrix in chicken (Gallus domesticus) brain. *Brain Research*, *1275*, 10-23. doi: 10.1016/j.brainres.2009.02.046

Morishita, H., Cabungcal, J. H., Chen, Y., Do, K. Q., & Hensch, T. K. (2015). Prolonged period of cortical plasticity upon redox dysregulation in fast-spiking interneurons. *Biological psychiatry*.

Moyer, Caitlin E., et al. (2012). Reduced glutamate decarboxylase 65 protein within primary auditory cortex inhibitory boutons in schizophrenia. *Biological psychiatry*, *72*(9), 734-743.

Murray, R.M. & Lewis, S.W. (1987). Is schizophrenia a neurodevelopmental disorder? *British Medical Journal (Clinical Research Edition)*, *295*(6600), 681-682.

Murray, R.M. & Van Os, J. (1998). Predictors of outcome in schizophrenia. *Journal of Clinical Psychopharmacology, 18*(2), 2-4.

Müller, N., Empel, M., Riedel, M., Schwarz, M.J., & Ackenheil, M. (1997). Neuroleptic treatment increases soluble IL-2 receptors and decreases soluble IL-6 receptors in schizophrenia. *European Archives of Psychiatry and Clinical Neurosciences*, *247*, 308-313.

Nagy, V., Bozdagi, O., & Huntley, G. W. (2007). The extracellular protease matrix metalloproteinase-9 is activated by inhibitory avoidance learning and required for long-term memory. *Learning & Memory*, *14*(10), 655-664.

Nakayama, D., Baraki, Z., Onoue, K., Ikegaya, Y., Matsuki, N., & Nomura, H. (2015). Frontal association cortex is engaged in stimulus integration during associative learning. *Current Biology, 25*, 117-123.

Nuechterlein K.H., Barch D.M., Gold J.M., Goldberg T.E., Green M.F., & Heaton R.K. (2004). Identification of separable cognitive factors in schizophrenia. *Schizophrenia Research, 72*, 29–39.

Norman K.A., & O'Reilly R.C. (2003). Modeling hippocampal and neocortical contributions to recognition memory: a complementary learning-systems approach. *Psychological Review*, *110,* 611–646.

Ozawa, K., Hashimoto, K., Kishimoto, T., Shimizu, E., Ishikura, H., & Iyo, M. (2006). Immune activation during pregnancy in mice leads to dopaminergic hyperfunction and cognitive impairment in the offspring: a neurodevelopmental animal model of schizophrenia. *Biological Psychiatry, 59*(6), 545-54.

Pantazopoulos, H., Woo, T.U., Lim, M.P., Lange, N., & Beretta, S. (2010). Extracellular matrix-glial abnormalities in the amygdala and entorhinal cortex of subjects diagnosed with schizophrenia. *Archives of General Psychiatry, 67*(2), 155-66. doi: 10.1001/archgenpsychiatry.2009.1964.

Pantazopoulos, H., Boyer-Boiteau, A., Holbrook, E.H., Jang, W., Hahn, C.G., Arnold, S.E., & Beretta, S. (2013). Proteoglycan abnormalities in olfactory epithelium tissue from subjects diagnosed with schizophrenia. *Schizophrenia Research, 150*(2-3), 366-72. doi: 10.1016/j.schres.2013.08.013

Pantazopoulos, H., et al. (2015). Aggrecan and chondroitin-6-sulfate abnormalities in schizophrenia and bipolar disorder: a postmortem study on the amygdala. *Translational Psychiatry* 5(1), e496.

Passetti, F., Humby, T., Everitt, B. J., & Robbins, T. W. (2000). Mixed attentional and executive deficits in medial frontal cortex lesioned rats. *Psychobiology*, *28*(2), 261-271.

Patrich, E., Piontkewitz, Y., Peretz, A., Weiner, I., & Attali, B. (2015). Maturation-and sex-sensitive depression of hippocampal excitatory transmission in a rat schizophrenia model. *Brain, behavior, and immunity*.

Paxinos, G. Watson C (1986) The rat brain in stereotaxic coordinates. *New York: Academic*.

Perkins, D.O. (2004). Evaluating and treating the prodromal stage of schizophrenia. *Current Psychiatry Reports, 6*(4), 289-295.

Pesold, C., Liu, W.S., Guidotti, A., Costa, E., & Caruncho, H.J. (1999). Cortical bitufted, horizontal, and Martinotti cells preferentially express and secrete reelin into perineuronal

nets, nonsynaptically modulating gene expression. *Proceedings of the National Academy of Sciences, 96*(6), 3217-22.

Pietersen, C.Y., Mauney, S.A., Kim, S.S., Lim, M.P., Rooney, R.J., Goldstein, J.M., Petryshen, T.L., Seidman, L.J., Shenton, M.E., McCarley, R.W., Sonntag, K.C., & Woo, T.U. (2014). Molecular profiles of pyramidal neurons in superior temporal cortex in schizophrenia. *Journal of Neurogenetics*, 28(1-2), 53-69. doi: 10.3109/01677063.2014.882918

Pietersen, C.Y., Mauney, S.A., Kim, S.S., Passeri, E., Lim, M.P., Rooney, R.J., Goldstein, J.M., Petreyshen, T.L., Seidman, L.J., Shenton, M.E., McCarley, R.W., Sonntag, K.C., & Woo, T.U. (2014). Molecular profiles of parvalbumin-immunoreactive neurons in the superior temporal cortex in schizophrenia. *Journal of Neurogenetics*, *28*(1-2), 70-85. doi: 10.3109/01677063.2013.878339

Pizzorusso, T., Medini, P., Berardi, N., Chierzi, S., Fawcett, J.W., & Maffei, L. (2002). Reactivation of ocular dominance plasticity in the adult visual cortex. *Science*, 298(5596), 1248-51.

Pizzorusso, T., Medini, P., Landi, S., Baldini, S., Berardi, N., & Maffei, L. (2006). Structural and functional recovery from early monocular deprivation in adult rats. *Proceedings of the National Academy of Sciences*, *103*(22), 8517-8522.

Pomarol-Clotet, E., Canales-Rodriguez, E. J., Salvador, R., Sarró, S., Gomar, J. J., Vila, F., Ortiz-Gil, J., Iturria-Medina, Y., Capdevila, A., & McKenna, P. J. (2010). Medial prefrontal cortex pathology in schizophrenia as revealed by convergent findings from multimodal imaging. *Molecular psychiatry*, *15*(8), 823-830.

Piontkewitz, Y., Bernstein, H. G., Dobrowolny, H., Bogerts, B., Weiner, I., & Keilhoff, G. (2012). Effects of risperidone treatment in adolescence on hippocampal neurogenesis, parvalbumin expression, and vascularization following prenatal immune activation in rats. *Brain, behavior, and immunity*, *26*(2), 353-363.

Pratt, J. A., & Morris, B. J. (2015). The thalamic reticular nucleus: A functional hub for thalamocortical network dysfunction in schizophrenia and a target for drug discovery. *Journal of Psychopharmacology*, *29*(2), 127-137.

Radhu, N., Dominguez, L. G., Farzan, F., Richter, M. A., Semeralul, M. O., Chen, R., & Daskalakis, Z. J. (2015). Evidence for inhibitory deficits in the prefrontal cortex in schizophrenia. *Brain*, *138*(2), 483-497.

Rajkowska, G., Selemon, L. D., & Goldman-Rakic, P. S. (1998). Neuronal and glial somal size in the prefrontal cortex: a postmortem morphometric study of schizophrenia and Huntington disease. *Archives of General Psychiatry*, *55*(3), 215-224.

Ranganath C., Minzenberg M.J., & Ragland J.D. (2008). The cognitive neuroscience of memory function and dysfunction in schizophrenia. *Biological Psychiatry*, *64,* 18–25.

Reynolds, G. P. (1983). Increased concentrations and lateral asymmetry of amygdala dopamine in schizophrenia. *Nature, 305*, 527-529. doi:10.1038/305527a0

Rhodes, K.E., & Fawcett, J.W. 2004. Chondroitin sulphate proteoglycans: preventing plasticity or protecting the CNS? *Journal of Anatomy*, *204*(1), 33-48.

Richetto, J., Calabrese, F., Meyer, U., & Riva, M. A. (2013). Prenatal versus postnatal maternal factors in the development of infection-induced working memory impairments in mice. *Brain, behavior, and immunity*, *33*, 190-200.

Ripke, S., & Schizophrenia Psychiatric Genome-Wide Association Study (GWAS) Consortium. (2011). Genome-wide association study identifies five new schizophrenia loci. *Nature genetics*, *43*(10), 969-976.

Ripke, S., & Schizophrenia Working Group of the Psychiatric Genomics Consortium. (2014). Biological insights from 108 schizophrenia-associated genetic loci. *Nature*, *511*(7510), 421-427.

Roberts, A. C., Robbins, T. W., & Weiskrantz, L. E. (1998). *The prefrontal cortex: Executive and cognitive functions*. Oxford University Press.

Roberts, R.C., Roche, J.K., & Conley, C.C. (2005). Synaptic differences in the postmortem striatum of subjects with schizophrenia: a stereological ultrastructural analysis. *Synapse, 56*, 185–197.

Roberts, R.C., Roche, J.K., & Conley, C.C. (2005). Synaptic differences in the patch matrix compartments of subjects with schizophrenia: a postmortem ultrastructural study of the striatum. *Neurobiology of Disease, 20*, 324–335.

Romberg, C., Yang, S., Melani, R., Andrews, M.R., Horner, A.E., Spillantini, M.G., Bussey, T.J., Fawcett, J.W., Pizzorusso, T., & Saksida, L.M. 2013. Depletion of perineuronal nets enhances recognition memory and long-term depression in the perirhinal cortex. *Journal of Neuroscience*, *33*(16), 7057-65. doi: 10.1523/JNEUROSCI.6267-11.2013

Piontkewitz, Y., Bernstein, H. G., Dobrowolny, H., Bogerts, B., Weiner, I., & Keilhoff, G. (2012). Effects of risperidone treatment in adolescence on hippocampal neurogenesis, parvalbumin expression, and vascularization following prenatal immune activation in rats. *Brain, behavior, and immunity*, *26*(2), 353-363.

Pizzorusso, T., Medini, P., Berardi, N., Chierzi, S., Fawcett, J.W., & Maffei, L. (2002). Reactivation of ocular dominance plasticity in the adult visual cortex. *Science*, *298*(5596), 1248-51.

Pomarol-Clotet, E., Canales-Rodriguez, E. J., Salvador, R., Sarró, S., Gomar, J. J., Vila, F., Ortiz-Gil, J., Iturria-Medina, Y., Capdevila, A., & McKenna, P. J. (2010). Medial prefrontal cortex pathology in schizophrenia as revealed by convergent findings from multimodal imaging. *Molecular psychiatry*, *15*(8), 823-830.

Sangha, S., Greba, Q., Robinson, P. D., Ballendine, S. A., & Howland, J. G. (2014). Heightened fear in response to a safety cue and extinguished fear cue in a rat model of maternal immune activation. *Frontiers in behavioral neuroscience*, *8*.

Saykin, A. J., Gur, R. C., Gur, R. E., Mozley, P. D., Mozley, L. H., Resnick, S. M., Kester, S.M., & Stafiniak, P. (1991). Neuropsychological function in schizophrenia: selective impairment in memory and learning. *Archives of general psychiatry*,*48*(7), 618-624.

Saykin A.J., Shtasel D.L., Gur R.E., Kester D.B., Mozley L.H., Stafiniak P., & Gur, R.C. (1994) Neuropsychological deficits in neuroleptic naive patients with first-episode schizophrenia. *Archives of General Psychiatry*, 51, 124–131

Selemon, L. D., Rajkowska, G., & Goldman-Rakic, P. S. (1995). Abnormally high neuronal density in the schizophrenic cortex: a morphometric analysis of prefrontal area 9 and occipital area 17. *Archives of general psychiatry, 52*(10), 805-818.

Seshadri, S., Zeledon, M., & Sawa, A. (2013). Synapse-specific contributions in the cortical pathology of schizophrenia. *Neurobiology of Disease, 53*, 26-35. doi: 10.1016/j.nbd.2013.01.009

Smith, S.E.P., Li, J., Garbett, K., Mirnics, K., & Patterson, P.H. (2007). Maternal immune activation alters fetal brain development through Interleukin-6. *Journal of Neuroscience, 27*(40), 10695-10702.

Smolders, S., Smolders, S. M., Swinnen, N., Gärtner, A., Rigo, J. M., Legendre, P., & Brône, B. (2015). Maternal immune activation evoked by polyinosinic: polycytidylic acid does not evoke microglial cell activation in the embryo. *Frontiers in cellular neuroscience*, *9*.

Sham P.C., MacLean, C.J., & Kendler, K.S. (1994). A typological model of schizophrenia based on age at onset, sex and familial morbidity. *Acta Psychiatrica Scandinavica, 89*(2), 135-141.

Shah, A., & Lodge, D.J. (2013). A loss of hippocampal perineuronal nets produces deficits in dopamine system function: relevance to the positive symptoms of schizophrenia. *Translation Psychiatry*, 3, e215.

Sohal, V. S., Zhang, F., Yizhar, O., & Deisseroth, K. (2009). Parvalbumin neurons and gamma rhythms enhance cortical circuit performance. *Nature*, *459*(7247), 698-702.

Spencer, K. M., Niznikiewicz, M. A., Shenton, M. E., & McCarley, R. W. (2008). Sensory-evoked gamma oscillations in chronic schizophrenia. *Biological psychiatry*, *63*(8), 744-747.

Stephan, K.E., Friston, K.J., & Frith, C.D. (2009). Dysconnection in schizophrenia: from aberrant synaptic plasticity to failures of self-monitoring. *Schizophrenia Bulletin, 39*(2), 199-209. doi: 10.1017/S0033291708003863

Stone, M., Gabrieli, J. D., Stebbins, G. T., & Sullivan, E. V. (1998). Working and strategic memory deficits in schizophrenia. *Neuropsychology*, *12*(2), 278.

Suddath, R. L., Casanova, M. F., Goldberg, T. E., Daniel, D. G., Kelsoe, J. R., & Weinberger, D. R. (1989). Temporal lobe pathology in schizophrenia: a quantitative magnetic resonance imaging study. *Am J Psychiatry*, *146*(4), 464-472.

Sugiyama, S., Di Nardo, A. A., Aizawa, S., Matsuo, I., Volovitch, M., Prochiantz, A., & Hensch, T. K. (2008). Experience-dependent transfer of Otx2 homeoprotein into the visual cortex activates postnatal plasticity. *Cell*, *134*(3), 508-520.

Sullivan, E. V., Lim, K. O., Mathalon, D., Marsh, L., Beal, D. M., Harris, D., ... & Pfefferbaum, A. (1998). A profile of cortical gray matter volume deficits characteristic of schizophrenia. *Cerebral Cortex*, *8*(2), 117-124.

Sun, Y., Farzan, F. Barr, M.S., Kirihara, K., Fitzgerald, P.B., Light, G.A., & Daskalakis, Z.J. (2011). Gamma oscillations in schizophrenia: mechanisms and clinical significance. *Brain Research, 1413*, 98-114.

Sur, M., Frost, D.O., & Hockfield, S. (1988). Expression of a surface-associated antigen on Y-cells in the cat lateral geniculate nucleus is regulated by visual experience. *Journal of Neuroscience, 8*, 874-882.

Suvisaari, J.M., Taxell-Lassas, V., Pankakoski, M., Haukka, J.K., Lönnqvist JK, & Häkkinen LT. (2013). Obstetric complications as risk factors for schizophrenia spectrum psychoses in offspring of mothers with psychotic disorder. *Schizophrenia Bulletin, 39*(5), 1056-66. doi: 10.1093/schbul/sbs109

Sweet, R. A., Henteleff, R. A., Zhang, W., Sampson, A. R., & Lewis, D. A. (2009). Reduced dendritic spine density in auditory cortex of subjects with schizophrenia. *Neuropsychopharmacology*, *34*(2), 374-389.

Sweet, R. A., Bergen, S. E., Sun, Z., Sampson, A. R., Pierri, J. N., & Lewis, D. A. (2004). Pyramidal cell size reduction in schizophrenia: evidence for involvement of auditory feedforward circuits. *Biological psychiatry*, *55*(12), 1128-1137.

Takesian, A. E., & Hensch, T. K. (2013). Balancing plasticity/stability across brain development. *Progress in Brain Research*, *207*, 3-34.

Takeuchi, O., & Akira, S. (2007). Recognition of viruses by innate immunity. *Immunology Review*, *220*, 214–224.

Thomas, P., Mathur, P., Gottesman, I. I., Nagpal, R., Nimgaonkar, V. L., & Deshpande, S. N. (2007). Correlates of hallucinations in schizophrenia: A cross-cultural evaluation. *Schizophrenia research*, *92*(1), 41-49.

Traynor, T. R., Majde, J. A., Bohnet, S. G., & Krueger, J. M. (2004). Intratracheal double-stranded RNA plus interferon-γ: a model for analysis of the acute phase response to respiratory viral infections. *Life sciences*, *74*(20), 2563-2576.

Troyano-Rodriguez, E., Lladó-Pelfort, L., Santana, N., Teruel-Martí, V., Celada, P., & Artigas, F. (2014). Phencyclidine inhibits the activity of thalamic reticular gamma-aminobutyric acidergic neurons in rat brain. *Biological psychiatry*, *76*(12), 937-945.

Uhlhaas, P.J., & Singer, W. (2010). Abnormal neural oscillations and synchrony in schizophrenia. *Nature Reviews Neuroscience, 11*(2), 100-113.

Van Rossum, J. M. (1967). The significance of dopamine-receptor blockade for the action of neuroleptic drugs. *Neuropsychopharmacology*, *5*, 321-323.

Vo, T., Carulli, D., Ehlert, E.M., Kwok, J.C., Dick, G., Mecollari, V., Moloney, E.B., Neufield, G., de Winter, F., Fawcett, J.W., & Verhaagen, J. (2013). The chemorepulsive axon guidance protein semaphorin3A is constituent of perineuronal nets in the adult rodent brain. *Molecular & Cellular Neuroscience, 56*, 186-200.

Volk, D. W., & Lewis, D. A. (2002). Impaired prefrontal inhibition in schizophrenia: relevance for cognitive dysfunction. *Physiology & behavior*,*77*(4), 501-505.

Volk, D.W., & Lewis, D.A. (2013). Prenatal ontogeny as a susceptibility period for cortical GABA neuron disturbances in schizophrenia. *Journal of Neuroscience, 284*, 154-64. doi: 10.1016/j.neuroscience.2013.06.008

Volk, D.W., & Lewis, D.A. (2014). Early Developmental Disturbances of Cortical Inhibitory Neurons: Contribution to Cognitive Deficits in Schizophrenia. *Schizophrenia Bulletin, 40*(5), 952-957.

Volk, D.W., Matsubara, T., Li, S., Sengupta, E.J., Georgiev, D., Minabe, Y., Sampson, A., Hashimoto, T., & Lewis, D.A. (2012). Deficits in transcriptional regulators of cortical parvalbumin neurons in schizophrenia. American Journal of Psychiatry, 169, 1082-1091.

Vorhees, C. V., Graham, D. L., Braun, A. A., Schaefer, T. L., Skelton, M. R., Richtand, N. M., & Williams, M. T. (2015). Prenatal immune challenge in rats: Effects of polyinosinic–polycytidylic acid on spatial learning, prepulse inhibition, conditioned fear, and responses to MK-801 and amphetamine. *Neurotoxicology and teratology*, *47*, 54-65.

Webster, M. J., Knable, M. B., Johnston-Wilson, N., Nagata, K., Inagaki, M., & Yolken, R. H. (2001). Immunohistochemical localization of phosphorylated glial fibrillary acidic protein in the prefrontal cortex and hippocampus from patients with schizophrenia, bipolar disorder, and depression. *Brain, behavior, and immunity*, *15*(4), 388-400.

Weinberger, D.R. (1987). Implications of normal brain development for the pathogenesis of schizophrenia. *Archives of General Psychiatry*, *44*(7), 660-669.

Wiese, S., Karus, M., & Faissner, A. (2012). Astrocytes as a source for extracellular matrix molecules and cytokines. *Frontiers in pharmacology*, *3*.

Weiss, A. P., Schacter, D. L., Goff, D. C., Rauch, S. L., Alpert, N. M., Fischman, A. J., & Heckers, S. (2003). Impaired hippocampal recruitment during normal modulation of memory performance in schizophrenia. *Biological psychiatry*, *53*(1), 48-55.

Weiss, A. P., Zalesak, M., DeWitt, I., Goff, D., Kunkel, L., & Heckers, S. (2004). Impaired hippocampal function during the detection of novel words in schizophrenia. *Biological psychiatry*, *55*(7), 668-675.

Winter, C., Djodari-Irani, A., Sohr, R., Morgenstern, R., Feldon, J., Juckel, G., & Meyer U. (2009). Prenatal immune activation leads to multiple changes in basal neurotransmitter levels in the adult brain: implications for brain disorders of neurodevelopmental origin such as schizophrenia. *International Journal of Neuropsychopharmacology, 12*(4), 513-24. doi: 10.1017/S1461145708009206

Woo, T.U., Spencer, K., & McCarley, R.W. (2010). Gamma oscillation deficits and the onset and early progression of schizophrenia. *Harvard Review of Psychiatry, 18*(3), 173-189.

Wooley, D.W., & Shaw, E. (1954). A Biochemical and Pharmacological suggestion about certain mental disorders. *Proceedings of the National Academy of Sciences of the United States of America, 40*(4), 228-231.

Wright, J. W., Brown, T. E., & Harding, J. W. (2006). Inhibition of hippocampal matrix metalloproteinase-3 and-9 disrupts spatial memory. *Neural plasticity*, *2007*.

Wright, I. C., Rabe-Hesketh, S., Woodruff, P. W., David, A. S., Murray, R. M., & Bullmore, E. T. (2014). Meta-analysis of regional brain volumes in schizophrenia. *American Journal of Psychiatry*.

Xu, M. Q., Sun, W. S., Liu, B. X., Feng, G. Y., Yu, L., Yang, L., ... & He, L. (2009). Prenatal malnutrition and adult schizophrenia: further evidence from the 1959-1961 Chinese famine. *Schizophrenia bulletin*, sbn168.

Yamada, J., Ohgomori, T., & Jinno, S. (2015). Perineuronal nets affect parvalbumin expression in GABAergic neurons in the mouse hippocampus. *European Journal of Neuroscience, 41*(3), 386-371.

Yamamori, H., Hashimoto, R., Ishima, T., Kishi, F., Yasuda, Y., Ohi, K., ... & Takeda, M. (2013). Plasma levels of mature brain-derived neurotrophic factor (BDNF) and matrix metalloproteinase-9 (MMP-9) in treatment-resistant schizophrenia treated with clozapine. *Neuroscience letters*, *556*, 37-41.

Ye, Q., & Miao, Q. L. (2013). Experience-dependent development of perineuronal nets and chondroitin sulfate proteoglycan receptors in mouse visual cortex. *Matrix Biology*, *32*(6), 352-363.

Zahrt, J., Taylor, J. R., Mathew, R. G., & Arnsten, A. F. (1997). Supranormal stimulation of D1 dopamine receptors in the rodent prefrontal cortex impairs spatial working memory performance. *The Journal of neuroscience*, *17*(21), 8528-8535.

Zalcman, S., Green-Johnson, J.M., Murray, L., Nance, D.M., Dyck, D., Anisman, H., & Greenberg, A.H. (1994). Cytokine-specific central monoamine alterations induced by interleukin-1, -2, and -6. *Brain Research, 643*, 40-49.

Zhang Y., Cazakoff B. N., Thai C. A., Howland J. G. (2012). Prenatal exposure to a viral mimetic alters behavioural flexibility in male, but not female, rats. *Neuropharmacology*, *62*, 1299–1307 10.1016/j.neuropharm.2011.02.022

Zuckerman, L., Rehavi, M., Nachman, R., & Weiner, I. (2003). Immune activation during pregnancy in rats leads to a postpubertal emergence of disrupted latent inhibition, dopamine hyperfunction, and altered limbic morphology in the offspring: a novel neurodevelopmental model of schizophrenia. *Neuropsychopharmacology, 28*, 1778-1789.